AUGUST 31, 1993

SUBMITTED BY

AUBURN UNIVERSITY
COLLEGE OF ENGINEERING
AND ENGINEERING EXPERIMENT STATION
DEPARTMENT OF AEROSPACE ENGINEERING
AUBURN UNIVERSITY, AL 36849

SUBMITTED TO

NATIONAL AERONAUTICS AND SPACE ADMINISTRATION
GEORGE C. MARSHALL SPACE FLIGHT CENTER
HUNTSVILLE, AL 35812

UNDER

CONTRACT NAS8-39131
DELIVERY ORDER NO. 15

AERODYNAMIC FLIGHT CONTROL TO INCREASE PAYLOAD
CAPABILITY OF FUTURE LAUNCH VEHICLES

FINAL REPORT

PREFACE

This report summarizes the work done under Delivery Order No. 15 of Contract NAS8-39131 between Marshall Space Flight Center and Auburn University during the period 14 December 1992 through August 31, 1993. The NASA Technical Representative was Ms. Chris Barrett. Numerous individuals in the Department of Aerospace Engineering contributed to this effort. The authors of this report, besides the Principal Investigator, were Mr. Y-M Cheng, Mr. Todd Leleux, Mr. Scott Bigelow, and Mr. William Hasbrook. Mr. Hasbrook also provided expert assistance in developing graphics for the report. A good deal of the background information on composite materials, as used for flight control surfaces, was provided by Ms. Maurine Wimsatt and Dr. R. S. Gross. Mrs. Marjorie McGee typed most of the final manuscript.

John E. Cochran, Jr.
Principal Investigator

PAGE ii INTENTIONALLY BLANK

PRECEDING PAGE BLANK NOT FILMED

THIS PAGE LEFT INTENTIONALLY BLANK

TABLE OF CONTENTS

LIST OF FIGURES

LIST OF TABLES

1. INTRODUCTION

1.1 Background

During the development of launch vehicles, there have been periods of time, especially in the early years of the space program, when some countries used fins on certain vehicles to either produce static stability with respect to angle of attack, or to reduce static instability of the vehicles, or to provide aerodynamic control, or a combination of these purposes. For example, members of the Saturn family of vehicles had fixed fins [1] to improve their stability characteristics. Launch vehicles with fins from some other countries are discussed in Section 2 of this report. For several reasons, most probably because of the obvious fact that fins add weight and because of the good reliability of automatic stabilization using thrust vectoring of gimballed engine nozzles, the use of aerodynamic surfaces on launch vehicles has decreased during recent years. A notable exception is the air-launched vehicle, Pegasus [1,2] that uses aerodynamic surfaces for attitude control and trajectory modification.

In any case, fins were not a part of the original design of the National Launch System (NLS) 1.5 Stage Vehicle [3] (see Fig. 1.1). However, during the NLS design process, the possibility of interchanging the locations of the liquid oxygen (LOX) and liquid hydrogen (LH) tanks was considered and preliminary estimates of the associated savings in structural weight and plumbing range from 5,000 to 10,000 pounds.

When the locations of the LOX and LH tanks are interchanged, the center of mass of the NLS 1.5 Stage Vehicle is moved aft, while the location of its aerodynamic center remains unchanged. This results in a vehicle design that is more statically unstable with respect to a disturbance in angle of attack than the original. In this context, fins can play two roles. First, fixed fins added to the rear of the vehicle result in a more aft location of the vehicle's

1

aerodynamic center, and thus, a more stable vehicle. Even if the vehicle is statically unstable at certain Mach numbers before the fins are added and the fins are not large enough to produce a statically stable vehicle, the addition of the fins will make an unstable vehicle less unstable and thus easier to control. Second, if the fins can be rotated with respect to the vehicle's body, then aerodynamic torques that are functions of the deflection can be generated for attitude control. To summarize, the prospect of converting the weight savings of the new "LOX aft" design into payload is enough incentive for further investigation of the use of fins.
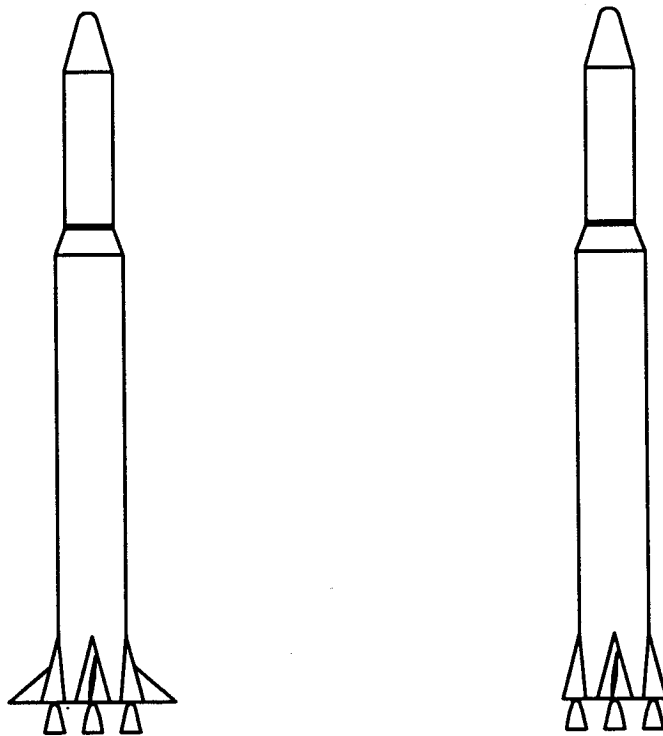
Fig. 1.1 Sketches of an NLS 1.5 Stage vehicle with and without fins.

Regarding the negating effect of the weight of fins, recent advances in composite material technology have resulted in the fabrication of light-weight aerodynamic surfaces for aircraft, missiles and launch vehicles (e.g., Pegasus). Thus, the weight penalty should be minimal.

From the foregoing, it follows that a decision to interchange the LOX and LH tanks must

be based on a complete analysis of the system, including appropriate fins. The purpose of the work reported herein has been to support the performance of such an analysis by Marshall Space Flight Center personnel.

1.2 Report Organization

In the next section, we provide some examples of French, Russian, Chinese, and Japanese launch vehicles that have utilized fins in their designs. Next, the aerodynamic design of the fins is considered in Section 3. Some comments on basic static stability and control theory are followed by a brief description of an aerodynamic characteristics prediction code that was used to estimate the characteristics of a modified NLS 1.5 Stage vehicle. Alternative fin designs are proposed and some estimated aerodynamic characteristics presented and discussed. Also included in Section 3 is a discussion of possible methods of enhancement of the aerodynamic efficiency of fins, such as, vortex generators and jet flaps.

We consider the construction of fins for launch vehicles in Section 4 and offer an assessment of the state-of-the-art in the use of composites for aerodynamic control surfaces on high speed vehicles. We also comment on the use of smart materials for launch vehicle fins.

The dynamic stability and control of a launch vehicle that utilizes both thrust vector control (engine nozzle gimballing) and movable fins is the subject addressed in Section 5. We give a short derivation of equations of motion for a launch vehicle moving in a vertical plane above a spherical earth, discuss the use of a gravity-turn nominal trajectory, and give the form of the period equations linearized about such a nominal. We then consider feedback control of vehicle attitude using both engine gimballing and fin deflection.

Conclusions are stated and recommendations made in Section 6. An appendix contains aerodynamic data in tabular and graphical formats.

# 2. USE OF FINS ON FRENCH, RUSSIAN, CHINESE, AND JAPANESE LAUNCH VEHICLES

2.1 General Comments

Many past launch vehicle configurations have included fins and several still do. In most current vehicles, fins are used only for stability enhancement and not to control the attitude of the vehicle. In the following subsections, we present some information regarding French, Russian, Chinese and Japanese launch vehicles that have fins. The majority of this information was taken from Ref. 1 which is apparently the most complete reference on launch vehicles.

2.2 French Vehicles

We place the Ariane [1] vehicle family under "French" vehicles, because France has provided the largest percentage of the funding for these European launch vehicles. Actually around 50 different countries have contributed to the design and construction of the Ariane vehicles. Ariane 1, 2, and 3, now out of production (see Fig. 2.1), had fins for improvement in the vehicles' aerodynamic stability. Although no information on the size or construction of the 4 fins on each of the first three Ariane vehicles was found, they were probably the same size as those on Ariane 4, i.e., 21 sq. ft. Also, since the construction of Ariane is steel, the material used for the fins was alos most likely steel. Maximum dynamic pressure for these vehicles should be about 835 lb/ft^2.

2.3 Russian Vehicles

Although most of the current Russian launch vehicles do not have aerodynamic fins [1], some earlier vehicles, in particular the Kosmos vehicle (see Fig. 2.1) are exceptions. The out-of-production vehicles, SL-1, SL-2, and SL-5, each had four small triangular fins with areas of approximately 4 sq. ft. The Kosmos, or C-1, is a small launch vehicle with a length of about 105 ft. and a diameter of 7.9 ft. The distance from tip to tip of the fins is 14.4 ft. Their individual areas are around 5 sq. ft. These fins are probably made of an aluminum alloy. The maximum dynamic pressure experienced by the vehicle is unavailable.

Fig. 2.1 French and Russian launch vehicles.

Ariane 44LP
European Space Administration
Fin Area — 21 ft^2

SL-4 Soyuz
Soviet Space Administration
Fin Area — 4 ft^2
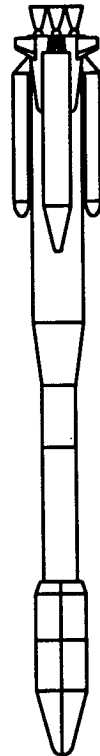
2.4 Chinese Vehicles

Several of the Long March [1] vehicles have fins. Based on sketches of these it appears that three different fin planforms and sizes are used. The Long March CZ-1D (CZ for Chang Zeng) is now out of production. Each of its fins had a trapezoidal planform and an area of about 25 sq.ft. These fins were probably made of a steel alloy. The Long March 2E is shown in Fig. 2.2.

The fins used on the CZ-3 vehicles have tapered planforms with swept leading edges and straight trailing edges. The fins on the CZ-3A and CZ-4 vehicles are also tapered with swept leading edges and straight trailing edges. The area of each of the fins is about 22 sq.ft. The CZ-3 and CZ-4 fins are probably made of an aluminum alloy.

MS-3S-II
Japan
Fin Area — 17 ft^2

Long March 2E
People's Republic of China
Fin Area — 25 ft^2
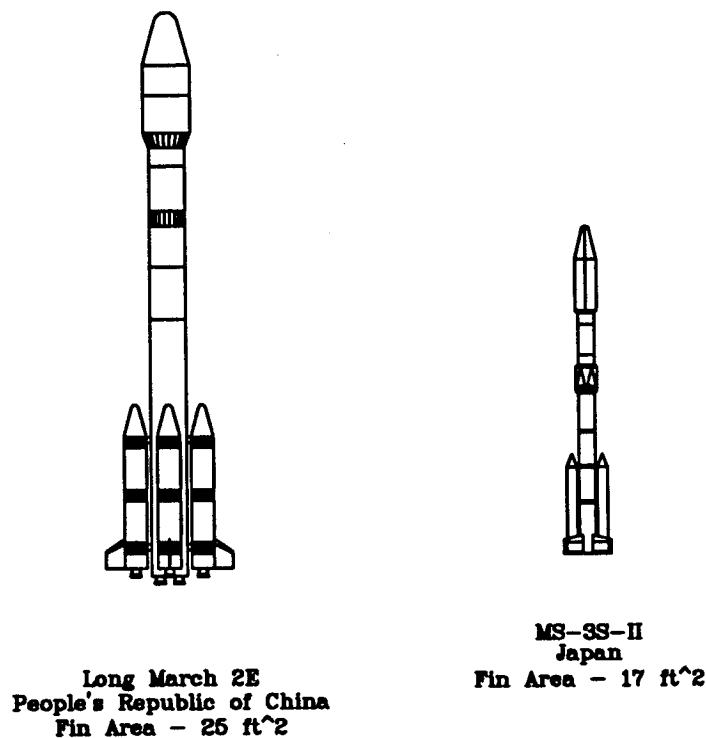
Fig 2.2 Chinese and Japanese launch vehicles.

6

2.5 Japanese Vehicles

The Japanese have two launch vehicle families, the H-vehicles and the M-vehicles [1,2]. The H-vehicles do not have fins. The M-vehicles, built by the Aeronautical and Space Division of Nissan Motor Co., do. The two M-vehicles in current production are the M-3S-II (see Fig. 2.2) and the M-V. Both of these are relatively small, the M-3S-II has a lift-off weight of 136,000 lb while the M-V's launch weight is 287,000 lb. Solid (Rocket) Motors for Roll Control (SMRC) are built into the fins of these vehicles. The fins are tapered, with swept leading edges and straight trailing edges. For the M-V vehicles, "[t]he fins are so designed that they guarantee aerodynamic stability up to Mach 2. Thereafter, the vehicle remains slightly unstable until separation of the first stage from the rest." [Ref. 1, page 95] The fins on the M-V vehicle have an area of about 28 sq.ft., while those on the M-3S-II each have an area of approximately 17 sq. ft. Steel is probably the material used for both types of fins.

More along the line of the modern approaches envisioned by NASA, Ref. 1 gives some possibilities of M-vehicle growth. On page 102, of Ref. 1, a sketch of a winged vehicle similar to Pegasus is shown that has a total wing area of 167 sq. ft. The materials suggested for this Institute of Space & Astronautical Science (ISAS) design are carbon fiber reinforced plastics (CFRP). The ISAS predicts that the wing surface of this vehicle will produce an acceleration of 0.2g at 20° angle of attack.

3. AERODYNAMIC DESIGN OF FINS

3.1 Basic Static Stability and Control

3.1.1 Forces and Moments

Most launch vehicles are intended to fly at zero angle of attack to minimize aerodynamic loads including drag. At the same time, it is desired that the vehicle be reasonably insensitive to winds and that its attitude motion be controllable using thrust vectoring. Thus, conventional launch vehicles are ordinarily not designed to be extremely statically stable and hence become very responsive to variations in angle of attack. On the other hand, it is not desirable that a launch vehicle be extremely unstable with respect to perturbations in angle of attack for the same reasons as stated above, plus the fact that the vehicle will tumble if control is not maintained.

To illustrate the basics of the situation, we use Fig. 3.1, where we show the axial and normal forces and the pitching moments on the body (A_b, N_b, and M_b) and vehicle (A, N, and M), and the normal force (N_f) on the fins of a rigid body model of a launch vehicle. Also, shown is the resultant thrust vector $\underline{F}_T$ which we assume acts in the xz-plane at an angle δ_e with respect to the x-axis. The summations of the aerodynamic and thrust forces acting on the vehicle in the x- and z-directions, respectively, for zero linear acceleration, are

$$\sum F_x = -A_b - A_f + F_T \cos\delta_e \qquad (3\text{-}1)$$

$$\sum F_y = -N_b - N_f + F_T \sin\delta_e \qquad (3\text{-}2)$$
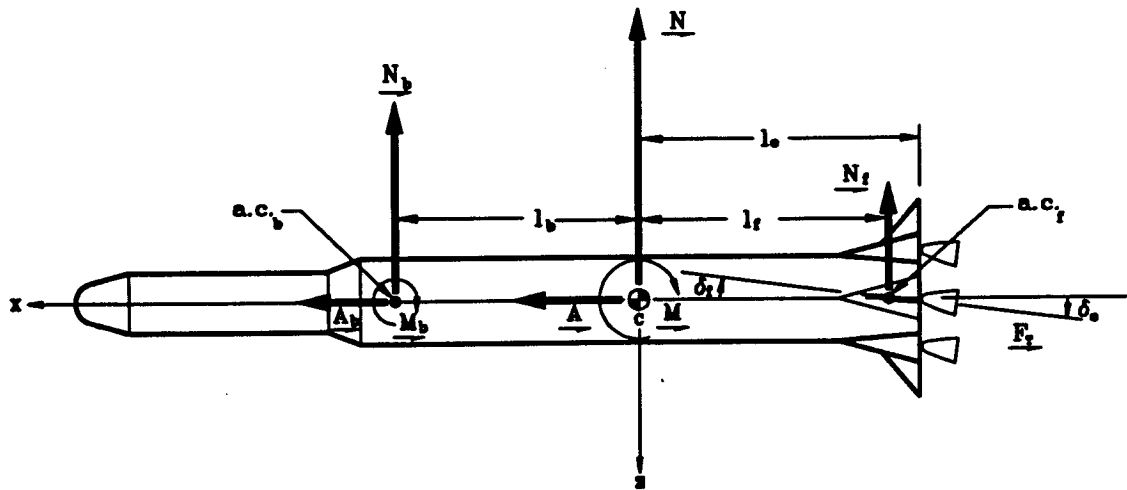
Fig. 3.1 Geometry for static stability and analyses.

Also, for zero angular acceleration, the sum of the moments about the y-axis is

$$\sum M_y = -\ l_b\ N_b\ -\ \ l_f\ N_f\ +l_e\ F_T\ \sin\delta_e \qquad (3\text{-}3)$$

Since the vehicle is axially symmetric, the pitching moment when N_b is zero is also zero.

From the aerodynamic characteristics prediction code (described later in this section), we can obtain the pitching moment coefficients and the normal force coefficients for the body alone and the total vehicle. Therefore, we can find the locations of the aerodynamic centers of the body (a.c.$_b$)

$$l_b\ =M_b/N_b \qquad (3\text{-}4)$$

and the fin (a.c.$_f$)

$$l_f\ =\ -M_f\ /N_f \qquad (3\text{-}5)$$

9

If the position of the center of gravity (c.g.) is referenced to the nose of the vehicle, then the distance l_e can be found from

$$l_e = L - x_{c.g.} \tag{3-6}$$

where L *is* the length of the vehicle and $x_{c.g.}$ is the distance from the vehicle's nose to the c.g. Once we have the distances l_b, l_e, and l_f then we can find the moment about any reference point. We can then find the moment about any center of mass location using Eq. (3-3).

As long as the aerodynamic center of the vehicle is behind the vehicle center of mass, we say the vehicle is statically stable with respect to a disturbance in angle of attack, or "statically stable" for short. If the a.c. and c.m. coincide, we say that the vehicle is "neutrally stable," and if the a.c. is forward of the c.m., we say that the vehicle is "statically unstable." As noted above, we may not want the vehicle to be statically stable. What is always required, however, is that the vehicle be controllable.

For a vehicle with both gimballed engines and movable fins, we can discuss *controllability* by using the ratio of the moment that can be generated by the engines <u>and</u> the fins, to the moment that will be generated by a disturbance in angle of attack. The aerodynamic parts of this ratio are of course related through the dynamic pressure and the angle of attack. Because our vehicle is statically unstable without fins (and probably with them, unless they are very large), we define a controllability ratio R as

$$R = (q_\infty S d \, C_{m_\delta} - F_T \, l_e \, \sin\delta_e)/(q_\infty S d \, C_{m_\alpha}) \tag{3-7}$$

where q_∞ is the dynamic pressure, S is the reference area, and d is the reference length.

10

Since the pitching moment due to the fins is negative if the fin deflection is zero, it follows that R is non-positive for zero fin deflection. For positive fin deflection, R is negative when the gimball angle is positive. The magnitude of R is a measure of controllability. If $|R| > 1$, there is more control torque than disturbance torque. We do not require that the fins make the vehicle statically stable; we only require that they assist the engines in controlling the attitude. Later in this section, after a discussion of the prediction of aerodynamic characteristics and alternative designs, we present some example results for various calculations of R.

3.2 Aerodynamics Characteristics Prediction

When we were tasked to recommend designs for fins for the NLS 1.5 Stage vehicle, we initially thought that numerous computer codes would be available for prediction of characteristics. However, we found only one, MISSILE DATCOM [4], that seems to give good results. We checked the operation of MISSILE DATCOM by using a separate code, AERODSN [5], to predict aerodynamic coefficients for a simple configuration. We also compared some results from MISSILE DATCOM with published test data. Wind tunnel tests would also be helpful in checking the validity of the program. One problem with MISSILE DATCOM is that it cannot (at least as far as we can tell) be used to model a missile design that included shrouding around the engines. Therefore, our model of the NLS 1.5 Stage vehicle does not include shrouds.

3.3 Geometrical Characteristics of the NLS 1.5 Stage

A sketch of the NLS 1.5 Stage vehicle is presented in Fig. 3.2. Some of the vehicle's characteristics are given in Table 3.1; others are given on Fig. 3.2.

All dimensions
in feet.
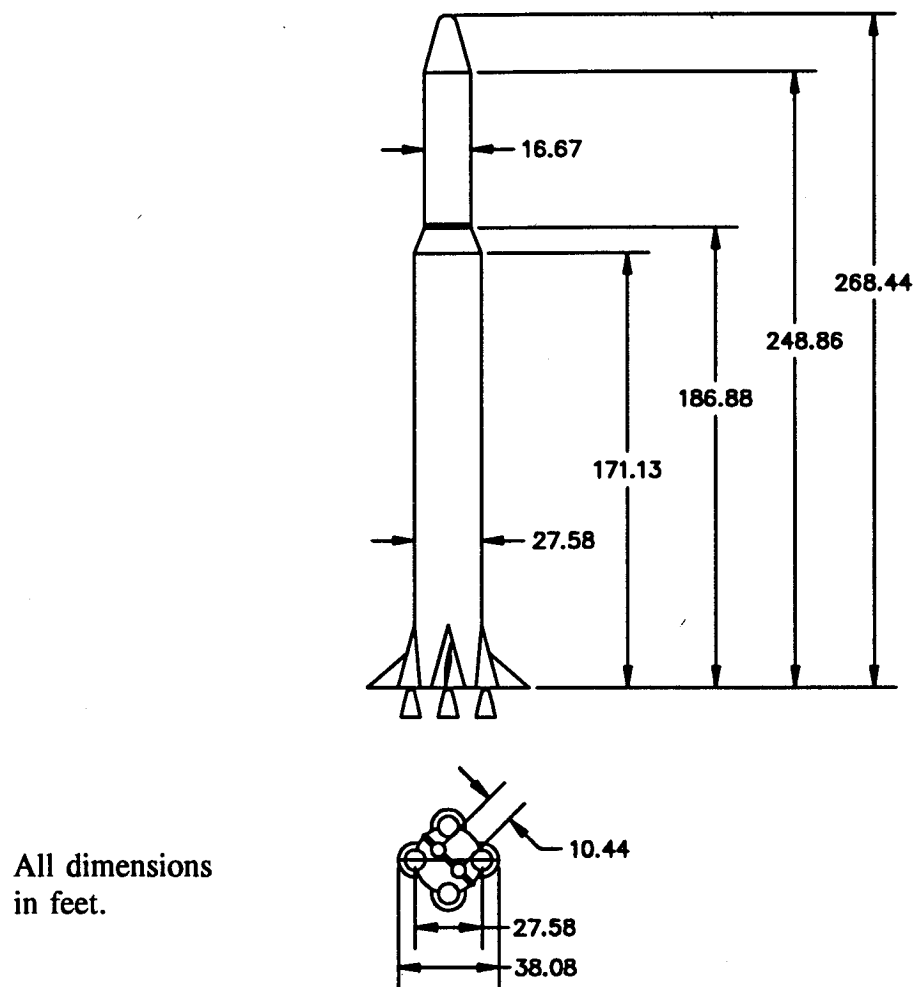
Fig 3.2 Sketch of the NLS 1.5 Stage vehicle.

Table 3.1 Geometrical Characteristics of the NLS 1.5 Stage Vehicle Model.

Length:	268.44 ft	Reference Diameter:	27.4 ft
Reference Area	593.96 ft^2	Moment Center:	256.62 ft

3.4 Estimated Aerodynamics of the NLS 1.5 Stage Vehicle.

Estimated aerodynamics of the NLS 1.5 Stage were calculated using MISSILE DATCOM for the configuration without fins and the vehicle with fins. Initially, we used 100 ft^2 fins and tried a variety of planforms and airfoil sections which are illustrated in Figs. 3.3 and 3.4. A comparison of the data for these 15 fins lead to the selection of a triangular planform and a lenticular, or "arc" cross section. From several computer simulations it was determined that, for a given surface area, a triangular planform results in a greater aft movement of the vehicle aerodynamic center than the others. The arc airfoil section appeared to be better for reducing wave drag.

A moment reference center at 256.62 ft from the vehicle's nose was chosen so that comparisons of the estimated data to data from wind tunnel tests could be made. Normal force coefficients (C_N) versus angle of attack (α_x) for the "body alone" (meaning the vehicle without fins) are shown in Fig. 3.5 for a range of Mach numbers. Corresponding pitching moment coefficients (C_m) are given in Fig. 3.6. Tabulated data is given in the Appendix.

Fig. 3.3 Fin configurations.

14
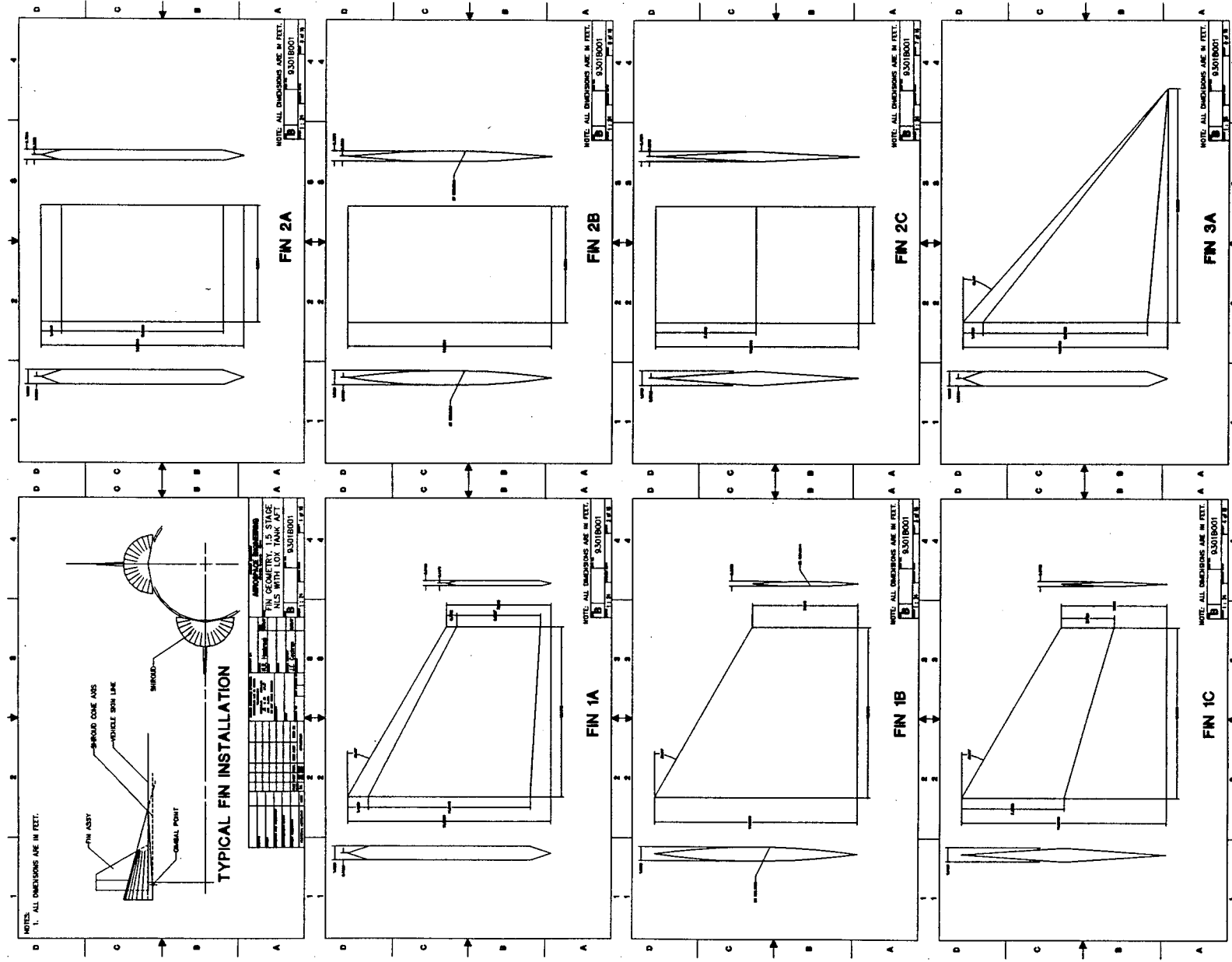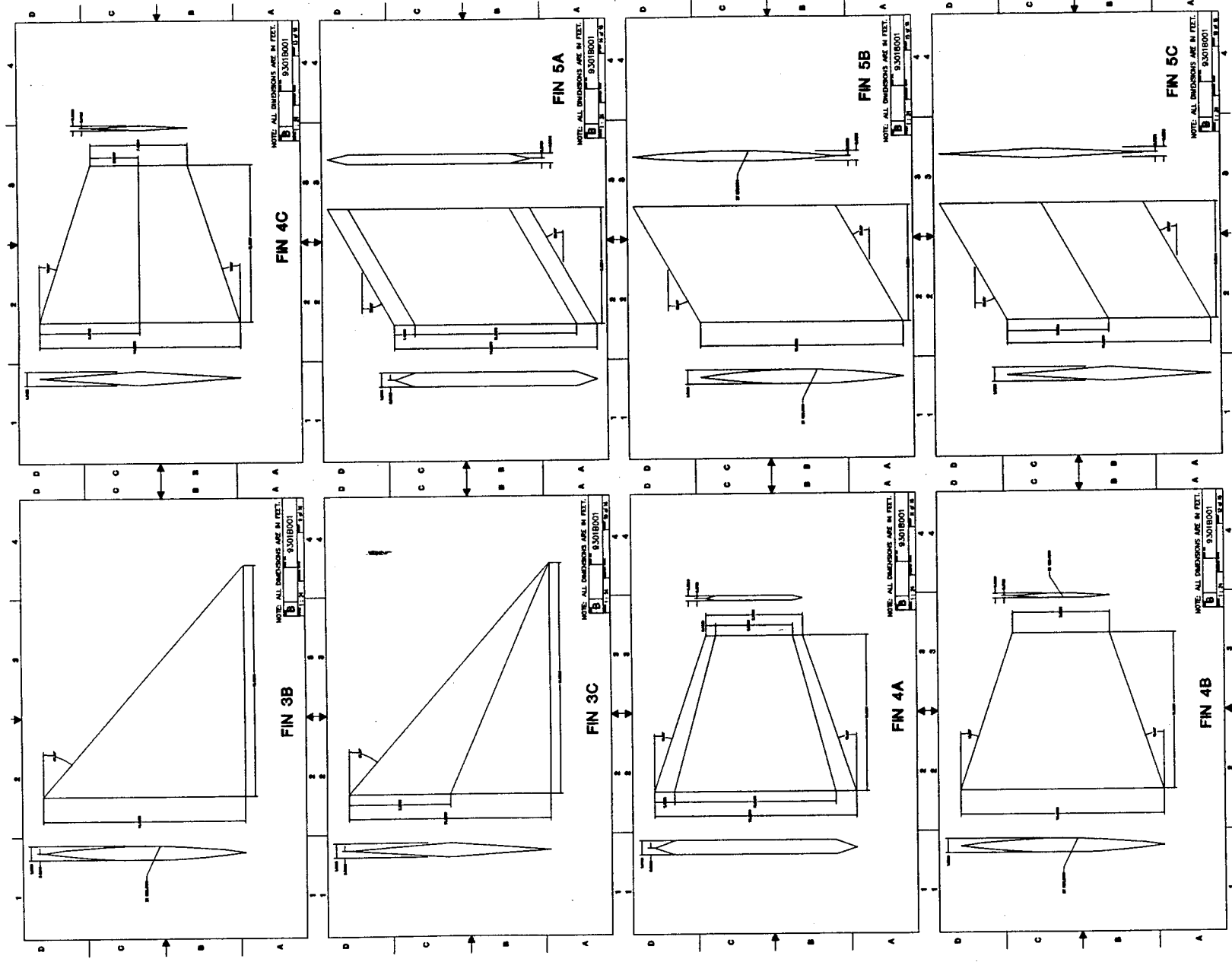
Fig. 3.4 Fin configurations continued.

15
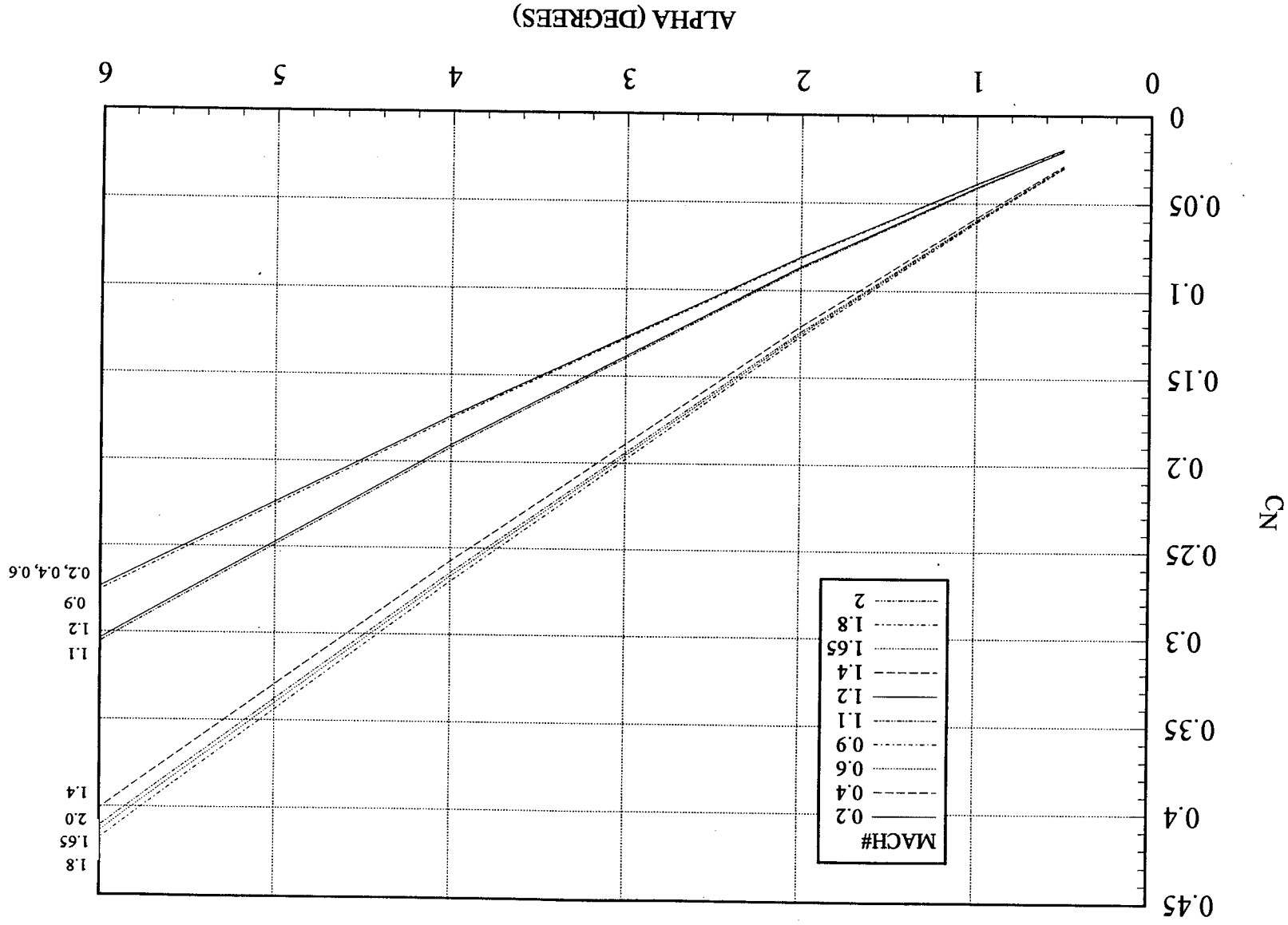
Fig 3.5 Aerodynamic normal force coefficient for the LOX-tank-aft
NLS 1.5 Stage vehicle (body alone, x c.g. = 256.63 ft).

ALPHA (DEGREES)

C_N

MACH#
2
1.8
1.65
1.4
1.2
1.1
0.9
0.6
0.4
0.2
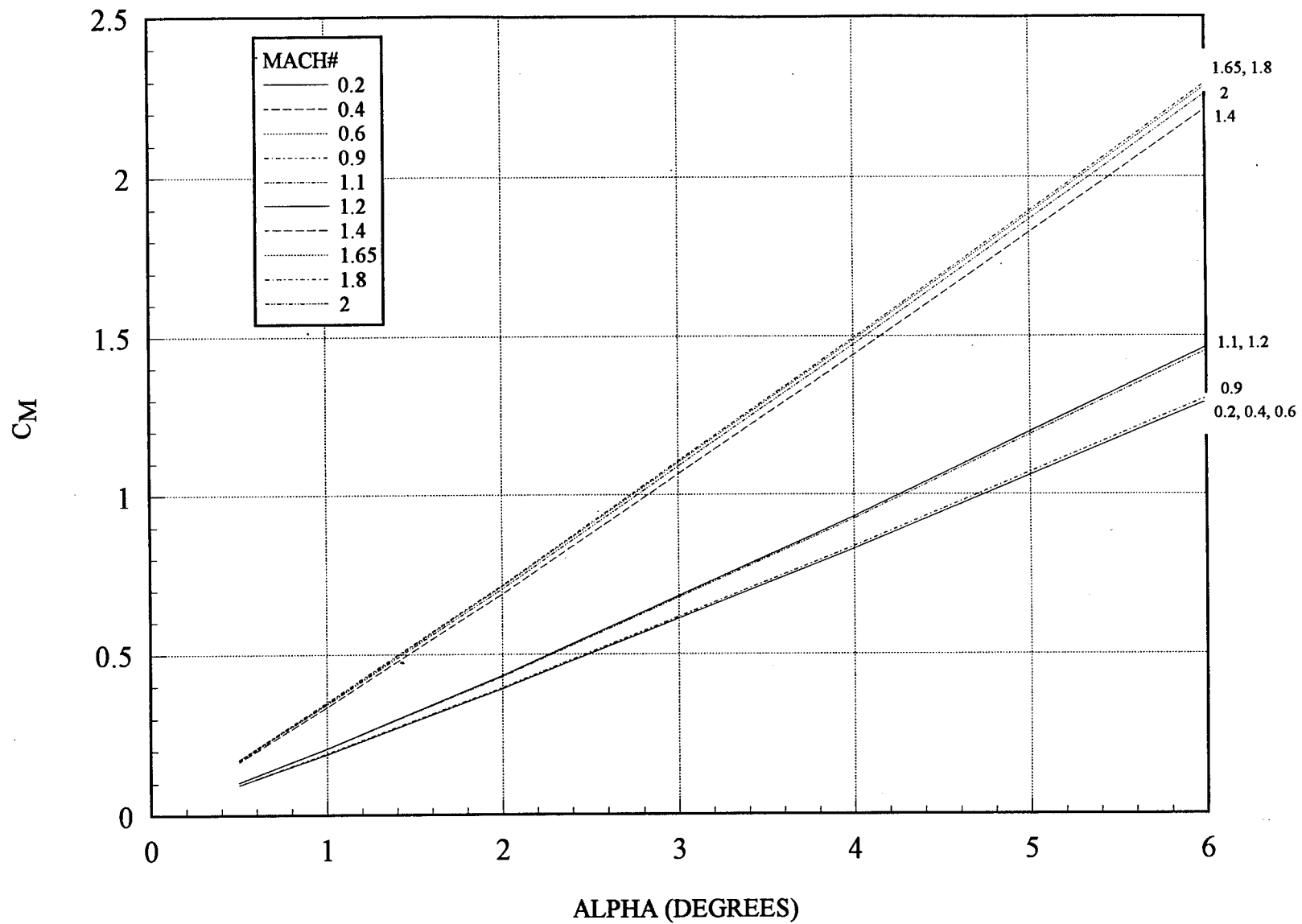
Fig 3.6   Aerodynamic pitching moment coefficients for the LOX-tank-aft
NLS 1.5 Stage vehicle (body alone, $x_{c.g.}$= 256.63 ft).

Note that, for the chosen moment reference, the vehicle is very unstable with respect to angle of attack disturbances. Also, even though the slopes of the C_m versus α_x for more forward reference points are not as steep, we found that, for even the most forward possible c.g. position, the vehicle alone was statically unstable.

Due to the need to limit structural weight, we have considered the effects of adding reduced size fins (50 ft²) on the normal force and pitching moment coefficients. Initially, NASA proposed using fins with a surface area of 100 ft². The results from this portion of our investigation are illustrated in Figs. 3.7 and 3.8. These show C_m as a function of α_x for three different Mach numbers and a range of fin deflection angles. We note that the slopes of the C_m versus α_x curves are reduced by the addition of the fins. Perhaps more importantly, we note that the deflections of the fins result in zero pitching moments for angles of attack less than about 0.1°. This means that, to a limited extent of course, the fins may be used to control the vehicle's attitude. That is, the fins can be used to "trim out" angle of attack perturbations less than about 0.1° if the c.g. were at the moment reference center near the aft end of the vehicle. Actually, the c.g will be much further forward, say at a distance of 212 ft from the vehicle nose. For this reasonable c.g. location, we obtained the control ratio plot shown in Fig. 3.9. THis plot is for a fixed angle of attack of 4°. A relatively simple computer program was provided to NASA that can be used to calculate $|R|$ for parameters of interest.

Note that with no fin deflection, the engine gimball angle to trim ($|R| = 0$) at $\alpha_x = 4°$ is around 4.2°. For a 6° fin deflection, only a 3.8° gimball angle is needed. This is around a 10% decrease in the gimball angle. For more forward c.g. positions the fins help more in two ways: (1) they make the vehicle less unstable and (2) they provide a larger control torque.
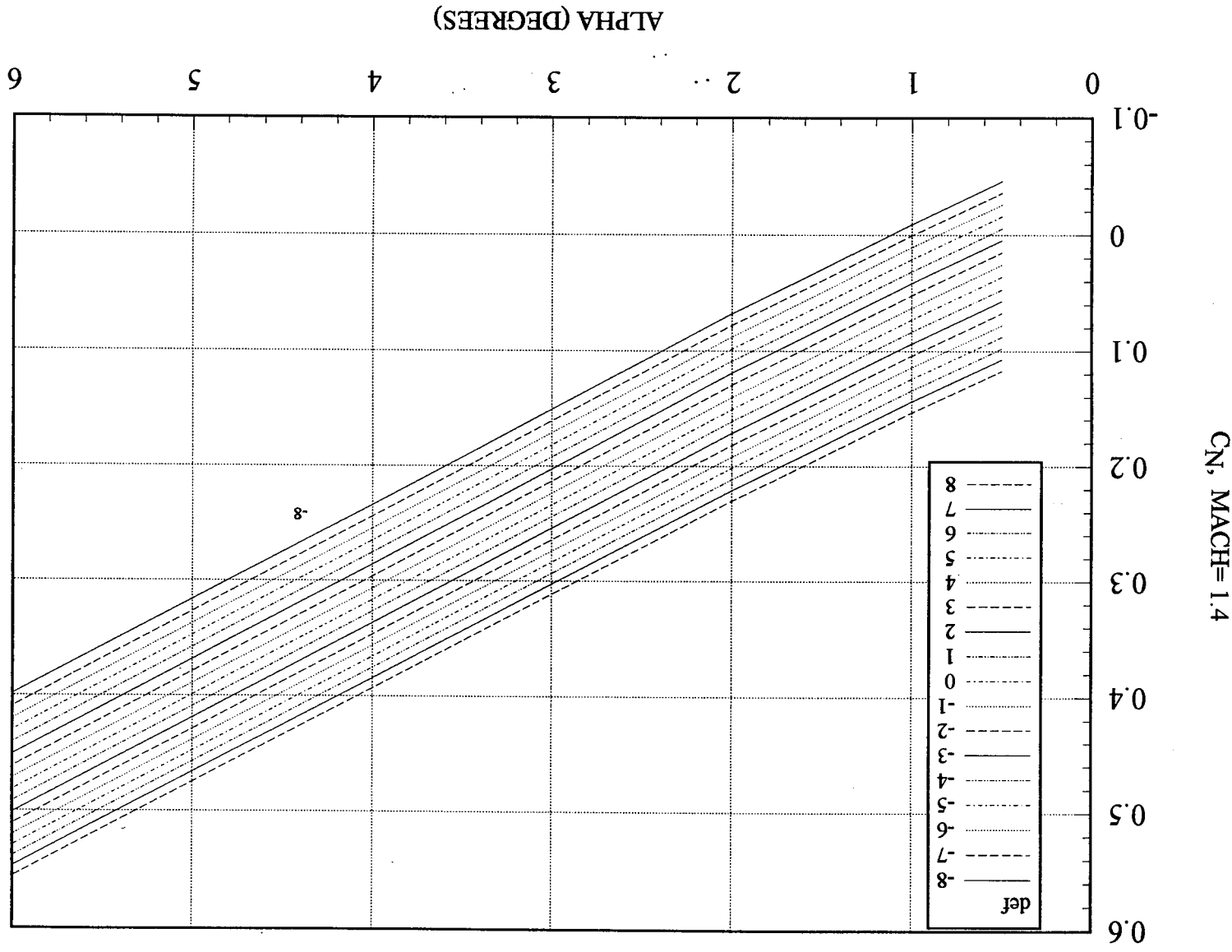
Fig. 3.7 Normal force coefficients for the vehicle with fins (x c.g. = 256.63 ft).
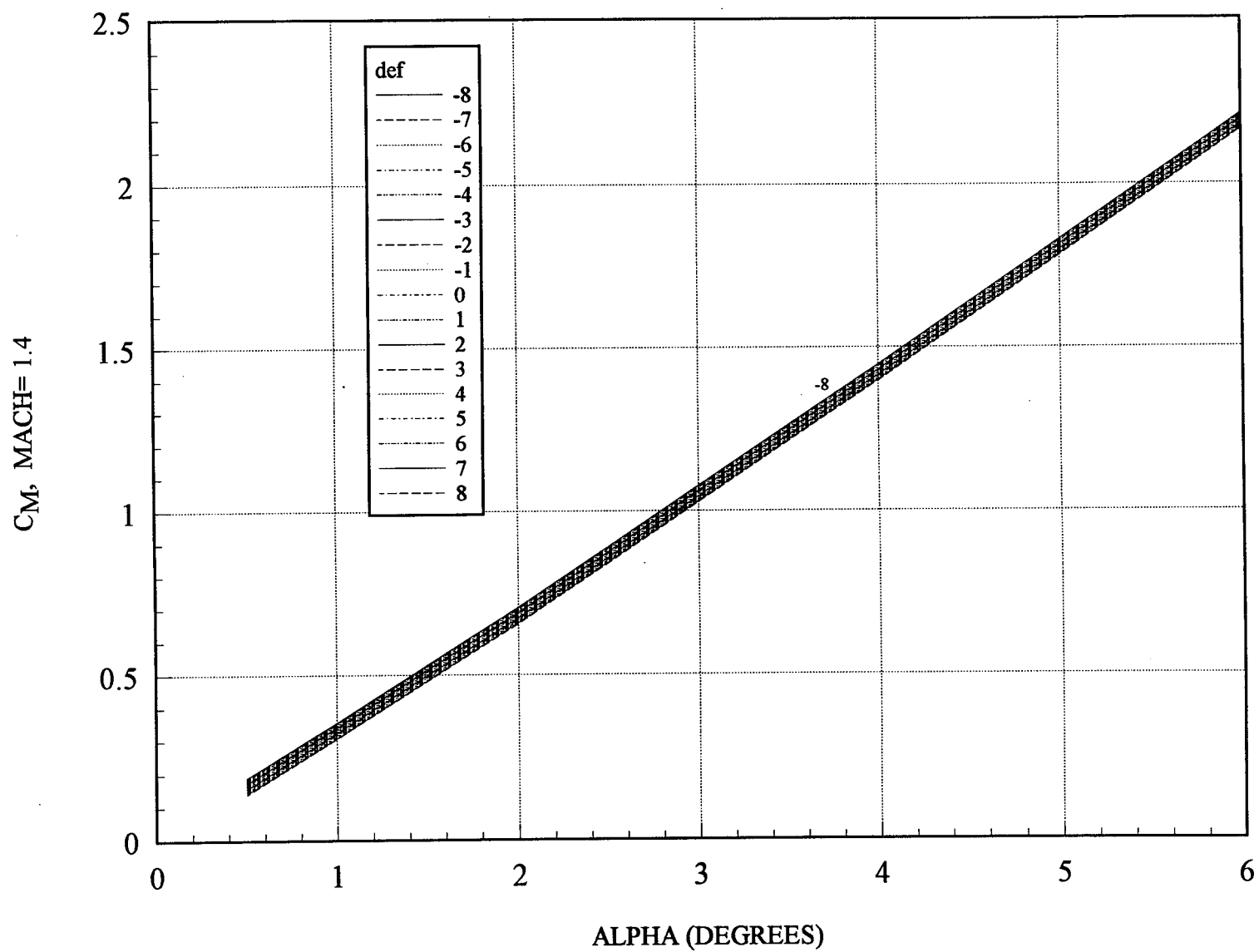
Fig. 3.8   Pitching moment coefficients for vehicle with fins ($x_{c.g.}$= 256.63 ft).
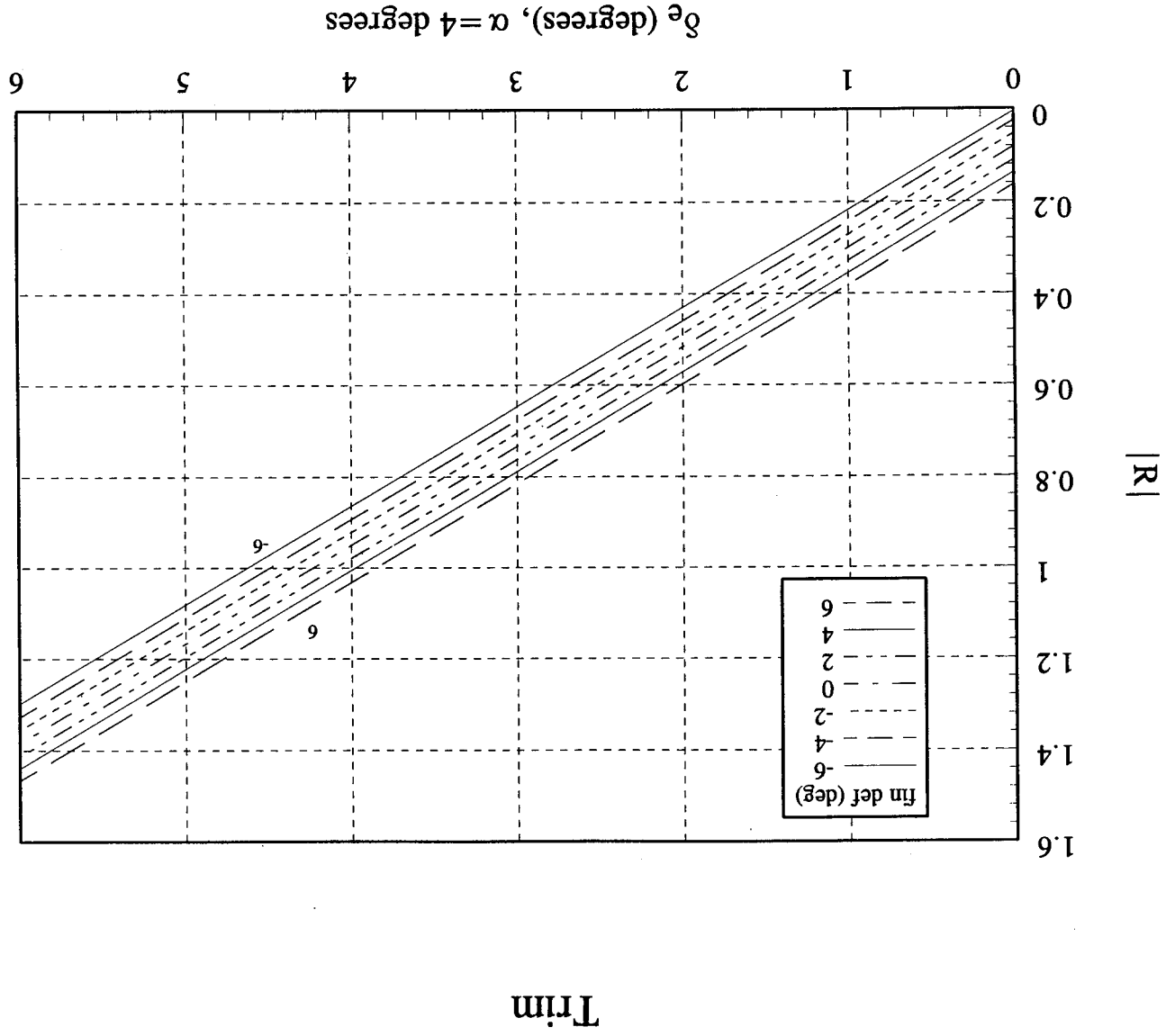
Fig. 3.9 Static control ratio for vehicle with fins (x c.g. = 212.44 ft).

3.5 Vortex Generators

Vortex generators have become widely employed as a method for controlling the boundary layer characteristics. For most purposes, boundary layer control is important in preventing premature separation of the boundary layer and the resulting loss of airfoil effectiveness. This is especially important on control surfaces such as those to be utilized on the NLS.

Several methods have been employed to produce vorticity in the boundary layer. In initial investigations, small obstructions (fins), mounted vertical to the flow surface, were placed upstream of a rapidly thickening boundary layer in a region of pressure rise (See Fig. 3.10) [7]. Such an area commonly occurs on the aft section of an airfoil, just downstream from the center of lift. The fins were placed with angles of attack relative to the flow at the surface creating trailing vortices. When such vortices are shed, the high momentum of the freestream fluid is entrained into the boundary layer which increases its kinetic energy. By energizing the fluid contained in the boundary layer in this manner, the "mixing" mechanism of the boundary layer is enhanced and separation is forestalled. It should be noted that for the NLS application, a turbulent boundary layer is assumed so there is no requirement for "tripping" the boundary layer.

Other methods of energizing the boundary layer include the addition of higher energy flow. Partial removal of boundary layer fluid at the surface will also serve as a method of delaying separation. Both of these methods are much more complex than conventional vortex generators, and their effectivenesses are harder to predict, especially in the supersonic regime. More research into this area is required before such mechanisms could be recommended for an NLS application.
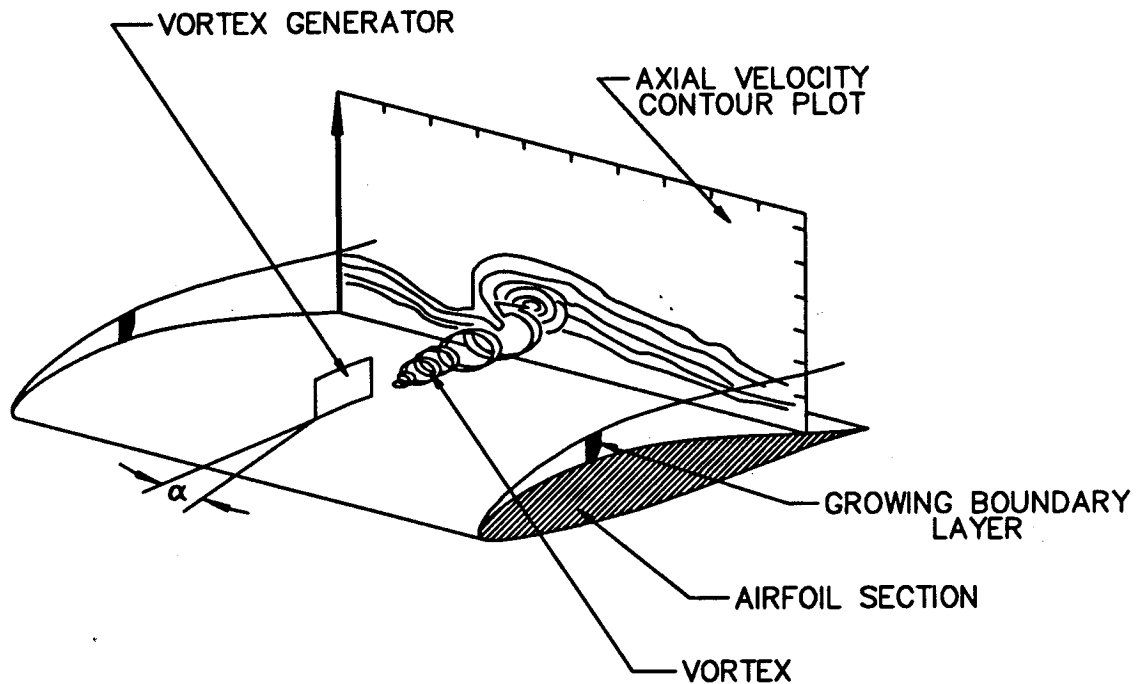
Fig. 3.10 Vortex generator mounted on an airfoil at an angle α
to the freestream velocity vector.

As demonstrated in Fig. 3.11, several different types of obstructions have been developed

which will produce the desired vortex structure. Types of conventional generators include the

constant chord, stepped chord, wedge-type, and "christmas tree" generators. Cylindrical devices

protruding into the flow have also been employed to generate counter-rotating vortices. Other

vortex generation methods include wedges, ramps, scoops, and tapered fins, all with varying

degrees of effectiveness.
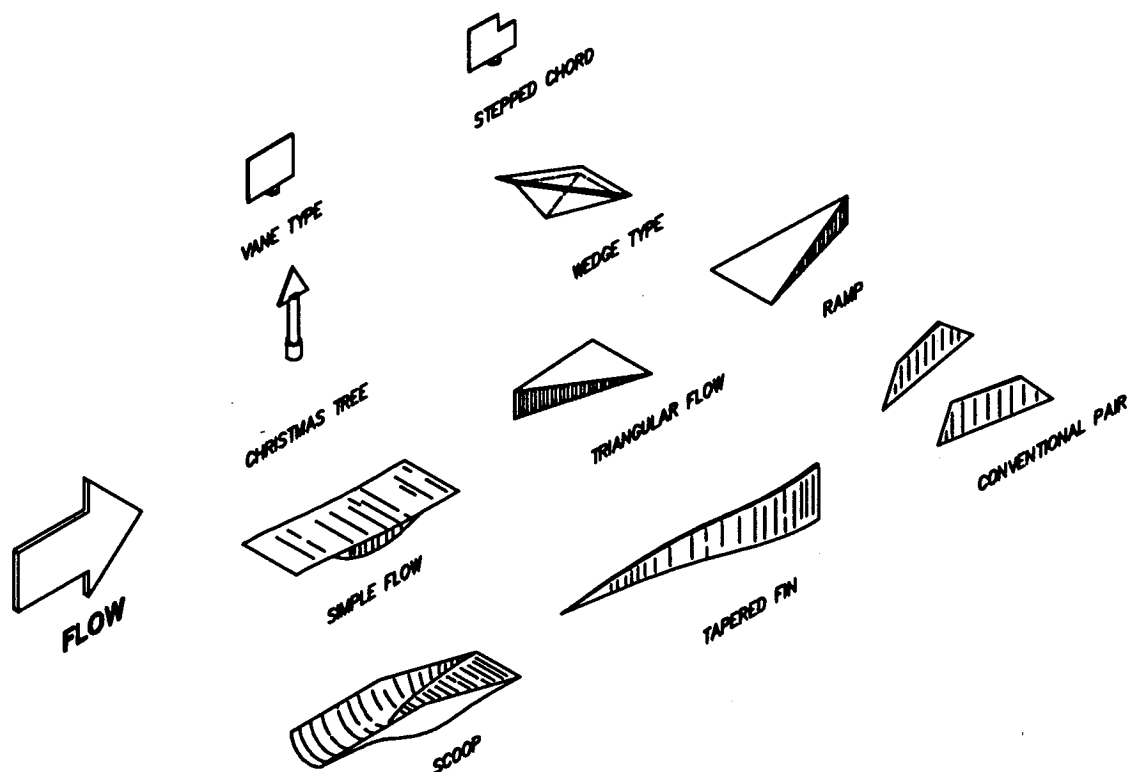
Fig. 3.11 Examples of vortex generating devices.

The actual effectiveness of vortex generating systems in the supersonic flow field that would be encountered on the NLS is yet to be determined. The complexities of the interaction of the vortices and the shock waves require much more research than time permitted within the scope of this investigation; however, a literature research is under way. Conversations with various authors of documents relating to the subject are also being initialized. The use of Auburn University's supersonic wind tunnel facilities is also being considered for a systematic study of various supersonic vortex generating systems if future investigations were warranted.

SECTION 4. FIN CONSTRUCTION

4.1 General Comments

One reason fins are not used on launch vehicles is that they add weight and thus decrease payload. This is especially true if the fins are fabricated of steel or even a light weight alloy. However, advances in the state-of-the-art in composite materials have resulted in the capability for manufacturing very light weight, structurally strong aerodynamic surfaces for aircraft [7] and launch vehicles [1]. Moreover, advances in the field of "smart structures" will foreseeably produce the capability for producing aerodynamic control surfaces that adapt to changing conditions (pressure, temperature, etc.) in such a way that additional damping is produced within the structure and/or its natural frequency is modified.

In this section, we present a review of some of the literature on the use of composite material in high-speed aircraft and launch vehicles and on the use of smart materials.

4.2 Use of Composites in High Speed Aircraft and Launch Vehicles

4.2.1 General Comments.

Primary structures manufactured from composite materials are becoming increasingly common in both commercial and military aerospace vehicles because they provide the designer with the potential to dramatically reduce structural weight and the total manufacturing costs of a structural component compared to an all metallic design. The term "potential" is emphasized here to indicate that composite materials are different from metals and must be treated differently during the design phase if full potential for weight and cost savings is to be realized. Many early aerospace structural designs employing composite materials simply replaced standard

aluminum alloys with the "new" composite materials without really changing the overall design geometry or philosophy. Such designs are referred to as "black aluminum" designs. It is not surprising that such a procedure rarely led to a substantial reduction in the weight or cost. The successful use of composite materials in structural design requires a new design philosophy, one that concentrates on the utilization of the composite material's high strength-to-weight and stiffness-to-weight ratios coupled with the unique ability of these materials to allow for the fabrication of large, complex, low part count structures [8].

During the late 1960's and the 1970's composite materials were used sparingly in aerospace structures and then only on secondary structures. However, since the early 1980's composites have been used to replace metals in several primary aerospace structures [9]. Some of the recent commercial composite structures fall into the category of large aerodynamic control surfaces such as vertical and horizontal stabilizers. In the military and space arena, some recent fighter aircraft (the F-22) and commercial launch vehicles (the Pegasus air-launched vehicle) employ fairly large composite wing designs. As pointed out in Section 2, the Japanese are planning to use composites in the form of Carbon Fiber Reinforced Plastic (CFRP) in an advanced M-Vehicle.

The four designs reviewed in this section were selected as typical of large aerodynamic control surface structures. They are the designs of the Airbus A310, Lockheed L-1011, McDonnell Douglas DC-10 vertical stabilizer and of the delta wing for the first stage of the Pegasus launch vehicle [8,9,10].

4.2.2 Airbus A310 Vertical Stabilizer

Airbus was the first commercial manufacturer to use composite materials for a primary structure in a production aircraft. Between 1980 and 1985, the vertical stabilizer for the A310

aircraft was designed and manufactured out of a carbon/epoxy composite material. This design resulted in significant cost and weight savings, and the elimination of environmental corrosion as a major problem in the component.

Figure 4.1 shows the 27'3" high, 25'7" wide (maximum chord width) composite vertical fin. The use of composite materials resulted in a 22% weight reduction as compared to the original aluminum stabilizer, and a decrease of almost 2000 parts (only 95 parts were required compared to 2076 parts used in the aluminum counterpart). This reduction in complexity, combined with an automated production process, provided a significant reduction in assembly and manufacturing costs.

The assembly process is begun by wrapping the prepreg [a ready-to-mold product consisting of the reinforcement material (carbon fibers) and partially cured matrix material (epoxy resin)]around three-piece aluminum modules that constitute the web of the stringers and the rib shear tie. The prepreg is then pressed onto the mold to form the external skin and the stringer bottom flange. The aluminum modules are then assembled into the mold and unidirectional prepreg tape is laid on the stringer (spanwise) to form the upper flanges. The part is then ready for curing in an autoclave, a closed vessel that applies pressure and heat to cure the part. The pressure is applied to the skin and stringer flanges by the autoclave and to the stringer webs by thermal expansion of the aluminum modules. A large number of similar modules are then set in a fixed grid to form the fin.

4.2.3 Lockheed L-1011 Vertical Fin

The Lockheed Co. selected composites in the design of their L-1011 vertical fin box. The original all-metal fin design was modified to incorporate a large amount of composite material so that the final design was a hybrid of composite and metallic materials. Layers of

(a) Fin skin with integral stiffeners

Section A-A

(b) Schematics

Three-piece aluminum module

Prepreg bandage

Stringer-strips

Module

Fin-box

Skin

Rib-web

Upper-stringerstrip

Lower-stringertip

(c) Module usage
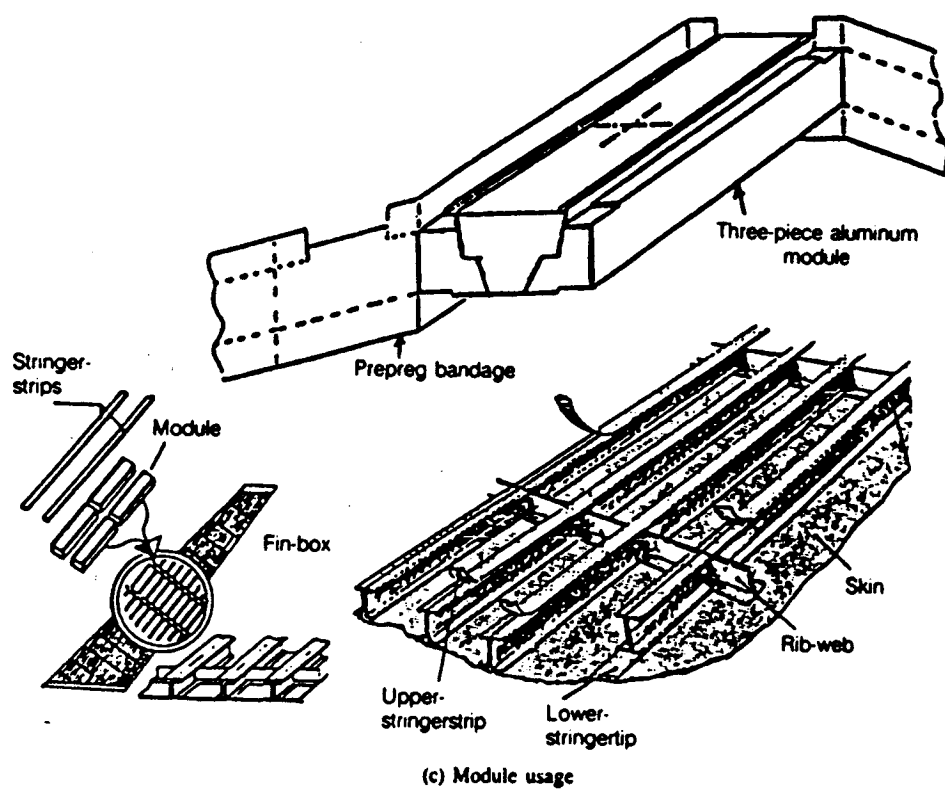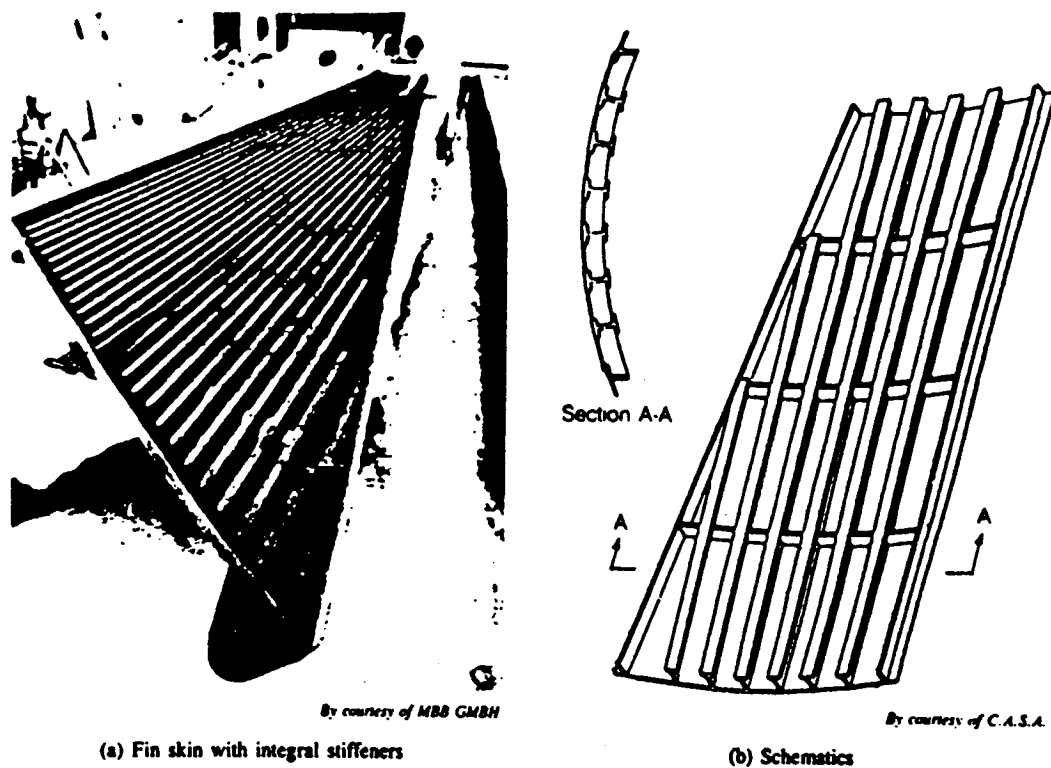
Fig. 4.1 A310 composite vertical stabilizer assembly.

unidirectional prepreg tape were used to form laminates for the skins because this type of design possesses better mechanical properties than aluminum and can be implemented in an automated layup process. This results in a considerable redution in fabricating costs. A tape laying machine is especially effective in significantly lowering the costs of fabrication of flat, single curvature composite parts such as the NLS fins. These machines use pre-impregnated unidirectional tape and are the most attractive form in terms of cost and production properties. By utilizing this method, Lockheed was able to reduce the number of ribs from 17 (all-metal) to 11 (hybrid). The basic structure is illustrated in Fig. 4.2.

The three upper ribs were solid graphite/epoxy laminates with integrally molded caps and bead stiffeners. Integral molding involves laying up and curing parts as a single, complex, continuous structure. This eliminates the need for many mechanical fasteners thereby reducing the overall weight and complexity of the structure. The eight lower ribs combined graphite/epoxy caps with extruded aluminum truss webs. The covers are solid laminates with integral co-cured hat stiffeners, which is lighter than a honeycomb structure. Co-cured parts are those in which laminates are cured and simultaneously bonded to some other prepared surface during the same cycle.

4.2.3 McDonnell Douglas DC-10

McDonnell Douglas used yet another manufacturing method in the DC-10 vertical stabilizer. It is formed from honeycomb sandwich skins and a four-spar and thirteen-rib substructure as shown in Figure 4.3. The skins are graphite/epoxy facesheets over Nomex core, with two plies on the outer surface and one on the inner surface. The spars and ribs are made of graphite fabric/epoxy sine wave webs in most areas.

(ii) Composite

	Aluminum	Composite
Weight (lb)	141	104
No. of ribs	18	10
No. of parts	398	205
No of fasteners	5253	2574

(a) Inboard aileron

	Aluminum	Composite
Weight (lb)	858	623
Assemblies	21	15
Parts	714	229
Fasteners	40800	10150
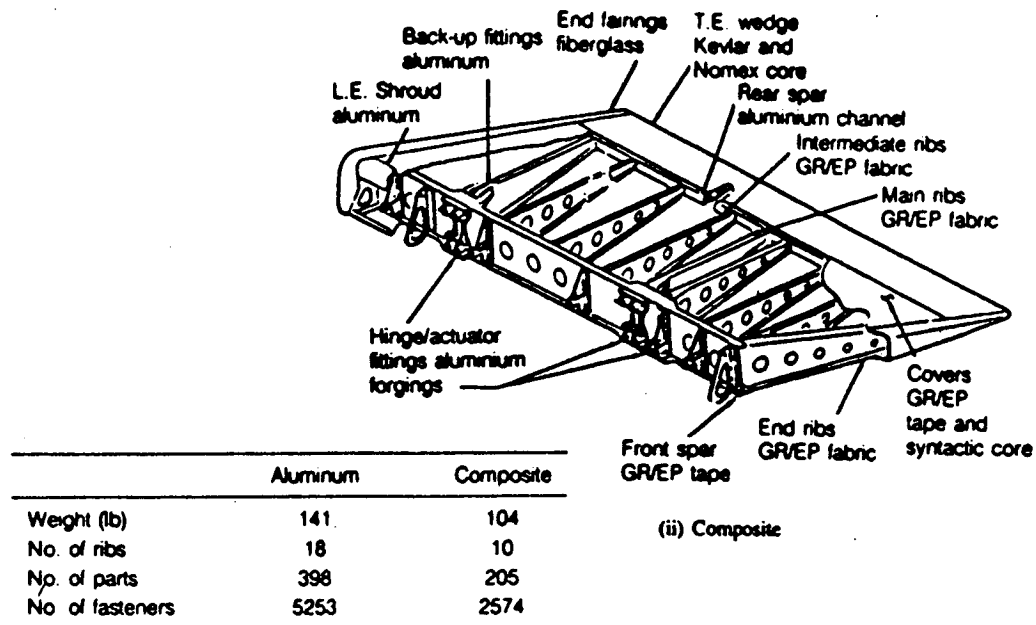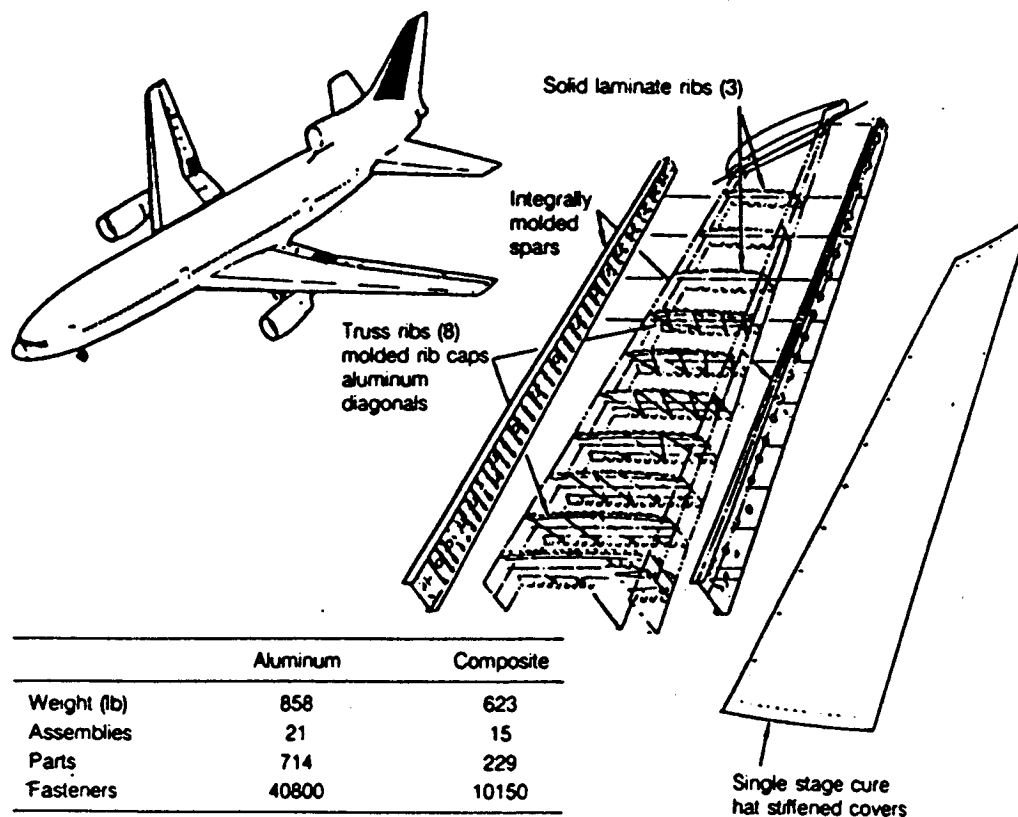
(b) Vertical fin box.

Fig. 4.2 Comparison of composite vertical stabilizer to aluminum counterpart.

Main frames

1.10 m

7.37 m

Antenna

Access panels

6.95 m

2.07 m

(a) Structural arrangement
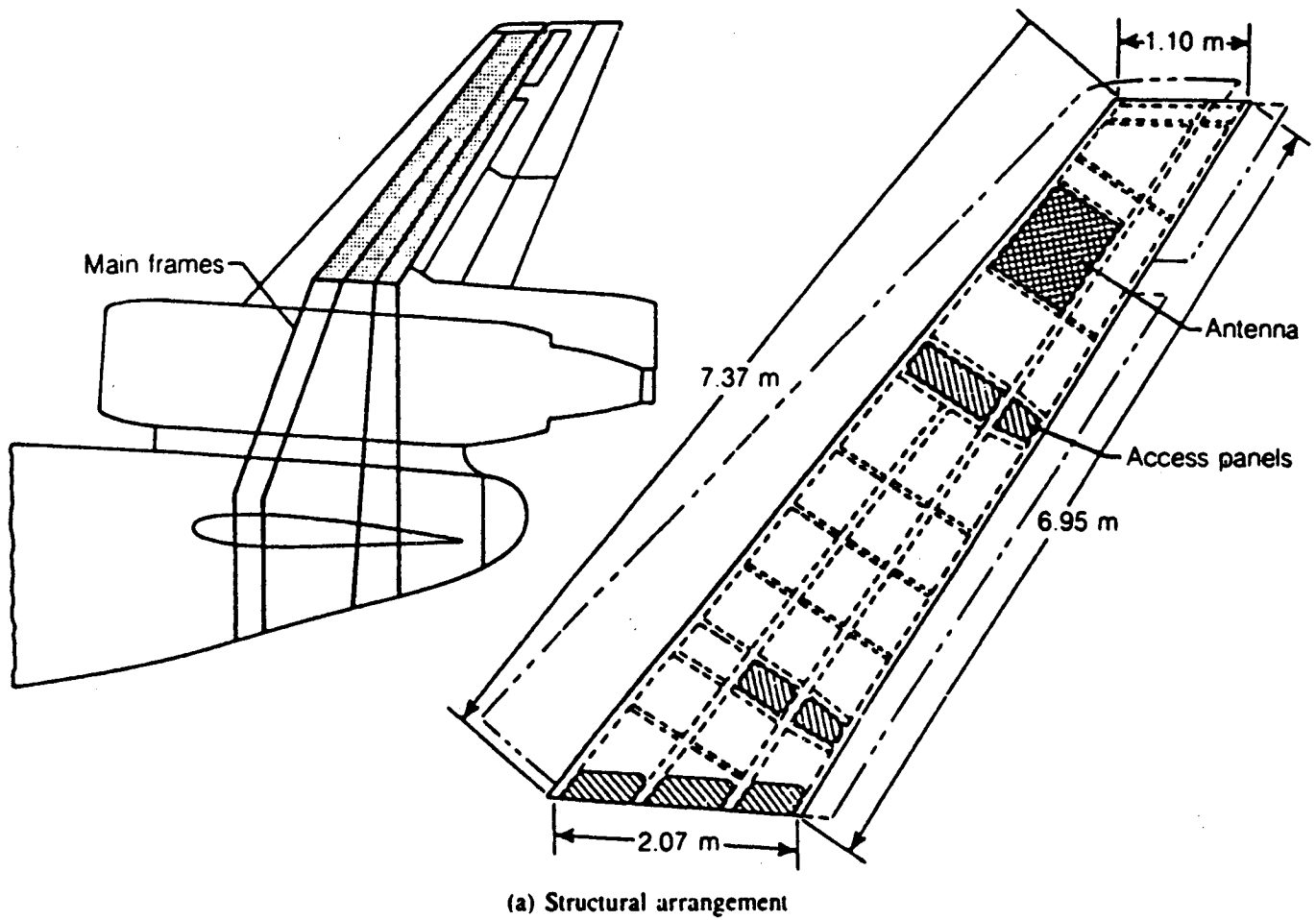
Fig. 4.3 DC-10 composite vertical stabilizer assembly.

4.2.4 Pegasus Wings

Pegasus, the small, air-launched, vehicle produced by Orbital Sciences Corporation, possesses a winged first stage booster. The wing is a one piece delta configuration that is subjected to substantial aerodynamic loading during flight. The wingspan is approximately 13 feet and the maximum chord dimension is approximately 8 feet. Scaled Composites, Inc. designed and constructed the Pegasus wings, which are composed almost entirely of composite materials. In the wing design and construction, the manufacturing flexibility of composite materials was used to produce a lightweight and low part count structure.

4.2.5 Summary

In summary, the design and fabrication of large aerodynamic control surfaces employing composite materials is no longer limited to experimental programs. Commercial production of these large composite structures is well established and they are becoming almost as common as metallic structures in the aerospace industry. Significant weight and cost reductions can be realized as long as the full flexibility of these materials is used to advantage during the design process. Furthermore, the ability to design and fabricate this type of composite structure is no longer limited to the large aerospace contractors. Small and medium size companies have also developed the expertise required to successfully produce various aerospace vehicles component parts including fins, wings, and control surfaces.

4.3 Smart Materials and Structures

4.3.1 General Comments

Smart materials and smart structures are new concepts in materials and structural design. The smart materials concept involves the development of materials that respond in predictable ways to stimuli such heat and electrical current. Smart structures are systems composed of smart materials that have been integrated into the microstructure of the system. The end result is expected to reduce the structure's size and decrease the energy expenditure required to foster adaptive functionality [11]. For example, the integration of actuators, sensors, and controls within a material or structural component creates a smart structure. Craig A. Rogers, from the Center of Intelligent Materials Systems and Structures at Virginia Polytechnic Institute and State University, suggests the following analogies of smart structural system components and various human body systems: actuators, or motors, behave like muscles; sensors have the architecture and processing features similar to the nervous system and memory; and communication and computational networks represent the motor control system and are analogous to the brain [8].

4.3.2 Applications of Smart Structures

Since smart structures are capable of sensing their surroundings and adapting to them, they offer many applications in the aerospace industry. For example, beam-like structures, such as wings and propeller blades, can be designed utilizing smart structure technology to actively damp vibrations. Wings, propellers, and helicopter blades can be shape-controlled, thus eliminating the need for flaps or ailerons as a means for attitude control. Loads can be redirected within a structural element through active strain resistance, thus extending fatigue life. An added benefit would be that strains within a structure could be monitored and recorded. The advantages of such applications are numerous:

- Lighter, smaller vibration control of structures.

- Increased fatigue resistance.

- Increased efficiency, maneuverability, and speed of aircraft wings and propellers.

- Monitoring of a structures "health" status.

- Ability of wings/structures to adapt to changing temperature, speed, and weight.

4.3.3 Key Technologies

Additional advancement of smart structural systems technology depends upon research in a vast array of subjects including composite materials, controls, fiber-optics, metal alloys, microelectronics, and many others. The critical areas of smart structures deal with the development of actuators, sensors and control methods. The latest in each of these fields is detailed below.

<u>Actuator Materials</u>

- Shape Memory Alloys (SMA's):

Shape Memory Alloys retain the ability to reverse strains that have been induced. The heating of SMA's above their phase transformation temperature causes these strains to be recovered. An electric resistive heater is normally employed to heat the structure. Constraining the resulting strain reversal allows large forces to be generated. Nickel-Titanium alloys that have been developed allow strains of up to 8% to be reversed [12]. Copper-based alloys allow up to 4% of strain reversed [11]. Copper-based alloys allow up to 4% of strain reversal [8], at one-tenth the cost of Nickel-Titanium. However, shape memory alloys are typically characterized by slow response times as compared to some of the other actuating materials.

- Shape Memory Alloy Hybrid Composites:

SMA hybrid composite materials contain SMA fibers or films that can be stiffened or

controlled by heat. Two techniques have been developed using SMA hybrid composites [12]. "Active Property Tuning" allows for the tuning or modifying the model response of a structure by heating the SMA fibers embedded in the composite. In the application of another technique, termed "Active Strain Energy Tuning," SMA fibers are placed in a structure in such a way that there are no resulting deflections when activated. Instead, the structure is placed in a residual state of strain. The resulting stored strain energy changes the model response of the structure [13].

Hybrid composite materials developed at Virginia Polytechnic Institute and State University employ Nitinol (Nickel Titanium alloy, patented at the Naval Ordnance Laboratory) fibers embedded in a graphite epoxy prepreg. These hybrid composites were used to test a variety of applications including natural frequency testing, acoustic control testing, and transient vibration control testing [15]. The results of each of these tests will be discussed below.

For all of the test procedures, the Nitinol fibers were induced with a 5% strain prior to being embedded in the graphite epoxy matrix. Because the maximum service temperature of the graphite epoxy is 300° F, the composite material was tested from room temperature up to 300°F. For the natural frequency tests, a nitinol hybrid composite beam was heated, and the natural frequencies for the first three modes of the beam were monitored. Fig. 4.4 illustrates the increase of the natural frequencies as temperature increased.
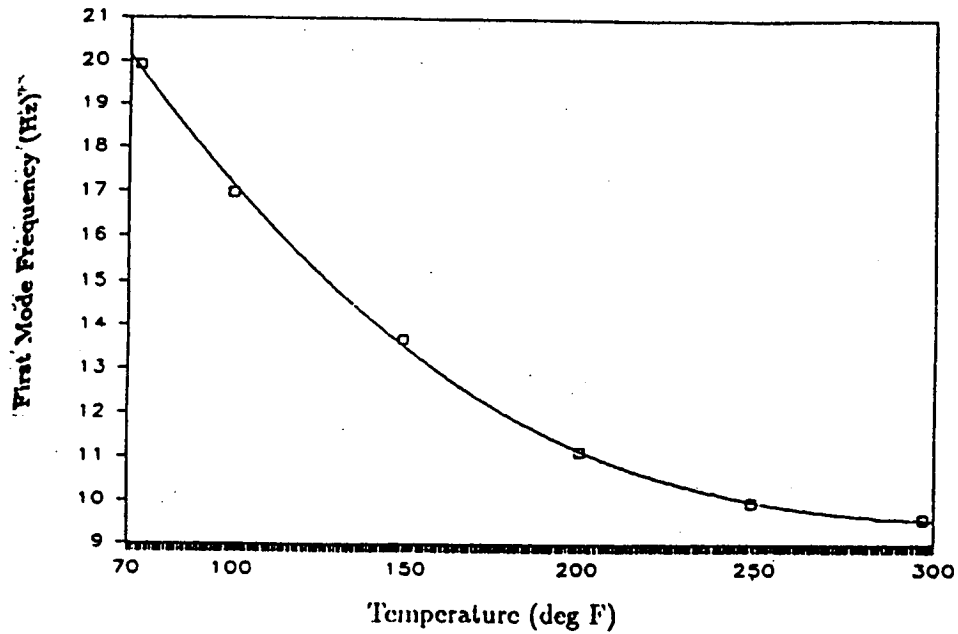
Fig. 4.4 Natural frequency versus temperature.

For acoustic control testing of the hybrid composite material, sound radiation of a vibrating beam was actively controlled by shifting the beam resonances away from harmonic disturbance frequencies. A closed-loop control system sensed input from a microphone to adjust the beam natural frequencies in order to damp out disturbances. Fig. 4.5 shows the time history of the damping of a 35 Hz disturbance frequency. This control system was used to minimize disturbance frequencies up to 324 Hz.
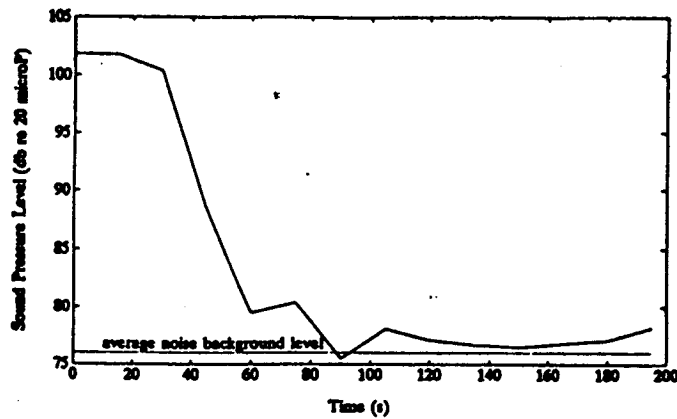
Fig. 4.5 Harmonic disturbance damping.

Another study was performed at Virginia Tech to determine the control power, authority, and frequency response for an actuator design used to control beam vibrations. In this application, the nitinol fibers were actively heated via electrical resistivity and then cooled either actively or passively. Fig. 4.6 shows the free vibration time history as well as the closed-loop control response of the first bending mode of a cantilever beam.
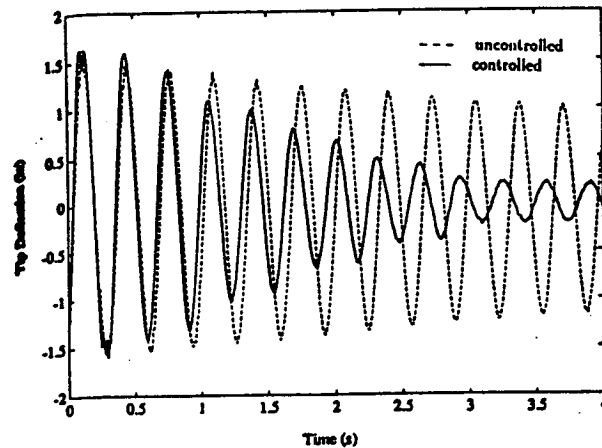
Fig. 4.6 Controlled versus uncontrolled vibration.

- Shape Memory Polymers:

Shape memory polymers are materials capable of large, reversible changes in elastic modulus across the glass transition temperature. With shape memory polymers, an increase in temperature allows the material to become more flexible [11].

- Electrorheological (ER) fluids:

ER fluids are materials that maintain the ability to alter their flow characteristics [15]. This is done by the introduction of an electric field. ER fluids consist of particles dispersed in a carrier fluid, and their response to an electric field is a progressive gelling proportional to the electric field strength. The fluid is free-flowing with no field present, but stiffens as field strength increases. ER fluids are noted for fast response times on the order of milliseconds .

37

- Piezoelectric and Magnetostrictive actuators:

Piezoelectric materials are capable of exerting mechanical forces in response to an applied voltage. This occurs as the materials change shape when their electrical dipoles spontaneously align in electric fields, causing deformation of the crystalline structure. Constraining these small deformations generates large mechanical forces proportional to the applied voltages [11]. Magnetostrictive actuators act similar to piezoelectrics, but respond to magnetic rather than electric fields [11].

4.3.5 Sensors

- Optical fibers:

Optical fibers can be used extrinsically, or intrinsically, in sensing applications of smart structures. Extrinsic use implies that a the fiber-optic doesn't act as a sensor, but merely transmits light. When the light path is broken, position changes can be detected. Intrinsic optical fiber sensing relies on changes in light transmission characteristics. NASA Langley has been researching such technology since 1979 [11].

There are numerous advantages to using fiber-optics as sensors:

immunity to electrical and magnetic disturbances.

high transmission rates.

unidirectional signal if desired.

simple signal multiplexing by a variety of means.

- Piezoelectric materials:

Piezoelectric ceramics and polymers can be used as smart structure sensors because they produce a measurable electric charge when subjected to mechanical stresses. Polymers can be formed into thin films and bonded to many surfaces. Ceramics, however, are of more limited

use due to their brittleness.

4.3.5 Processing and Controls

Adaptive controls and neural networks are currently under development to allow the capability to process information and control smart structural systems.

4.3.6 Current Progress.

Several smart structural systems are under development throughout the United States [13]. Numerous research efforts exist to develop shape memory alloy and SMA hybrid composite applications. At Martin-Marietta Space Systems in Denver, a vibration damping system for the Space Shuttle antenna mast has been developed using shape memory alloys. At Catholic University of America in Washington, D.C., SMA hybrid composites are being used to alter the shape of helicopter blades. At Georgia Tech, SMA hybrid composites are used for a different application involving helicopter blades where stiffening fibers are activated to damp vibrations when detected. Researchers at Virginia Tech in Blacksburg have designed a SMA composite beam that is capable of contracting to heal cracks. At Michigan State, researchers are currently developing a prototype helicopter main rotor blade that damps vibrations using electrorheological fluids embedded within the structure [14].

Several research efforts are underway concerning piezoelectric actuators and sensors. At the University of Maryland, piezoelectric sensors and actuators embedded in a helicopter blade serve to combat vibrations [15]. Similar applications are also being researched at Georgia Tech [12]. At MIT, piezoelectric ceramic material serves as an actuator in a helicopter blade system with a flap that rises and falls to compensate for changes in lift [15]. Innovative Dynamics has designed a wing de-icing system using piezoelectric film to sense changes in with vibration signature resulting from ice buildup [14]. Finally, at Grumman Aircraft in Bethpage,

N. Y., a smart hydraulics system using Terfenol-D, a magnetostrictive alloy, is being developed for the control of aircraft flight surfaces. The alloy is being used to change the shape of the wings in-flight in order to maximize efficiency [14].

4.3.6 Summary

The concept of a smart structural system has numerous applications to the aerospace industry. Advantages include improved efficiency, structural adaptability, as well as health monitoring of structural systems. The technology behind this concept has been tested and developed for a number of applications by a variety of researchers, and work continues in the exploration of this field. The use of smart materials in the construction of fins for advanced launch vehicles appears to be a good idea.

5. DYNAMIC STABILITY AND CONTROL

5.1 Introduction

One of the tasks set for completion during this project was to perform a "rigid body dynamic stability analysis" of the LOX-Tank-Aft NLS 1.5 Stage vehicle with fins. This section contains a description of the model used as a basis for the required analysis and some typical results based on estimated aerodynamic characteristics. Exhaustive studies of stability and controllability were not undertaken due to the lack of test data and the limited scope of this effort.

5.2 System Model

5.2.1 Assumptions

The stability analysis of the motion of the LOX-Tank-Aft NLS 1.5 Stage vehicle with fins is based primarily on the following assumptions:

1. The earth can be modeled as spherical with an inverse-square gravity field.

2. The rotation of the earth may be neglected.

3. The launch vehicle is a structurally rigid body, but its mass and moments of inertia are time-varying.

4. The motion of the launch vehicle to be considered is restricted to a fixed vertical plane so that the vehicle has three degrees of freedom, two in translation and one (pitch) in rotation.

5. The deflection of the fins and/or the gimbaling of engines do not affect the motion except through the changes in external forces and moments (The thrust is treated as an external force.).

6. The motion of the vehicle for which stability is to be investigated is a typical gravity-turn launch trajectory.

7. Stability of the motion can be determined by considering the stability at various points along the trajectory.

41

8. Since the vehicle is statically unstable, active control using the engines and/or aerodynamic surfaces is assumed.

5.2.2 Model and Equations of Motion

The model we have adopted is depicted in Fig. 5.1. The spherical earth has center E and radius R_E. The position of the center of mass of the vehicle is located using the radial distance R and the "latitude" λ. The attitude of the vehicle is defined by the pitch angle θ (measured with respect to the local vertical) and the angle λ. The vehicle pitch rate Q is

$$Q = \dot{\theta} + \dot{\lambda} \qquad (5\text{-}1)$$

and, since $\underline{R} = R\underline{i}_v$, where $\underline{i}_v$ is one of the triad of unit vectors attached to the local vertical coordinate system, the velocity of the center of mass of the vehicle is

$$\underline{V} = \underline{\dot{R}} = \dot{R}\,\underline{i}_v - R\,\dot{\lambda}\underline{k}_v \qquad (5\text{-}2)$$

Also, we may write the velocity as

$$\underline{V} = V\underline{i}_w \qquad (5\text{-}3)$$

where V is the speed and $\underline{i}_w$ is one of the triad of unit vectors attached to the "wind," or velocity, coordinate system $Cx_w\,y_w z_w$. From the geometry of Fig. 1, we also have

$$\underline{V} = V \cos \gamma \underline{i}_v - V \sin \gamma \underline{k}_v \qquad (5\text{-}4)$$

42
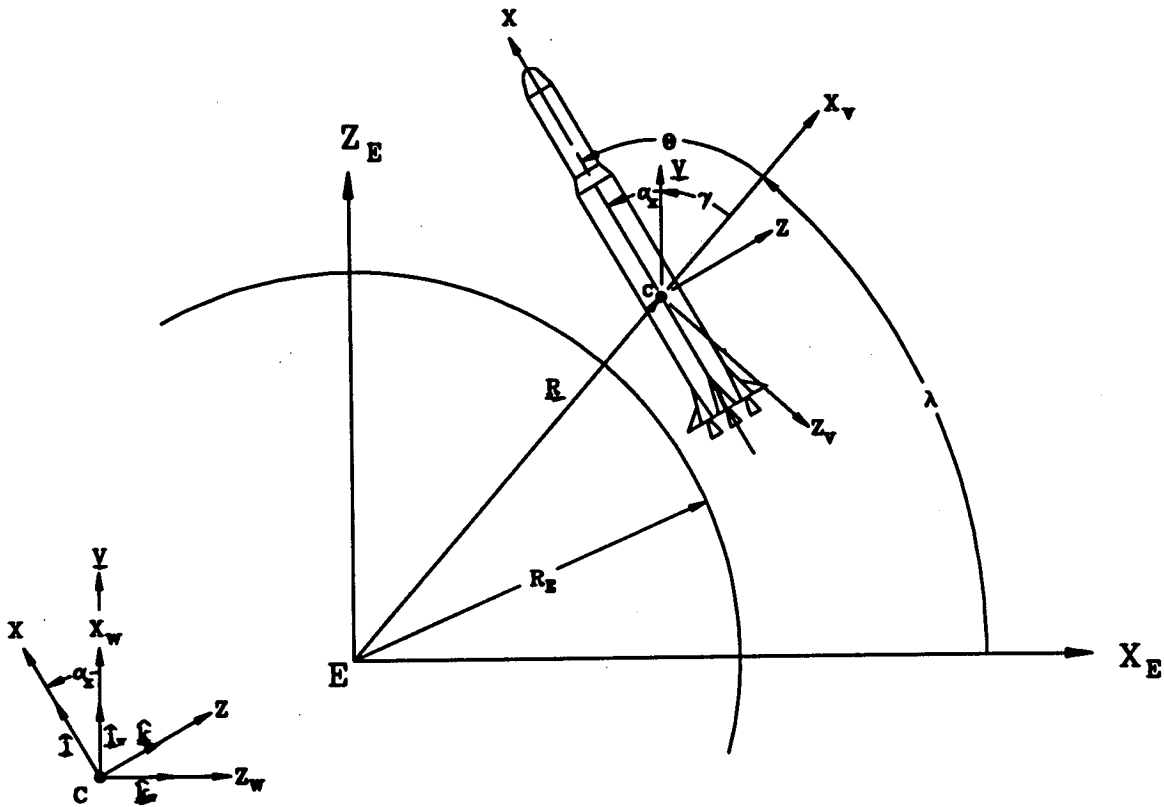
Fig. 5.1 Vehicle model and notation.

It follows from Eqs. (5-2) and (5-4) that

$$\dot{R} = V \cos \gamma \qquad (5\text{-}5)$$

and

$$\dot{\lambda} = (V \sin\gamma)/R \qquad (5\text{-}6)$$

Now, the angular velocity of the launch vehicle may be written as

$$\underline{\omega} = Q\hat{\underline{i}} \tag{5-7}$$

where $\hat{\underline{i}}$ is one of the triad of unit vectors attached to the Cxyz body-fixed coordinate system that is fixed in the launch vehicle with its x-axis along the longitudinal axis of the vehicle. Thus, from Eqs. (5-1), (5-6), and (5-7), we have

$$\dot{\theta} = Q - (V \sin \gamma)/R \tag{5-8}$$

Equations (5-5), (5-6) and (5-8) are the required kinematic equations.

We can apply Newton's second law of motion and treat the thrust force $\underline{F}_T$ as an external force, to write the translational equation of motion as

$$m\dot{\underline{V}} = m\underline{g} + \underline{F}_A + \underline{F}_T \tag{5-9}$$

where $\underline{g} = -g_E(R_E/R)^2 \hat{\underline{i}}_v$, g_E is the value of the gravitational acceleration at

$R = R_E$, and

$$\underline{F}_A = X \hat{\underline{i}} + Z \hat{\underline{k}} \tag{5-10}$$

or

$$\underline{F}_A = -D \hat{\underline{i}}_w - L \hat{\underline{k}}_w \tag{5-11}$$

In Eq. (5-11), D is the drag, L is the lift, and X and Z are related to D and L through the equations,

$$X = - D \cos\alpha + L \sin\alpha \qquad (5\text{-}12)$$

and

$$Z = - D \sin\alpha - L \cos\alpha \qquad (5\text{-}13)$$

where α is the angle of attack of the longitudinal axis of the vehicle. Note that only when there is no ambient wind $\alpha_x = \alpha$ (i.e. α_x is caused by the motion of the vehicle only).

The thrust may be written as

$$\underline{F}_T = (F_T \cos\delta_e) \, \hat{\underline{i}} - (F_T \sin\delta_e) \, \hat{\underline{k}} \qquad (5\text{-}14)$$

where δ_e is the gimbal angle. Note that even through the launch vehicle has six engines that can be individually gimballed, we assume here that all are gimbaled the same amount, in the same direction, to control pitching motion. This assumption may easily be removed by changing F_T in Eq. (5-12) to the value of the thrust used for pitch control if that is less than F_T, or by defining the thrust of each engine using a separate gimbal angle.

The time rate of change of the angular momentum of the vehicle (neglecting the effects of internal flow) is equal to the external torque. Since we are considering flight within the sensible atmosphere, we neglect the gravity-gradient torque to get

$$\dot{Q} = G_y / I_y \qquad (5\text{-}15)$$

where

$$G_y = M - F_T \ell \sin\delta_e \qquad (5\text{-}16)$$

Here, ℓ is the moment arm of the thrust and the aerodynamic pitching moment, M, can be expressed as

45

$$M = 1/2\ \rho S d V^2 C_m \qquad (5\text{-}17)$$

In Eq. (5-17) ρ is the atmospheric density, S is the reference area, d is the reference length and C_m is the aerodynamic pitching moment coefficient. We can write C_m as

$$C_m = C_{m_s}(\alpha, M, \delta_r) + c_{m_q}(\frac{d}{2V})Q + C_{m_\alpha}(\frac{d}{2V})\dot{\alpha} \qquad (5\text{-}18)$$

where C_{M_s} is the "static" part of C_m, C_{m_q} is the pitch damping derivative, and C_{m_α} is the change in C_m due to the time rate of change in angle of attack.

We may use the fact that $\Theta = \alpha_x + \gamma$ and collect the above equations and write the following set:

$$\dot{R} = V \cos \gamma$$
$$\dot{\lambda} = (V/R)\sin \gamma$$
$$mV\dot{\gamma} = -m(V^2/R)\sin \gamma + mg \sin \gamma + F_T \sin(\alpha_x + \delta_e) + L$$
$$m\dot{V} = -mg\cos\gamma + F_T \cos(\alpha_x + \delta_e) \qquad (5\text{-}19)$$
$$mV\dot{\alpha}_x = mVQ + m(V^2/R)\sin \gamma - mg \sin \gamma - F_T \sin(\alpha_x + \delta_e) - L$$
$$I_y\dot{Q} = \frac{1}{2}\rho V^2 S d \left[C_{m_s} + C_{m_q}\left(\frac{d}{2V}\right)Q + C_{m_\alpha}\left(\frac{d}{2V}\right)\dot{\alpha} \right] - F_T \ell_r \sin\delta_e$$

Equations (5-19) are of the form,

$$\underline{\dot{X}} = \underline{f}(\underline{X}, \underline{U}, t) \qquad (5\text{-}20)$$

where $\underline{X} = (R\ \lambda\ \gamma\ V\ \alpha_x\ Q)^T$ is the state vector ("state"), and $\underline{U} = (\delta_e\ \delta_r)^T$ is the control vector ("control"). The time, t, appears explicitly because of the time-varying properties of the

46

system.

5.2.3 Linearized Equations

Let $\underline{X}^*(t)$ and $\underline{U}^*(t)$ denote nominal state and control, respectively. Then, we may set $\underline{X}$ = $\underline{X}^*(t) + \underline{x}$ and $\underline{U} = \underline{U}^*(t) + \underline{u}$, where $\underline{x}$ and $\underline{u}$ are perturbations in the state and control, respectively. Next, we may expand both sides of Eq. (5-19) and drop all terms that are nonlinear in elements of $\underline{x}$ and/or $\underline{u}$ to get the linear matrix equation,

$$\underline{\dot{x}} = A \, \underline{x} + B \, \underline{u} \tag{5-21}$$

where $A = (\partial \underline{f}/\partial \underline{X})_{\underline{x} = \underline{x}^*, \underline{U} = \underline{U}^*}$ and $B = (\partial \underline{f}/\partial \underline{U})_{\underline{x} = \underline{x}^*, \underline{U} = \underline{U}^*}$ are the system and control matrices, respectively.

5.3 Computer Program and Preliminary Results

A computer program has been written in the C language to (a) integrate the nonlinear equations of motion, (b) calculate numerical approximations to the system and control matrices, and (c) determining the quasi-steady stability characteristics of the system when different feedback control laws are used. Here, by "quasi-steady" we mean that the stability is determined by using the matrices A and B evaluated at particular times.

At the beginning of this project, it was planned that aerodynamic data from wind tunnel tests would be available for the final static stability and control and dynamic stability analyses. Because these data were not available, we have not conducted extensive analyses. However, as we did for the static analysis presented *supra*, we used the estimated aerodynamic data to obtain some representative results.

47

5.3.1 Nominal Trajectory

We integrated the nonlinear equations of motion holding $\alpha_x = 0$ and generated a nominal trajectory. For the integration, we used the data given in Table 5.1. The mass, moments of inertia, thrust and c.m. position were varied with time in a piece-wise linear manner. The trajectory is shown in Fig. 5.2, while the time histories of the state variables, except that for α_x which is zero, are shown in Figs. 5.3 to 5.5. This trajectory is not exactly the same as any of those generated by NASA for the NLS, but it is representative and suitable for our purposes. We have used nominals like this because we need more information than that usually provided, i.e., we need the nominal, plus the system and control matrices.
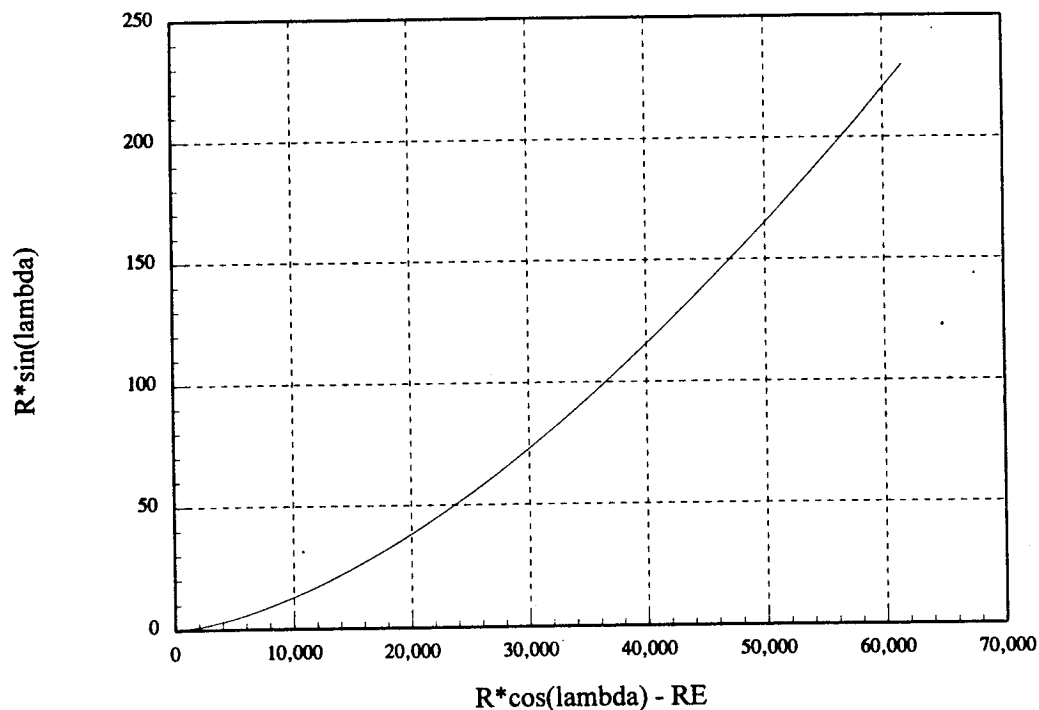
Fig. 5.2 Gravity-turn nominal trajectory.

48

Table 5.1 Physical Characteristics of the NLS 1.5 Stage Vehicle for Dynamic Analysis.

TIME (SEC)	WEIGHT (LBS)	MOMENT OF INERTIA, I_y
0	1972653.	124326000.
65	1449316.	103155496.
128	933563.	90071384.

MACH NUMBER	THRUST (LBS)	MACH NUMBER	THRUST (LBS)
0.61	3491867.00	2.02	3199134.25
0.80	2913900.75	2.19	3212174.25
0.90	2965691.25	2.49	3227807.00
0.94	2985669.25	2.71	3234955.50
1.07	3033270.50	2.99	3240632.25
1.12	3051234.25	3.43	3244574.00
1.17	3068509.25	3.78	3247423.00
1.26	3093054.00	4.16	3248522.75
1.41	3123076.25	4.52	3899016.25
1.66	3161505.75	5.01	3899394.00
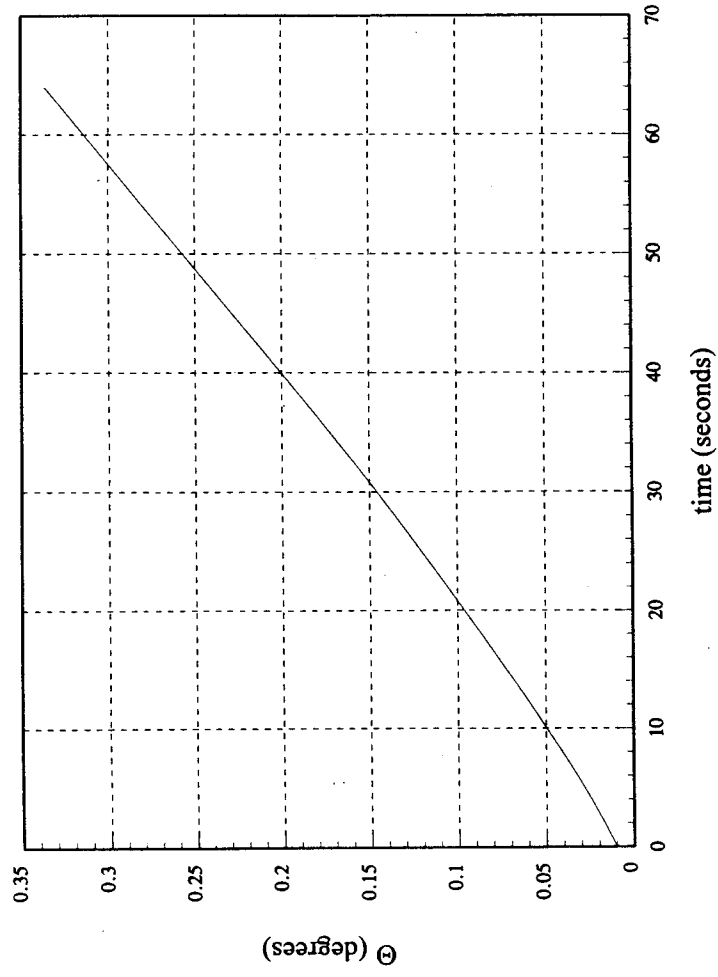
Fig. 5.3 Vehicle pitch angle, Θ.
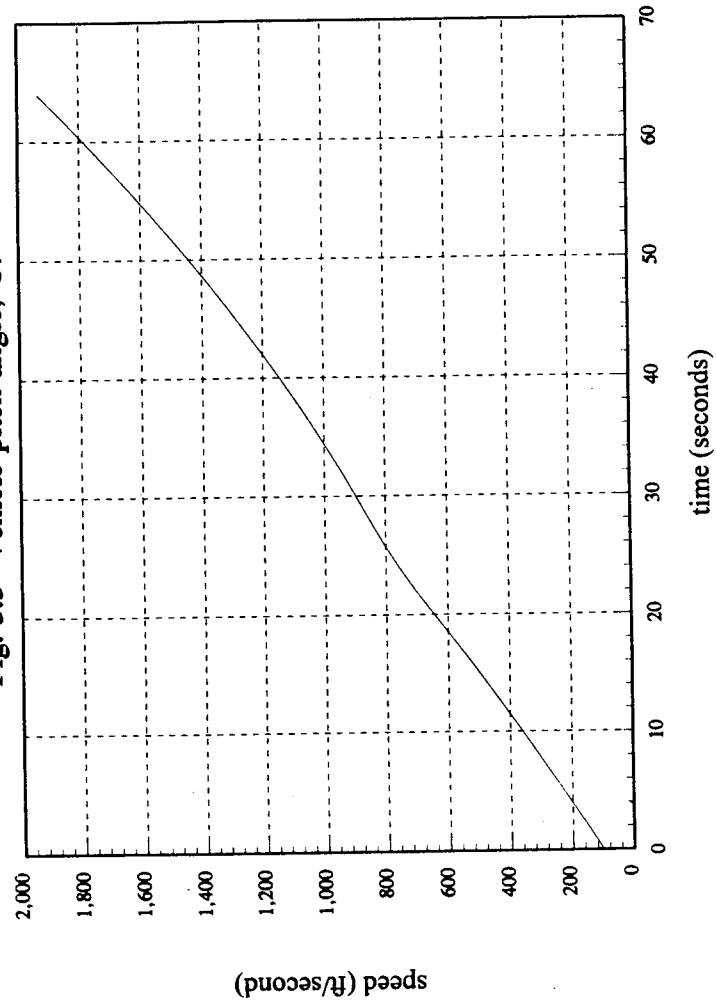
Fig. 5.4 Vehicle speed, V.

50
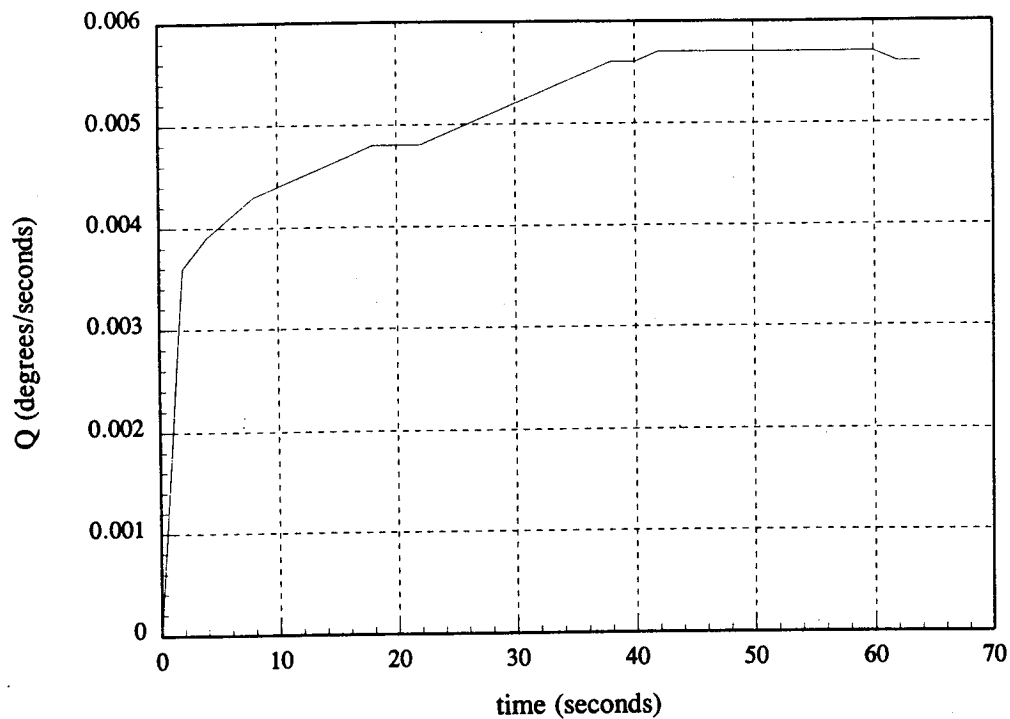
Fig. 5.5 Vehicle pitch rate, Q.

5.3.2 System and Control Matrices

The system and control matrices are calculated in the computer program using a forward

differences method because the form of the aerodynamic data is such that analytical partial

derivatives can not be found. The A and B matrices at times 10 sec and 60 sec in to the flight

are presented in Table 5.2. Note that due to the changes in mass, moment of inertia, and thrust

magnitude, there is a good deal of variation in the matrices and consequently in the eigenvalues

of A that are also shown in Table 5.2. The principal unstable mode is a divergence in pitch that

has a time-to-double of about 3.533 sec at t= 10 sec. The time to double of this mode

decreases to 0.721 sec at t = 60 sec. The control power matrix (B) also varies with time.

Elements b_{51} and b_{61} are "control powers" associated with the thrust. The elements b_{51} and b_{61}

are measures of the normal acceleration pitch acceleration, respectively, generated per radian

of engine deflection   At t = 60 sec, for example, b_{61} = -1.6999 On the other hand, the element a_{65} is the "over turning acceleration" per radian of angle of attack. At t = 60 sec, a_{65} =   0.96352.

Of great interest here is the control power due to the deflection of the fins. This is determined by b_{52} and b_{62}.   The ratio b_{62}/b_{61} is a measure of the effectiveness to the fins as compared to the engines. At t= 60 sec., from the estimated aerodynamic data, we predict that this ratio is about 0.03377. Although the absolute value of the torque due to the fins is smaller than that due to the engines, it is large enough to be of considerable benefit in controlling the unstable vehicle.

5.3.3 Effect of an Angle of Attack Perturbation.

Winds aloft are a major source of perturbations of launch vehicle motion. To see how a small perturbation will affect an uncontrolled vehicle we picked the "gust angle of attack" shown in Fig. 5.6. This was applied in our simulation beginning at t = 0. The trajectory is shown in Fig. 5.7. It is grossly different than the nominal one. In Figs. 5.8 and 5.9, we have plotted the pitch angle and pitch rate, respectively. Time histories of the other state variables are provided in Figs. 5.10 through 5.11.

Table 5.2 System and Control Power Matrices for Selected Times - Nominal Trajectory.

t = 10 sec

$$A = \begin{bmatrix} 0 & 0 & -3.0868E-1 & 1.0 & 0 & 0 \\ -7.1093E-16 & 0 & 1.719E-5 & 4.1358E-11 & 0 & 0 \\ 7.1094E-16 & 0 & 8.9421E-2 & -2.1523E-7 & 1.7784E-1 & 0 \\ 0 & 0 & 2.7502E-2 & 0 & -9.9863 & 0 \\ 0 & 0 & -8.9439E-2 & 2.1519E-7 & -1.7784E-1 & 1 \\ 1.9462E-13 & 0 & 0 & -2.1773E-11 & 1.0227E-1 & -8.6732E-5 \end{bmatrix}$$

$$B^T = \begin{bmatrix} 0 & 0 & 1.6506E-1 & 0 & -1.6506E-1 & -1.6151 \\ 0 & 0 & 2.947E-3 & -3.1983 & -2.9470E-3 & -2.5443E-2 \end{bmatrix}$$

Eigenvalues of A: 0, -4.0068E-1, 1.9532E-1, 1.1686E-1, -4.3393E-6, 4.4034E-6

Table 5.2 (continued)

t = 40 sec

$$A = \begin{bmatrix} 0 & 0 & -4.001 & 9.9999E\text{-}1 & 0 & 0 \\ -9.1157E\text{-}15 & 0 & 5.4642E\text{-}5 & 1.6682E\text{-}10 & 0 & 0 \\ 9.1157E\text{-}15 & 0 & 2.8050E\text{-}2 & -8.5972E\text{-}8 & 7.5657E\text{-}2 & 0 \\ 3.1420E\text{-}5 & 0 & 1.1243E\text{-}1 & 6.6340E\text{-}3 & -2.5947E2 & 0 \\ 0 & 0 & -2.8105E\text{-}2 & 8.5805E\text{-}8 & -7.5657E\text{-}2 & 1 \\ 8.6691E\text{-}13 & 0 & 0 & -6.3342E\text{-}12 & 5.4920E\text{-}1 & -2.3291E\text{-}4 \end{bmatrix}$$

$$B^T = \begin{bmatrix} 0 & 0 & 5.1999E\text{-}2 & 0 & -5.1999E\text{-}2 & -1.5366 \\ 0 & 0 & 6.7141E\text{-}3 & 4.7548E1 & -6.7141E\text{-}3 & -1.8008E\text{-}1 \end{bmatrix}$$

Eigenvalues of A: 0, -7.7859E-1, 7.0258E-1, -3.1962E-3, 9.8304E-3, 2.8162E-2
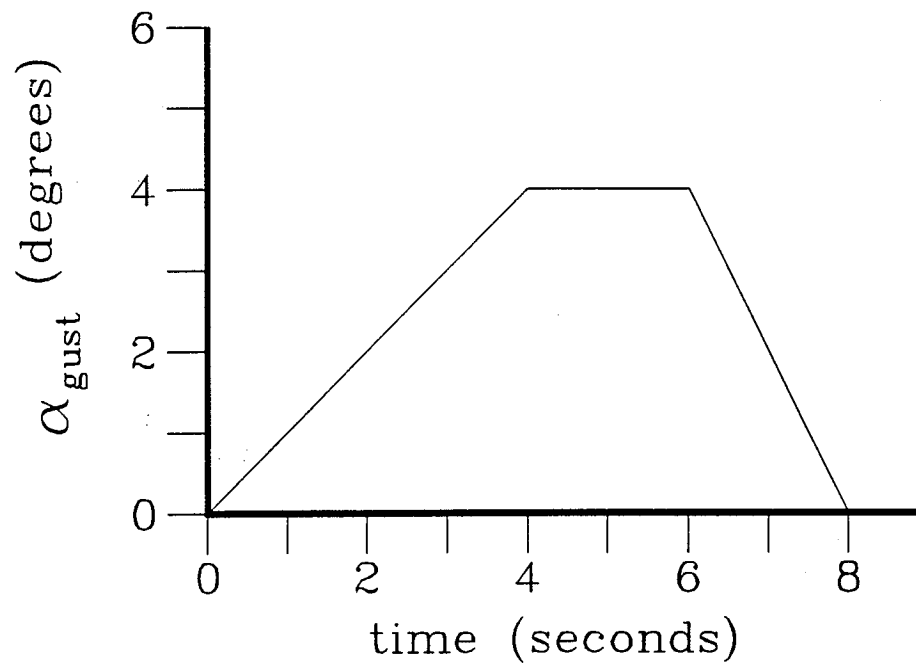
Fig. 5.6 Contribution to the aerodynamic angle of attack due to a gust.
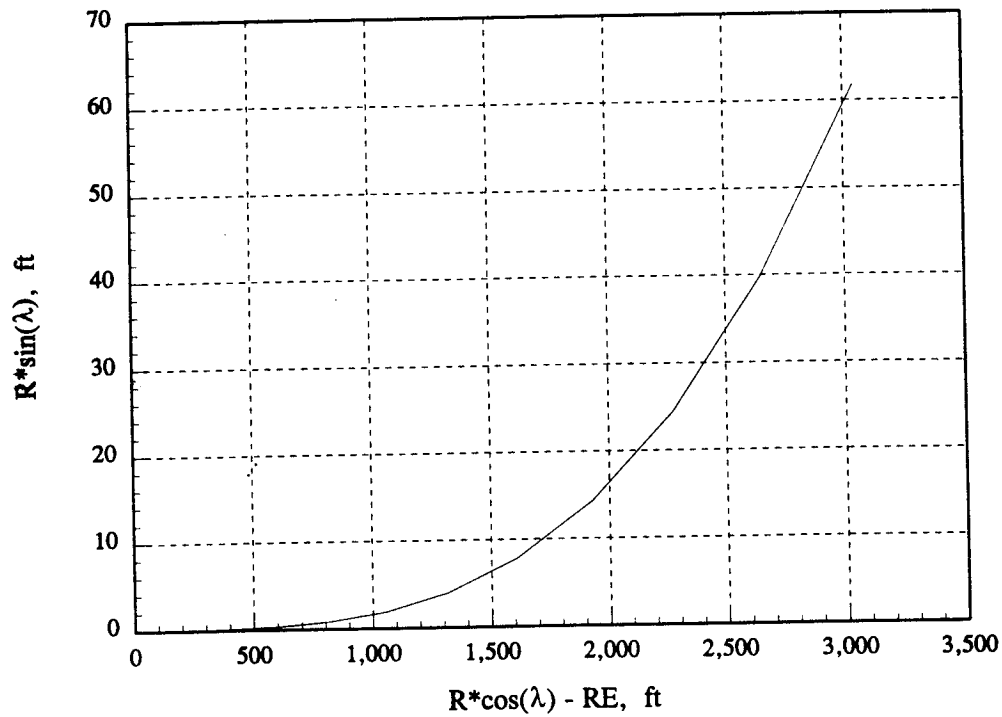
Fig. 5.7 Vehicle trajectory with gust.
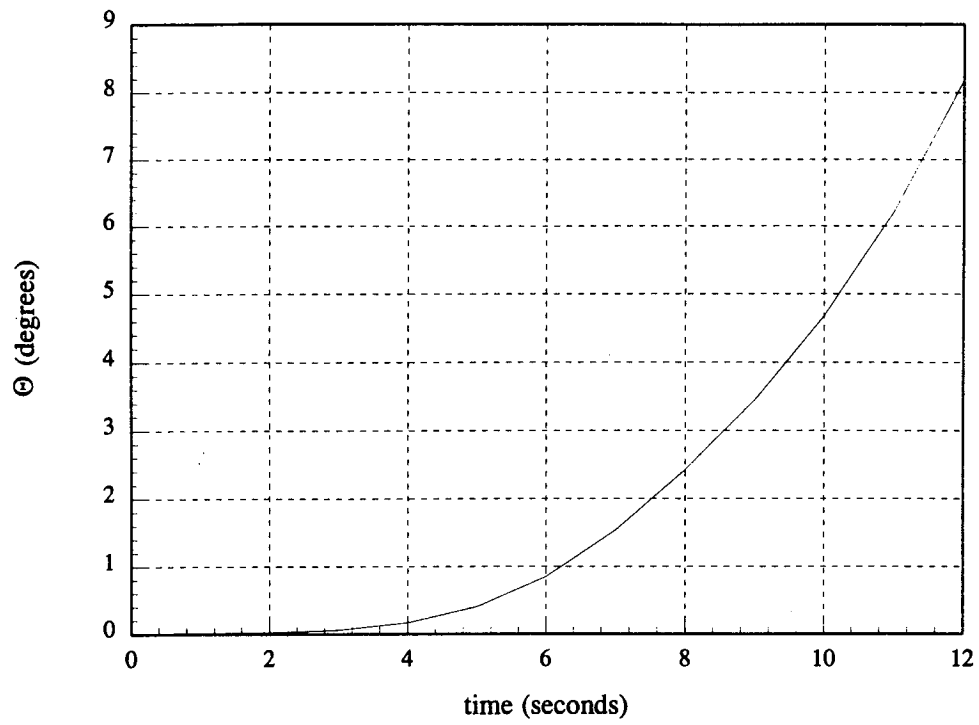
Fig. 5.8 Vehicle pitch angle, Θ.
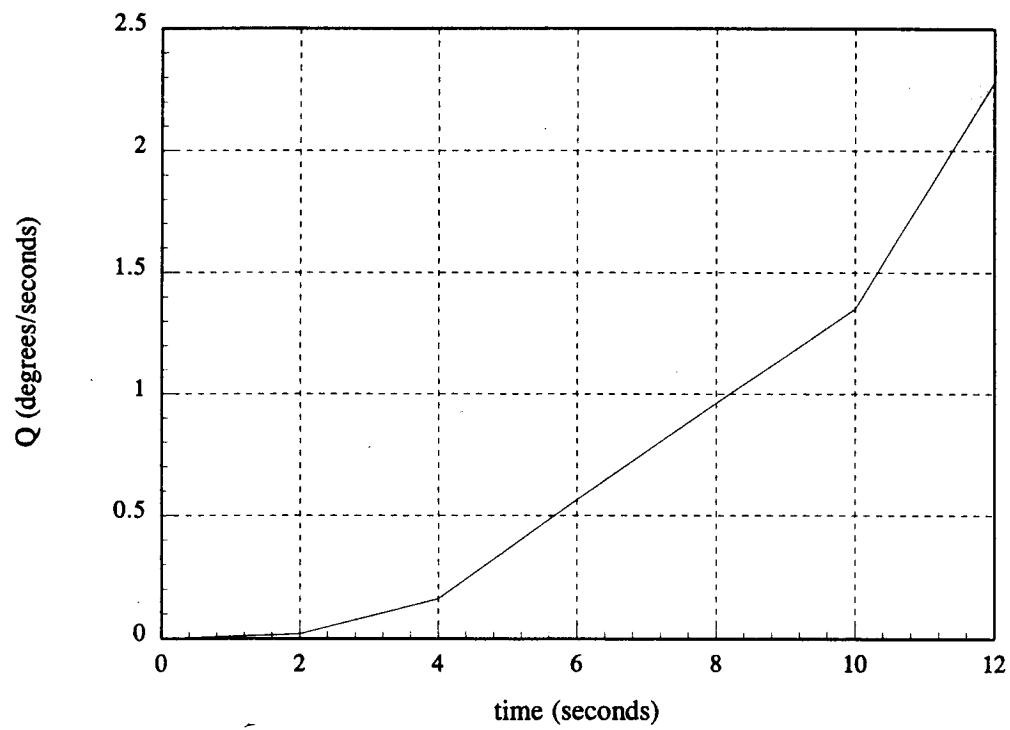
Fig. 5.9 Vehicle pitch rate, Q.
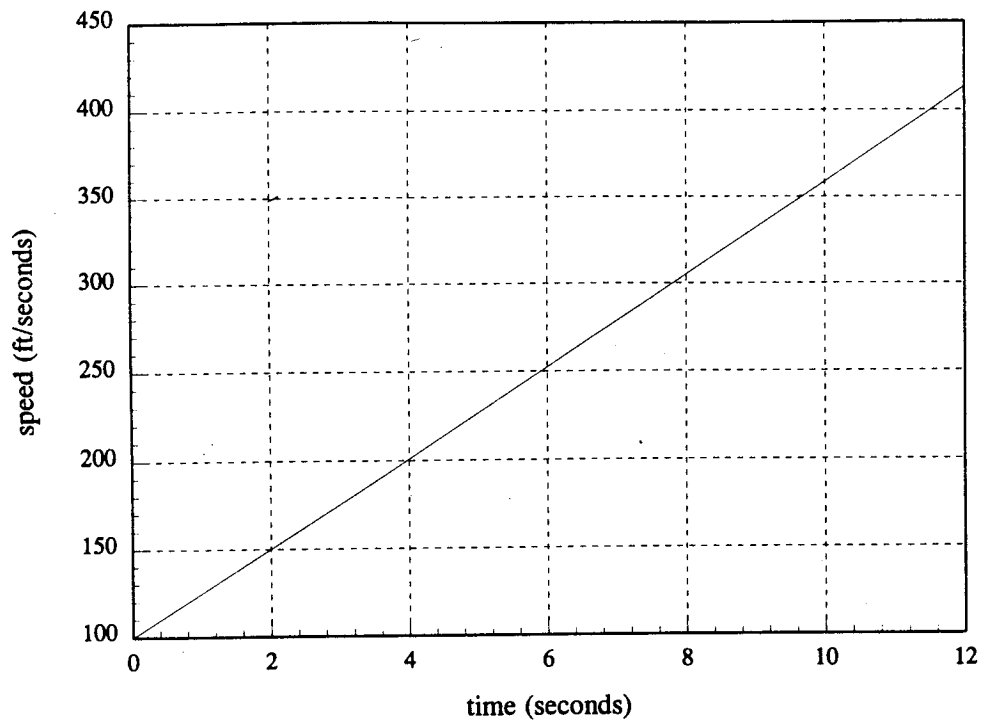
Fig. 5.10 Vehicle speed, V.
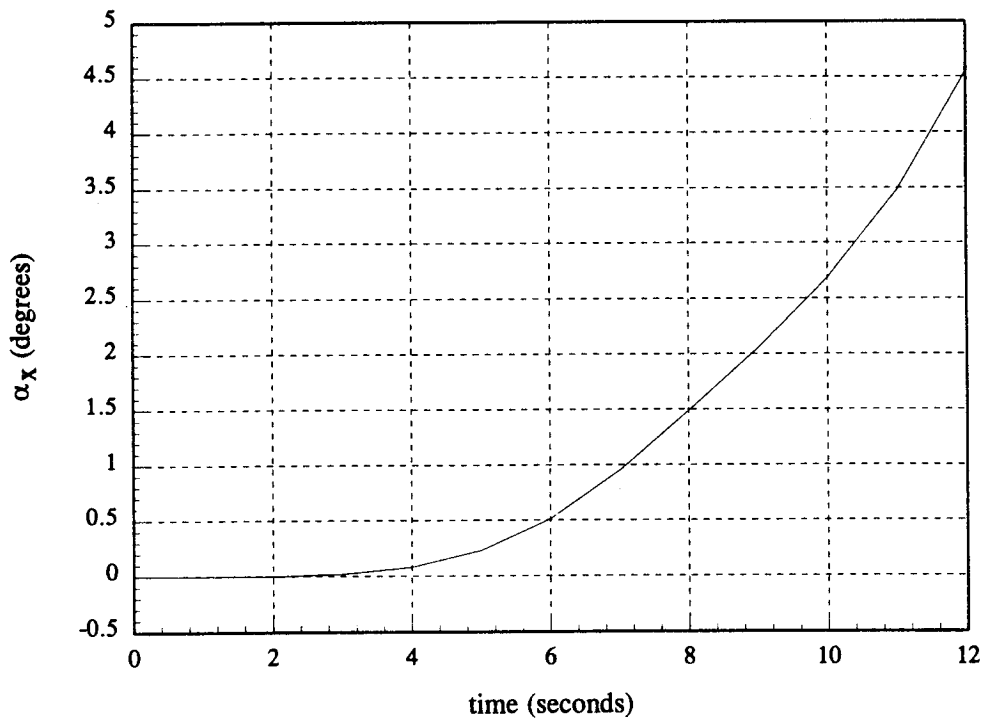
Fig. 5.11 Angle of attack, α_x.

5.3.4 Feedback Control

Because the vehicle is unstable with respect to an angle of attack, we must use some type of feedback if we want to achieve anything close to a nominal trajectory for comparison purposes. For the sake of simplicity, we decided to feedback α_x and Q. This assumes that α_x and Q can be measured. The pitch rate can be measured with a rate gyro, but the angle of attack of the x-axis will probably need to be estimated using the z-component of acceleration. Thus, we focused on a feedback control law of the form:

$$\begin{pmatrix} \delta_e \\ \delta_r \end{pmatrix} = K \begin{pmatrix} \alpha_x \\ Q - Q^* \end{pmatrix}$$

where Q^* is the nominal pitch rate. To date we have neglected Q^*. There are several methods that can be used to find the gain matrix K. We first tried a pole placement method from MATLAB Control System Toolbox, but we were not pleased with the results. We than decided on the established "root locus" method in which we first fixed the pitch rate gains at zero and then varied the gains on α_x. Using this method and some intuition, we settled on the following gain matrix:

$$K = \begin{bmatrix} 1.0 & 0.5 \\ 1.8 & 0.5 \end{bmatrix}$$

The closed-loop trajectory generated using K is shown in Fig. 5.12 and other state variables are plotted in Figs. 5-13 through 5-16. The steadily increasing pitch angle is due to the use of a feedback law that does not include pitch angle feedback, or feedback of the integral of the pitch angle. Adding such feedback terms is relatively straightforward and the objective of this exercise

to show that the engines and fins will effectively control the attitude motion of the vehicle has been achieved. In the next phase, we will devote more time to the attitude control and guidance aspects.
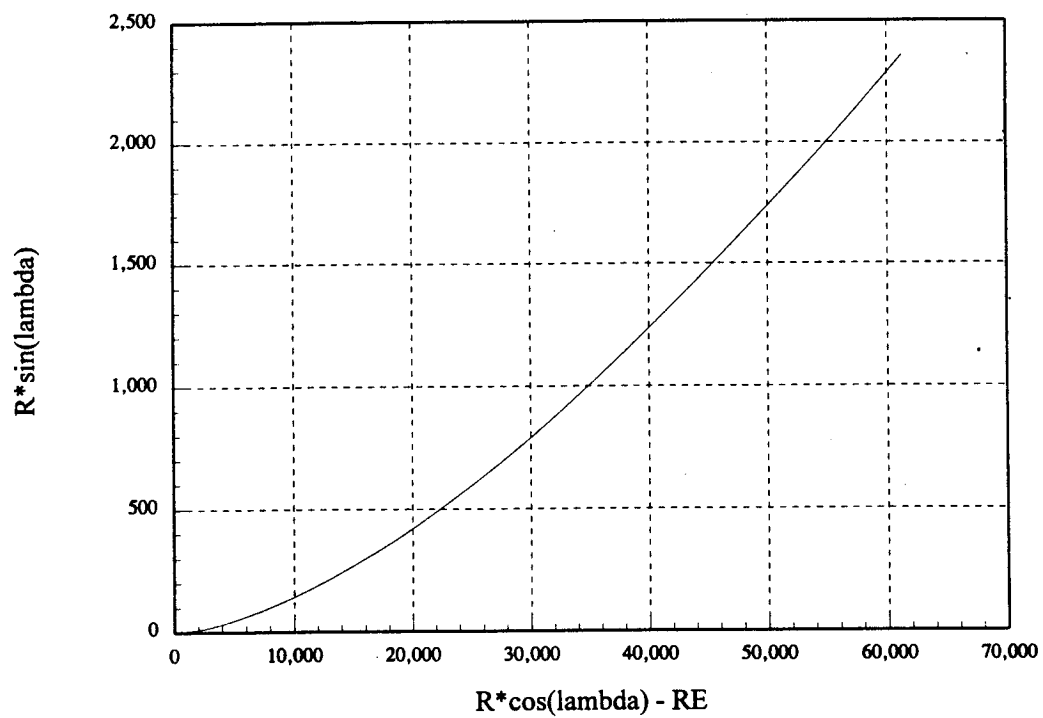
Fig. 5.12 Vehicle trajectory with attitude feedback control.
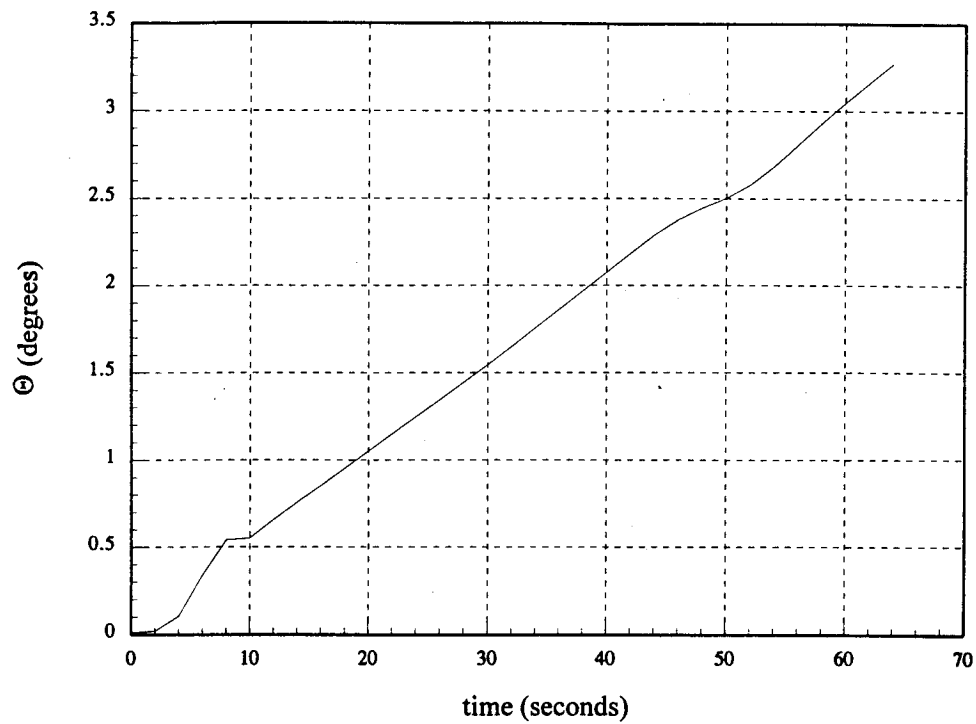
Fig. 5.13 Vehicle pitch angle, Θ.
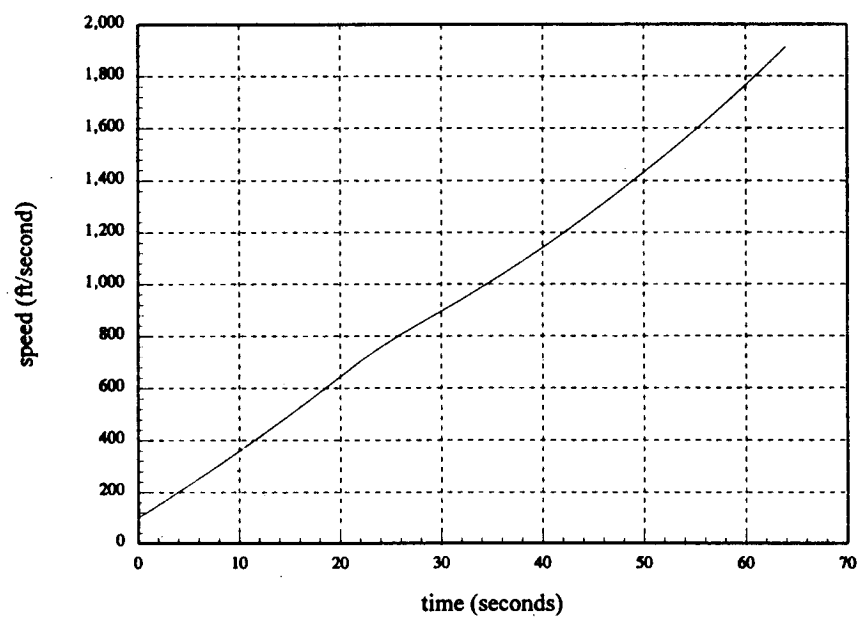
Fig. 5.14 Vehicle speed, V.
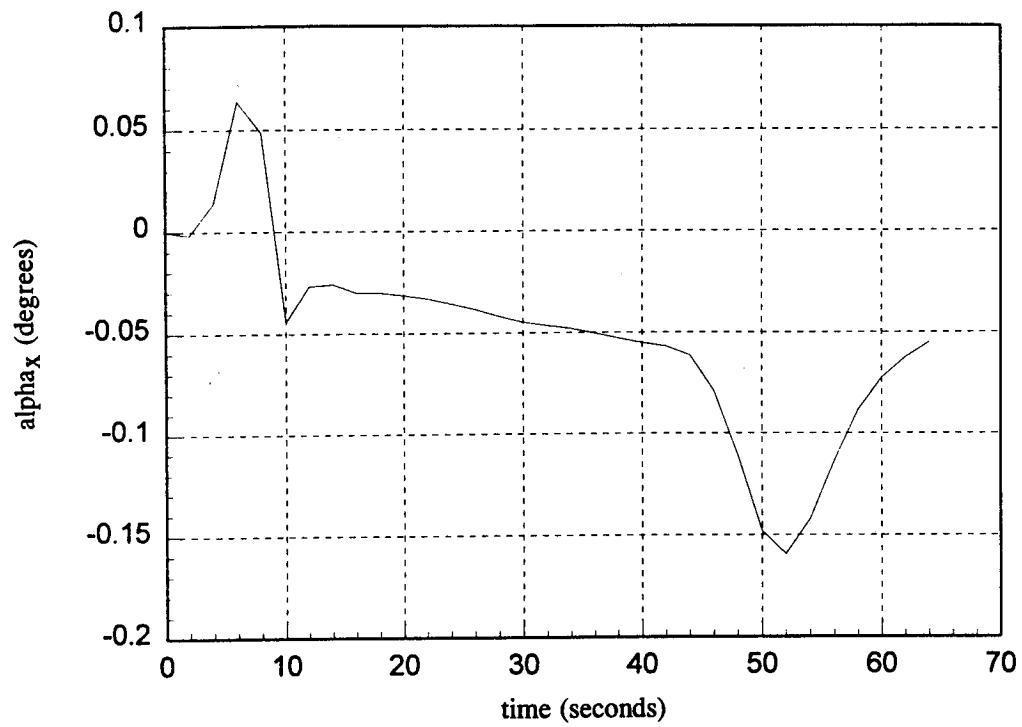
Fig. 5.15 Angle of attack, α_x.
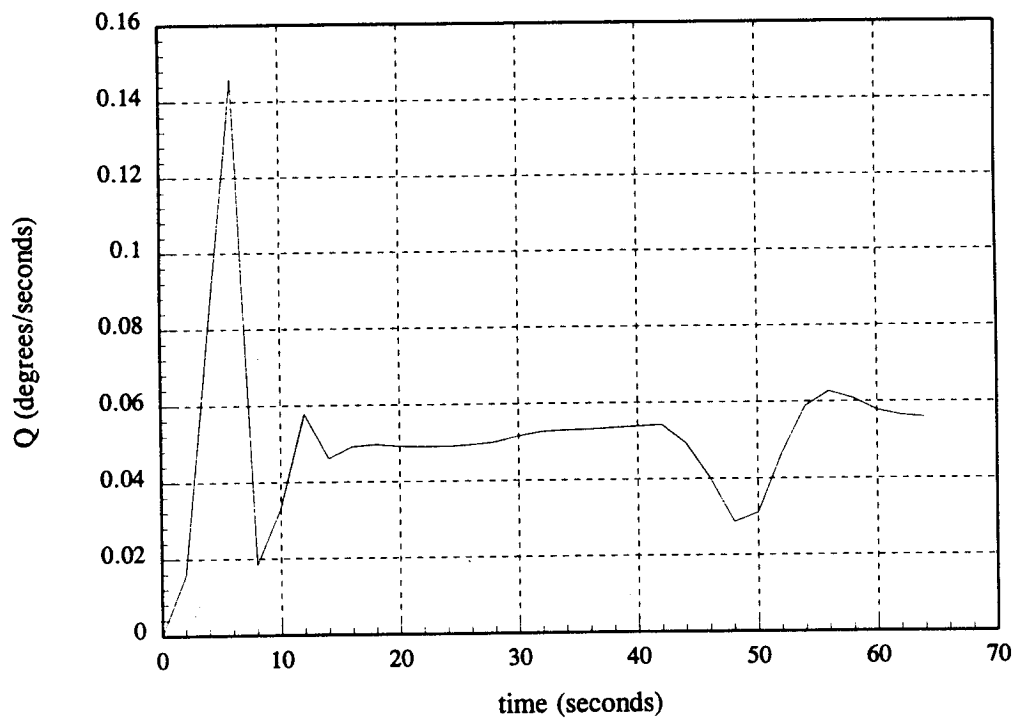
Fig. 5.16 Pitch rate, Q.

6. CONCLUSIONS AND RECOMMENDATIONS

6.1 Conclusions

The analysis we have conducted supports the use of fins on the LOX-Tank-Aft NSL 1.5 Stage vehicle. We considered a large number of fin planforms and airfoil sections and chose the best performing combination. Based on our predictions of the vehicle's aerodynamics, <u>four fins of 50 ft² planform area each will not stabilize the vehicle with respect to perturbations in angle of attack, but the fins will decrease the instability of the vehicle significantly. More importantly, if the fins are movable, by deflecting them, the vehicle can be trimmed at small positive and negative angles of angles of attack</u>. This means that the fins can be used to counteract small perturbations in angle of attack and to assist in counteracting large magnitude disturbances.

A static control, or trim, parameter R was defined as the sum of the torque due to thrust vectoring and the torque due to the fins divided by the aerodynamic torque on the vehicle without fins ("body alone"). For reasonable center of gravity positions, the fins provide an additional 10 to 20% of "control power."

The construction of aerodynamic surfaces for launch vehicles was considered and an indication of the state-of-the-art provided. It appears that carbon fiber reinforced plastics (CFRP) are a good choice for fins that will be exposed to temperatures no higher than 476 °F (stagnation temperature at Mach 2). For higher temperature applications, say up to 745 °F (stagnation temperature at Mach 3), more expensive titanium composites could be used. A combination of titanium leading edges with CFRP surfaces would also be a consideration to be examined.

A dynamic stability and control analysis of the NLS 1.5 Stage vehicle with four 50 ft² fins

was conducted. NLS data was used in a digital computer code to (a) produce a nominal gravity-turn trajectory, (b) compute system and control power matrices for the associated linear system and calculate the eigenvalues of the system matrices. A simple linear feedback controller that uses both thrust vectoring and fin deflections was developed to control the vehicle's attitude and successfully tested in the nonlinear simulation.

6.2 Recommendations

The following recommendations are made:

1. The use of movable fins on next generation launch vehicles should be considered further.

2. The planned wind tunnel tests of a model of the NLS 1.5 Stage vehicle should be carried out early in FY 1994 to determine if the predicted aerodynamic are qualitatively correct.

3. Further investigation of vortex generators for the fins and/or the vehicle are recommended.

4. Additional analytical work should be done to model the flexibility of the launch vehicle as well as sloshing of fuel and oxidizer.

5. Additional analytical work should be done to determine the effects of vehicle flexibility and sloshing when fins are used to assist in the control of the vehicle.

6. Additional consideration should be given to the construction of the fins and to estimating the weights of the fins and the actuators.

7. Depending on the success with which the MISSILE DATCOM code predicted the aerodynamics of the NLS 1.5 Stage vehicle, additional effort should be expended to determine if a better prediction code exists. If it is determined that a suitable code does not exist, then an attempt should be made to modify MISSILE DATCOM so that it produces adequate results.

REFERENCES

1. Isakowitz, Stephen J. <u>International Reference Guide to Space Launch Systems</u>, American Institute of Aeronautics and Astronautics, Washington, D.C., 1991.

2. <u>Jane's Space Flight Directory,</u> 1988-1989, Fourth Edition, Jane's Information Group, Inc., Alexandria, VA 22313-2036, 1989.

3. "National Launch System (NLS) Reference System Definition Executive Summary," 1-1532-1-16T, May 1991.

4. Bruns, K.D., Moore, M.E., Stoy, S.L., Vukelich, S.R., and Blake, W.B. "MISSILE DATCOM User's Manual - Rev 4/91," WL-TR-91-3039, Final Report, Contract f33615-87-C-3604, WPAFB, OH, 45433-6553, April 1991.

5. Washington, W.D. "AERODSN, Aerodynamics Prediction Code," U.S. Army Missile Command, Systems Simulation and Development Directorate, Redstone Arsenal, AL, 1988.

6. "NLS Mass Properties Status Report #5, Cycle O Configuration (Final)," NLS2TEL-2.COM, Configuration Definition Panel Systems Requirements and Integration Team, Marshall Space Flight Center, AL 35812, February 1992.

7. Wendt, B.J., Greber, I., and Hingst, W.R. <u>The Structure and Development of Streamwise Vortex Arrays Embedded in a Turbulent Boundary Layer</u>, NASA Technical Memorandum NASA-TM-105211 (N92-10012), 1992.

8. Middleton, D.H. <u>Composite Materials in Aircraft Structures</u>, Longman Scientific and Technical Book Company, Harlow, Essex, U.K., 1990.

9. Jones, Robert M. <u>Mechanics of Composite Materials</u>, Scripta Book Company, Washington, D..C., 197.

10. Niu, Michael C.Y. <u>Composite Airframe Structures</u>, Conmilit Press Ltd., Hong Kong, 1992.

11. Rogers, Craig A. "Intelligent Material Systems - The Dawn of a New Age," <u>Journal of Intelligent Material Systems and Structures</u>, January 1993, pp. 4-12.

12. Stevens, Tim. "Structures Get Smart (Part I)," <u>Materials Engineering</u>, October 1991, pp. 18-20.

13. Rogers, Craig A. "Intelligent Systems and Structures," <u>U.S.-Japan Workshop on Smart/Intelligent Materials and Systems</u>, 1990, pp. 11-33.

14. Boggs, Robert N. "'Smart' materials bolster helicopter blade design," <u>Design News</u>, April 22, 1991, p. 28.

15. Rogers, Craig A. "Active vibration and structural acoustic control of shape memory alloy hybrid composites: Experimental Results," <u>Journal of the Acoustical Society of America</u>, December 1990, pp. 2803-11.

16. Tessler, Sandra Rubin. "Smart Materials," <u>Technology Review</u>, April 1989, pp. 8-9.

17. Stevens, Tim. "Structures Get Smart (Part II)," <u>Materials Engineering</u>, November 1991,
pp. 26-28.

APPENDIX

ADDITIONAL AERODYNAMIC DATA

$X_{c.g.} = 212.44$ ft

ARC fin3, body alone
A = 50 ft^2

Cm body alone	Mach									
alpha	0.2	0.4	0.6	0.9	1.1	1.2	1.4	1.65	1.8	2
0.50	0.063	0.063	0.063	0.063	0.069	0.07	0.119	0.124	0.124	0.122
1.00	0.126	0.126	0.126	0.127	0.138	0.14	0.24	0.249	0.249	0.246
2.00	0.259	0.259	0.259	0.262	0.287	0.291	0.491	0.508	0.509	0.502
4.00	0.545	0.545	0.545	0.551	0.611	0.62	1.016	1.05	1.052	1.038
6.00	0.845	0.845	0.845	0.853	0.954	0.969	1.554	1.605	1.607	1.587

Cn body alone										
alpha	0.2	0.4	0.6	0.9	1.1	1.2	1.4	1.65	1.8	2
0.50	0.019	0.019	0.019	0.019	0.02	0.02	0.029	0.03	0.03	0.029
1.00	0.039	0.039	0.039	0.039	0.041	0.041	0.058	0.06	0.061	0.059
2.00	0.081	0.081	0.081	0.081	0.087	0.086	0.12	0.124	0.126	0.123
4.00	0.173	0.173	0.173	0.174	0.191	0.189	0.256	0.265	0.268	0.263
6.00	0.272	0.272	0.272	0.274	0.304	0.302	0.399	0.412	0.416	0.409

Cma body alone										
alpha	0.20	0.40	0.60	0.90	1.10	1.20	1.40	1.65	1.80	2.00
0.50	0.1238	0.1238	0.1238	0.1251	0.1351	0.1370	0.2373	0.2458	0.2462	0.2427
1.00	0.1301	0.1301	0.1301	0.1314	0.1438	0.1459	0.2461	0.2545	0.2550	0.2515
2.00	0.1381	0.1381	0.1381	0.1395	0.1551	0.1575	0.2567	0.2651	0.2655	0.2621
4.00	0.1464	0.1464	0.1464	0.1478	0.1669	0.1695	0.2659	0.2742	0.2747	0.2713
6.00	0.1531	0.1531	0.1531	0.1545	0.1766	0.1794	0.2720	0.2803	0.2807	0.2773

Cna body alone										
alpha	0.2	0.4	0.6	0.9	1.1	1.2	1.4	1.65	1.8	2
0.50	0.03763	0.03763	0.03763	0.03790	0.03976	0.03924	0.05639	0.05855	0.05925	0.05804
1.00	0.04045	0.04045	0.04045	0.04074	0.04370	0.04326	0.06037	0.06253	0.06322	0.06202
2.00	0.04410	0.04410	0.04410	0.04440	0.04881	0.04847	0.06523	0.06738	0.06807	0.06687
4.00	0.04793	0.04793	0.04793	0.04824	0.05422	0.05400	0.06976	0.07189	0.07258	0.07138
6.00	0.05110	0.05110	0.05110	0.05143	0.05877	0.05865	0.07306	0.07517	0.07585	0.07467

6/8/93

67

$X_{c.g.} = 2/2.44\ ft$

Cn, ARC fin3, A = 50 ft^2

Mach	alpha	-8	-7	-6	-5	-4	-3	-2	-1	0	1	2	3	4	5	6	7	8
0.2	0.2																	
	0.5	-0.067	-0.056	-0.044	-0.033	-0.021	-0.009	0.003	0.016	0.028	0.040	0.052	0.064	0.076	0.088	0.099	0.110	0.121
	1	-0.039	-0.028	-0.016	-0.005	0.007	0.019	0.032	0.044	0.056	0.068	0.081	0.092	0.104	0.116	0.127	0.138	0.149
	2	0.019	0.031	0.042	0.054	0.067	0.079	0.091	0.103	0.116	0.128	0.139	0.151	0.163	0.174	0.185	0.196	0.206
	4	0.146	0.158	0.170	0.182	0.194	0.206	0.218	0.230	0.242	0.254	0.265	0.276	0.287	0.298	0.307	0.317	0.325
	6	0.272	0.285	0.297	0.309	0.321	0.333	0.345	0.356	0.368	0.379	0.390	0.400	0.410	0.419	0.428	0.436	0.443
0.4	0.5	-0.069	-0.058	-0.046	-0.034	-0.022	-0.010	0.003	0.016	0.028	0.041	0.053	0.066	0.078	0.090	0.101	0.113	0.124
	1	-0.041	-0.030	-0.018	-0.006	0.006	0.019	0.031	0.044	0.057	0.069	0.082	0.094	0.106	0.117	0.129	0.140	0.151
	2	0.017	0.029	0.041	0.054	0.066	0.079	0.091	0.104	0.117	0.129	0.141	0.153	0.164	0.176	0.187	0.198	0.208
	4	0.145	0.157	0.170	0.182	0.195	0.207	0.220	0.232	0.244	0.256	0.267	0.279	0.289	0.300	0.310	0.319	0.327
	6	0.272	0.285	0.297	0.310	0.322	0.334	0.346	0.358	0.370	0.381	0.392	0.403	0.412	0.421	0.430	0.438	0.445
0.6	0.5	-0.073	-0.061	-0.049	-0.037	-0.024	-0.011	0.002	0.015	0.029	0.042	0.055	0.068	0.081	0.093	0.105	0.117	0.128
	1	-0.045	-0.033	-0.021	-0.008	0.005	0.018	0.031	0.044	0.058	0.071	0.084	0.097	0.109	0.121	0.133	0.144	0.155
	2	0.014	0.027	0.039	0.052	0.065	0.079	0.092	0.106	0.119	0.131	0.144	0.156	0.168	0.180	0.191	0.202	0.212
	4	0.143	0.156	0.169	0.183	0.196	0.209	0.222	0.235	0.247	0.259	0.271	0.283	0.294	0.304	0.314	0.323	0.331
	6	0.272	0.286	0.299	0.312	0.325	0.338	0.350	0.362	0.374	0.386	0.397	0.407	0.417	0.425	0.434	0.441	0.448
0.8	0.5	-0.089	-0.075	-0.061	-0.046	-0.031	-0.016	-0.001	0.015	0.030	0.046	0.061	0.076	0.091	0.106	0.120	0.134	0.147
	1	-0.059	-0.045	-0.030	-0.016	-0.001	0.015	0.030	0.046	0.061	0.077	0.092	0.107	0.121	0.136	0.150	0.163	0.176
	2	0.004	0.018	0.033	0.048	0.063	0.079	0.095	0.110	0.126	0.140	0.155	0.170	0.184	0.198	0.211	0.224	0.237
	4	0.139	0.155	0.170	0.186	0.201	0.216	0.231	0.246	0.261	0.275	0.290	0.303	0.317	0.329	0.341	0.353	0.364
	6	0.274	0.290	0.305	0.320	0.335	0.350	0.365	0.379	0.394	0.407	0.421	0.433	0.446	0.457	0.468	0.478	0.487
0.9	0.5																	
1.1	0.5	-0.097	-0.082	-0.066	-0.050	-0.034	-0.018	-0.001	0.016	0.032	0.049	0.066	0.082	0.098	0.114	0.130	0.145	0.160
	1	-0.065	-0.050	-0.034	-0.018	-0.002	0.015	0.032	0.049	0.065	0.082	0.098	0.115	0.131	0.146	0.162	0.177	0.191
	2	0.003	0.019	0.035	0.051	0.068	0.085	0.101	0.118	0.135	0.151	0.167	0.183	0.199	0.214	0.229	0.244	0.258
	4	0.153	0.169	0.186	0.203	0.220	0.236	0.253	0.269	0.285	0.301	0.316	0.332	0.346	0.361	0.374	0.388	0.400
	6	0.303	0.320	0.336	0.353	0.370	0.386	0.402	0.418	0.433	0.449	0.463	0.478	0.492	0.505	0.518	0.530	0.541

Cn, ARC fin3, A = 50 ft^2

O

1.2																	
0.5	-0.082	-0.069	-0.055	-0.041	-0.027	-0.013	0.001	0.016	0.031	0.045	0.060	0.074	0.088	0.102	0.115	0.129	0.142
1	-0.052	-0.038	-0.025	-0.011	0.004	0.018	0.032	0.047	0.062	0.076	0.090	0.104	0.118	0.132	0.146	0.159	0.172
2	0.013	0.027	0.041	0.055	0.069	0.084	0.099	0.113	0.128	0.142	0.156	0.170	0.183	0.197	0.210	0.223	0.235
4	0.157	0.171	0.185	0.200	0.214	0.229	0.243	0.257	0.271	0.285	0.299	0.312	0.325	0.338	0.350	0.362	0.373
6	0.301	0.315	0.330	0.344	0.358	0.373	0.387	0.400	0.414	0.428	0.441	0.453	0.466	0.478	0.489	0.500	0.511
1.4																	
0.5	-0.046	-0.036	-0.026	-0.016	-0.006	0.005	0.015	0.026	0.036	0.046	0.057	0.067	0.077	0.087	0.097	0.107	0.117
1	-0.009	0.001	0.011	0.021	0.031	0.041	0.052	0.062	0.073	0.083	0.093	0.104	0.114	0.124	0.134	0.143	0.153
2	0.067	0.077	0.088	0.098	0.108	0.119	0.129	0.140	0.150	0.160	0.170	0.181	0.191	0.200	0.210	0.220	0.229
4	0.233	0.243	0.253	0.264	0.274	0.285	0.295	0.305	0.315	0.325	0.335	0.345	0.355	0.364	0.374	0.383	0.391
6	0.397	0.407	0.418	0.428	0.439	0.449	0.459	0.469	0.479	0.489	0.499	0.508	0.518	0.527	0.536	0.545	0.553
1.65																	
0.5	-0.029	-0.021	-0.013	-0.005	0.003	0.011	0.019	0.027	0.035	0.044	0.052	0.060	0.068	0.076	0.084	0.092	0.100
1	0.007	0.015	0.023	0.031	0.039	0.047	0.055	0.063	0.071	0.080	0.088	0.096	0.104	0.112	0.120	0.128	0.135
2	0.083	0.091	0.099	0.107	0.115	0.123	0.131	0.139	0.148	0.156	0.164	0.172	0.180	0.188	0.196	0.204	0.211
4	0.247	0.255	0.263	0.271	0.279	0.287	0.295	0.303	0.311	0.319	0.327	0.335	0.343	0.351	0.359	0.366	0.374
6	0.409	0.417	0.425	0.433	0.442	0.450	0.458	0.466	0.474	0.482	0.490	0.498	0.506	0.513	0.521	0.528	0.535
1.8																	
0.5	-0.024	-0.016	-0.009	-0.002	0.006	0.013	0.021	0.028	0.035	0.042	0.050	0.057	0.065	0.072	0.080	0.087	0.094
1	0.012	0.020	0.027	0.034	0.042	0.049	0.056	0.064	0.071	0.078	0.086	0.093	0.101	0.108	0.116	0.123	0.130
2	0.088	0.096	0.103	0.110	0.118	0.125	0.132	0.139	0.147	0.154	0.162	0.169	0.177	0.184	0.192	0.199	0.206
4	0.251	0.258	0.266	0.273	0.280	0.288	0.295	0.303	0.310	0.318	0.325	0.333	0.340	0.348	0.355	0.362	0.369
6	0.413	0.420	0.428	0.435	0.442	0.450	0.457	0.465	0.473	0.480	0.488	0.495	0.503	0.510	0.517	0.525	0.532
2																	
0.5	-0.019	-0.012	-0.005	0.002	0.008	0.015	0.021	0.028	0.034	0.040	0.047	0.053	0.060	0.067	0.074	0.081	0.088
1	0.016	0.023	0.030	0.037	0.043	0.049	0.056	0.062	0.068	0.075	0.081	0.088	0.095	0.102	0.109	0.116	0.123
2	0.090	0.097	0.103	0.110	0.116	0.123	0.129	0.135	0.142	0.148	0.155	0.162	0.169	0.176	0.183	0.190	0.197
4	0.248	0.255	0.261	0.267	0.274	0.280	0.287	0.293	0.300	0.308	0.315	0.322	0.329	0.336	0.343	0.349	0.356
6	0.405	0.412	0.418	0.424	0.431	0.438	0.445	0.452	0.459	0.466	0.473	0.480	0.487	0.494	0.501	0.507	0.514

70

Cm, ARC fin3, A = 50 ft2

Mach	alpha	deflection																
		-8	-7	-6	-5	-4	-3	-2	-1	0	1	2	3	4	5	6	7	8
0.2	0.5	0.223	0.202	0.181	0.159	0.137	0.115	0.092	0.069	0.046	0.024	0.001	-0.021	-0.043	-0.065	-0.086	-0.107	-0.128
	1	0.271	0.25	0.229	0.207	0.185	0.162	0.139	0.116	0.094	0.071	0.048	0.026	0.005	-0.017	-0.038	-0.059	-0.079
	2	0.374	0.352	0.33	0.308	0.285	0.263	0.24	0.217	0.194	0.172	0.15	0.128	0.107	0.086	0.065	0.046	0.027
	4	0.597	0.575	0.552	0.529	0.506	0.484	0.461	0.439	0.417	0.396	0.374	0.354	0.333	0.314	0.296	0.279	0.263
	6	0.845	0.822	0.799	0.777	0.754	0.732	0.71	0.689	0.667	0.646	0.626	0.607	0.589	0.571	0.555	0.54	0.527
0.4	0.5	0.227	0.206	0.184	0.162	0.139	0.116	0.093	0.069	0.046	0.022	-0.001	-0.024	-0.046	-0.068	-0.09	-0.111	-0.132
	1	0.275	0.253	0.232	0.209	0.186	0.163	0.14	0.116	0.093	0.069	0.046	0.024	0.001	-0.02	-0.042	-0.063	-0.083
	2	0.377	0.355	0.332	0.309	0.286	0.263	0.239	0.216	0.192	0.17	0.147	0.125	0.103	0.082	0.061	0.041	0.022
	4	0.599	0.576	0.552	0.529	0.505	0.482	0.459	0.436	0.414	0.392	0.37	0.349	0.329	0.31	0.292	0.275	0.259
	6	0.845	0.821	0.798	0.775	0.752	0.729	0.707	0.685	0.663	0.642	0.622	0.602	0.584	0.567	0.552	0.537	0.524
0.6	0.5	0.235	0.213	0.19	0.167	0.144	0.119	0.096	0.07	0.046	0.02	-0.004	-0.028	-0.052	-0.076	-0.097	-0.119	-0.14
	1	0.282	0.26	0.237	0.214	0.19	0.165	0.14	0.116	0.091	0.066	0.042	0.018	-0.005	-0.028	-0.05	-0.071	-0.091
	2	0.383	0.36	0.336	0.312	0.288	0.263	0.238	0.213	0.189	0.165	0.141	0.118	0.096	0.074	0.053	0.033	0.014
	4	0.602	0.577	0.553	0.528	0.503	0.478	0.454	0.431	0.408	0.386	0.363	0.341	0.32	0.301	0.283	0.267	0.251
	6	0.845	0.82	0.795	0.771	0.747	0.723	0.7	0.677	0.655	0.633	0.613	0.594	0.576	0.559	0.544	0.53	0.518
0.9	0.5	0.265	0.239	0.213	0.185	0.168	0.129	0.101	0.072	0.043	0.014	-0.015	-0.043	-0.071	-0.098	-0.124	-0.15	-0.176
	1	0.311	0.284	0.257	0.23	0.202	0.173	0.144	0.116	0.086	0.061	0.029	0.001	-0.026	-0.063	-0.079	-0.105	-0.129
	2	0.407	0.38	0.352	0.324	0.296	0.266	0.237	0.208	0.18	0.151	0.124	0.097	0.07	0.044	0.018	-0.006	-0.029
	4	0.616	0.589	0.559	0.53	0.501	0.473	0.444	0.416	0.389	0.362	0.336	0.31	0.286	0.261	0.239	0.218	0.197
	6	0.853	0.824	0.795	0.767	0.738	0.711	0.683	0.666	0.63	0.604	0.579	0.555	0.533	0.511	0.491	0.472	0.455
1.1	0.5	0.293	0.264	0.234	0.204	0.173	0.142	0.11	0.078	0.046	0.014	-0.018	-0.049	-0.08	-0.11	-0.14	-0.169	-0.197
	1	0.342	0.312	0.282	0.251	0.22	0.189	0.167	0.126	0.093	0.061	0.029	-0.001	-0.032	-0.062	-0.091	-0.12	-0.148
	2	0.447	0.417	0.386	0.355	0.323	0.291	0.259	0.227	0.196	0.164	0.133	0.103	0.073	0.044	0.015	-0.013	-0.039
	4	0.683	0.652	0.62	0.588	0.556	0.524	0.493	0.462	0.431	0.401	0.371	0.342	0.314	0.287	0.261	0.235	0.211
	6	0.956	0.924	0.892	0.86	0.829	0.798	0.767	0.737	0.707	0.678	0.65	0.622	0.596	0.571	0.546	0.523	0.501

Cm, ARC fin3, A = 50 ft^2

1.2				0.187	0.16	0.133	0.105	0.078	0.05	0.022	-0.005	-0.033	-0.059	-0.086	-0.112	-0.137	-0.162	
0.5	0.265	0.24	0.214	0.187	0.16	0.184	0.156	0.128	0.101	0.073	0.046	0.019	-0.008	-0.034	-0.06	-0.085	-0.11	
1	0.317	0.292	0.265	0.239	0.211	0.184	0.156	0.128	0.101	0.212	0.184	0.158	0.131	0.105	0.079	0.054	0.03	0.006
2	0.43	0.404	0.377	0.35	0.323	0.295	0.267	0.239	0.212	0.184	0.437	0.411	0.386	0.361	0.337	0.313	0.291	0.269
4	0.683	0.655	0.628	0.6	0.572	0.545	0.518	0.491	0.464	0.437	0.411	0.68	0.656	0.633	0.611	0.59	0.57	
6	0.971	0.944	0.916	0.889	0.861	0.834	0.807	0.781	0.755	0.729	0.704	0.68	0.656	0.633				
1.4				0.204	0.185	0.165	0.145	0.125	0.105	0.085	0.065	0.046	0.026	0.007	-0.012	-0.031	-0.049	
0.5	0.261	0.242	0.223	0.204	0.185	0.165	0.145	0.125	0.105	0.085	0.065	0.046	0.026	0.007	0.114	0.095	0.077	0.059
1	0.368	0.35	0.33	0.311	0.291	0.272	0.252	0.232	0.212	0.192	0.172	0.153	0.133	0.114	0.337	0.319	0.301	0.283
2	0.592	0.572	0.553	0.533	0.514	0.494	0.474	0.454	0.434	0.414	0.395	0.375	0.356	0.337	0.792	0.775	0.758	
4	1.062	1.042	1.022	1.002	0.982	0.962	0.943	0.923	0.904	0.884	0.865	0.847	0.828	0.81	0.792	0.775	0.758	
6	1.558	1.538	1.519	1.499	1.479	1.459	1.44	1.42	1.401	1.382	1.364	1.346	1.328	1.31	1.293	1.277	1.26	
1.65				0.19	0.174	0.159	0.144	0.128	0.113	0.097	0.082	0.066	0.051	0.035	0.02	0.005	-0.01	
0.5	0.235	0.22	0.205	0.19	0.174	0.159	0.144	0.128	0.113	0.097	0.082	0.066	0.051	0.035	0.134	0.119	0.104	
1	0.35	0.334	0.319	0.304	0.288	0.273	0.258	0.242	0.227	0.211	0.196	0.18	0.165	0.149	0.371	0.357	0.342	
2	0.587	0.571	0.556	0.541	0.525	0.51	0.494	0.479	0.463	0.448	0.432	0.417	0.402	0.386	0.871	0.856	0.842	
4	1.085	1.07	1.054	1.039	1.024	1.008	0.993	0.977	0.961	0.946	0.931	0.915	0.9	0.886	1.396	1.382	1.369	
6	1.61	1.594	1.579	1.564	1.548	1.532	1.517	1.501	1.486	1.47	1.455	1.44	1.425	1.411				
1.8				0.184	0.17	0.156	0.142	0.128	0.114	0.1	0.086	0.072	0.057	0.043	0.029	0.015	0.001	
0.5	0.227	0.212	0.198	0.184	0.17	0.156	0.142	0.128	0.114	0.1	0.086	0.072	0.057	0.043	0.144	0.13	0.116	
1	0.342	0.328	0.313	0.299	0.285	0.271	0.257	0.243	0.229	0.215	0.201	0.187	0.172	0.158	0.383	0.369	0.355	
2	0.581	0.566	0.552	0.538	0.524	0.51	0.497	0.483	0.469	0.454	0.44	0.426	0.411	0.397	0.383	0.369	0.355	
4	1.083	1.07	1.056	1.042	1.028	1.014	1	0.985	0.971	0.956	0.942	0.928	0.913	0.899	0.885	0.871	0.857	
6	1.613	1.599	1.585	1.571	1.557	1.543	1.528	1.514	1.499	1.485	1.47	1.456	1.442	1.428	1.414	1.4	1.387	
2				0.175	0.162	0.15	0.138	0.126	0.113	0.101	0.089	0.077	0.064	0.051	0.037	0.024	0.01	
0.5	0.215	0.201	0.188	0.175	0.162	0.15	0.138	0.126	0.113	0.101	0.089	0.077	0.064	0.051	0.037	0.024	0.01	
1	0.328	0.315	0.302	0.289	0.277	0.265	0.253	0.241	0.228	0.216	0.204	0.191	0.178	0.165	0.151	0.138	0.124	
2	0.565	0.552	0.54	0.528	0.515	0.503	0.491	0.479	0.467	0.454	0.441	0.428	0.414	0.401	0.387	0.374	0.361	
4	1.066	1.054	1.042	1.029	1.017	1.005	0.993	0.98	0.966	0.953	0.939	0.925	0.912	0.899	0.886	0.873	0.86	
6	1.593	1.581	1.569	1.557	1.545	1.532	1.519	1.505	1.491	1.477	1.464	1.45	1.437	1.424	1.411	1.398	1.386	

71

XCG=212.44   Cna, ARC fin3, A = 50 ft^2

72

alpha	-8	-7	-6	-5	-4	-3	-2	-1	0	1	2	3	4	5	6	7	8
Mach = 0.2																	
0.5	0.05387	0.05408	0.05429	0.05462	0.05475	0.05498	0.05516	0.05524	0.05524	0.05514	0.05495	0.05474	0.05462	0.05431	0.05416	0.05393	0.05354
1	0.05688	0.05710	0.05732	0.05755	0.05776	0.05792	0.05800	0.05800	0.05792	0.05776	0.05756	0.05735	0.05714	0.05693	0.05667	0.05628	0.05575
2	0.06081	0.06104	0.06125	0.06142	0.06154	0.06158	0.06154	0.06144	0.06128	0.06109	0.06089	0.06066	0.06039	0.06006	0.05959	0.05900	0.05832
4	0.06330	0.06346	0.06357	0.06361	0.06359	0.06350	0.06338	0.06324	0.06307	0.06288	0.06263	0.06230	0.06188	0.06135	0.06075	0.06011	0.05942
6	0.06342	0.06345	0.06339	0.06327	0.06311	0.06295	0.06283	0.06272	0.06262	0.06243	0.06208	0.06157	0.06096	0.06033	0.05976	0.05923	0.05867
Mach = 0.4																	
0.5	0.05409	0.05434	0.05459	0.05487	0.05515	0.05545	0.05568	0.05579	0.05579	0.05565	0.05540	0.05514	0.05487	0.05461	0.05443	0.05416	0.05368
1	0.05714	0.05741	0.05768	0.05795	0.05822	0.05842	0.05863	0.05863	0.05842	0.05821	0.05796	0.05770	0.05744	0.05719	0.05688	0.05642	0.05580
2	0.06115	0.06143	0.06168	0.06190	0.06206	0.06210	0.06204	0.06190	0.06170	0.06146	0.06121	0.06093	0.06061	0.06021	0.05968	0.05901	0.05826
4	0.06370	0.06389	0.06402	0.06407	0.06402	0.06391	0.06375	0.06356	0.06335	0.06312	0.06281	0.06243	0.06194	0.06136	0.06069	0.05998	0.05923
6	0.06383	0.06386	0.06377	0.06359	0.06337	0.06316	0.06300	0.06287	0.06274	0.06251	0.06208	0.06150	0.06084	0.06018	0.05956	0.05899	0.05837
Mach = 0.6																	
0.5	0.05456	0.05486	0.05519	0.05556	0.05595	0.05638	0.05670	0.05686	0.05686	0.05685	0.05665	0.05630	0.05593	0.05555	0.05499	0.05464	0.05397
1	0.05768	0.05802	0.05838	0.05876	0.05912	0.05942	0.05967	0.05956	0.05940	0.05910	0.05874	0.05838	0.05804	0.05771	0.05730	0.05669	0.05588
2	0.06182	0.06219	0.06254	0.06284	0.06304	0.06311	0.06302	0.06282	0.06262	0.06218	0.06184	0.06148	0.06105	0.06062	0.05984	0.05902	0.05812
4	0.06448	0.06474	0.06491	0.06496	0.06488	0.06471	0.06447	0.06420	0.06392	0.06359	0.06318	0.06267	0.06206	0.06134	0.06055	0.05972	0.05885
6	0.06465	0.06467	0.06452	0.06423	0.06389	0.06358	0.06334	0.06317	0.06300	0.06268	0.06209	0.06132	0.06066	0.05986	0.05920	0.05851	0.05775
Mach = 0.9																	
0.5	0.05796	0.05829	0.05864	0.05900	0.05937	0.05977	0.06007	0.06022	0.06022	0.06003	0.05970	0.05935	0.05900	0.05866	0.05840	0.05803	0.05742
1	0.06111	0.06146	0.06182	0.06218	0.06253	0.06281	0.06296	0.06296	0.06279	0.06252	0.06218	0.06184	0.06160	0.06116	0.06076	0.06018	0.05947
2	0.06526	0.06562	0.06596	0.06625	0.06644	0.06661	0.06643	0.06624	0.06697	0.06664	0.06631	0.06496	0.06464	0.06404	0.06343	0.06271	0.06192
4	0.06759	0.06784	0.06801	0.06806	0.06800	0.06786	0.06763	0.06737	0.06710	0.06678	0.06640	0.06594	0.06540	0.06477	0.06408	0.06336	0.06260
6	0.06710	0.06713	0.06701	0.06676	0.06645	0.06617	0.06695	0.06677	0.06569	0.06529	0.06479	0.06416	0.06353	0.06284	0.06236	0.06176	0.06111
Mach = 1.1																	
0.5	0.06184	0.06217	0.06249	0.06281	0.06314	0.06348	0.06373	0.06386	0.06386	0.06370	0.06343	0.06313	0.06282	0.06262	0.06225	0.06189	0.06138
1	0.06607	0.06640	0.06672	0.06704	0.06734	0.06758	0.06771	0.06771	0.06758	0.06734	0.06706	0.06676	0.06645	0.06613	0.06576	0.06527	0.06468
2	0.07160	0.07193	0.07223	0.07248	0.07265	0.07271	0.07266	0.07250	0.07226	0.07189	0.07169	0.07137	0.07100	0.07067	0.07006	0.06945	0.06879
4	0.07504	0.07526	0.07541	0.07547	0.07542	0.07530	0.07512	0.07490	0.07466	0.07438	0.07406	0.07366	0.07321	0.07269	0.07213	0.07153	0.07090
6	0.07506	0.07509	0.07499	0.07479	0.07464	0.07431	0.07412	0.07396	0.07378	0.07363	0.07313	0.07266	0.07216	0.07169	0.07122	0.07073	0.07020

XCG = 212.44

Cna, ARC fin3, A = 50 ft^2

73

	-8	-7	-6	-5	-4	-3	-2	-1	0	1	2	3	4	5	6	7	8
Mach = 1.2																	
0.5	0.05855	0.05882	0.05908	0.05933	0.05958	0.05983	0.06003	0.06012	0.06001	0.05980	0.05958	0.05934	0.05911	0.05887	0.05859	0.05820	
1	0.06280	0.06307	0.06332	0.06357	0.06379	0.06397	0.06407	0.06407	0.06397	0.06380	0.06358	0.06312	0.06286	0.06267	0.06220	0.06176	
2	0.06834	0.06860	0.06883	0.06902	0.06915	0.06920	0.06916	0.06904	0.06887	0.06866	0.06843	0.06789	0.06756	0.06717	0.06673	0.06625	
4	0.07191	0.07209	0.07220	0.07225	0.07222	0.07214	0.07200	0.07184	0.07165	0.07144	0.07120	0.07058	0.07020	0.06979	0.06935	0.06889	
6	0.07221	0.07224	0.07217	0.07203	0.07186	0.07169	0.07155	0.07142	0.07129	0.07110	0.07082	0.07016	0.06983	0.06949	0.06914	0.06877	
Mach = 1.4																	
0.5	0.07050	0.07068	0.07084	0.07098	0.07111	0.07123	0.07133	0.07137	0.07137	0.07132	0.07122	0.07111	0.07099	0.07086	0.07052	0.07033	
1	0.07462	0.07479	0.07493	0.07506	0.07518	0.07527	0.07631	0.07632	0.07527	0.07519	0.07508	0.07497	0.07483	0.07468	0.07432	0.07411	
2	0.07967	0.07981	0.07993	0.08003	0.08010	0.08013	0.08011	0.08006	0.07998	0.07987	0.07975	0.07961	0.07945	0.07928	0.07908	0.07865	
4	0.08242	0.08251	0.08258	0.08261	0.08261	0.08257	0.08252	0.08244	0.08234	0.08223	0.08211	0.08196	0.08181	0.08164	0.08126	0.08104	
6	0.08196	0.08198	0.08196	0.08191	0.08184	0.08177	0.08170	0.08155	0.08155	0.08146	0.08136	0.08124	0.08112	0.08099	0.08053	0.08053	
Mach = 1.65																	
0.5	0.06997	0.07004	0.07010	0.07015	0.07016	0.07014	0.07012	0.07011	0.07012	0.07014	0.07017	0.07018	0.07016	0.07012	0.07007	0.06990	
1	0.07399	0.07405	0.07409	0.07411	0.07411	0.07409	0.07409	0.07410	0.07411	0.07414	0.07415	0.07413	0.07410	0.07405	0.07398	0.07378	
2	0.07887	0.07890	0.07892	0.07893	0.07893	0.07893	0.07895	0.07897	0.07898	0.07899	0.07897	0.07893	0.07879	0.07870	0.07870	0.07847	
4	0.08154	0.08155	0.08157	0.08158	0.08161	0.08163	0.08165	0.08166	0.08165	0.08163	0.08159	0.08146	0.08138	0.08129	0.08129	0.08106	
6	0.08113	0.08114	0.08118	0.08123	0.08127	0.08130	0.08129	0.08127	0.08124	0.08121	0.08116	0.08111	0.08105	0.08098	0.08091	0.08072	
Mach = 1.8																	
0.5	0.06999	0.07001	0.07001	0.06999	0.06992	0.06979	0.06968	0.06962	0.06963	0.06971	0.06985	0.06995	0.07000	0.07003	0.07002	0.07000	
1	0.07395	0.07394	0.07392	0.07386	0.07377	0.07367	0.07363	0.07364	0.07371	0.07381	0.07391	0.07397	0.07400	0.07401	0.07399	0.07395	
2	0.07872	0.07868	0.07862	0.07855	0.07850	0.07849	0.07854	0.07861	0.07871	0.07879	0.07884	0.07887	0.07887	0.07886	0.07884	0.07872	
4	0.08123	0.08119	0.08116	0.08116	0.08121	0.08128	0.08135	0.08143	0.08148	0.08151	0.08152	0.08152	0.08151	0.08148	0.08136	0.08128	
6	0.08065	0.08066	0.08074	0.08086	0.08099	0.08108	0.08111	0.08111	0.08110	0.08109	0.08108	0.08107	0.08104	0.08099	0.08087	0.08080	
Mach = 2.0																	
0.5	0.06831	0.06832	0.06809	0.06764	0.06732	0.06719	0.06713	0.06711	0.06711	0.06711	0.06715	0.06738	0.06784	0.06818	0.06831	0.06817	
1	0.07215	0.07197	0.07166	0.07135	0.07118	0.07112	0.07109	0.07110	0.07114	0.07123	0.07144	0.07177	0.07208	0.07224	0.07225	0.07203	
2	0.07659	0.07635	0.07613	0.07600	0.07595	0.07595	0.07599	0.07610	0.07627	0.07650	0.07675	0.07697	0.07707	0.07705	0.07697	0.07678	
4	0.07880	0.07870	0.07866	0.07866	0.07870	0.07878	0.07894	0.07913	0.07933	0.07950	0.07959	0.07959	0.07954	0.07947	0.07941	0.07929	
6	0.07817	0.07828	0.07835	0.07841	0.07851	0.07869	0.07898	0.07920	0.07922	0.07910	0.07893	0.07878	0.07873	0.07876	0.07877	0.07867	

Cms, ARC fin3, A = 50 ft^2

alpha	-8	-7	-6	-5	-4	-3	-2	-1	0	1	2	3	4	5	6	7	8
Mach = 0.2																	
0.5		0.09316	0.09276	0.09233	0.09191	0.09148	0.09115	0.09099	0.09100	0.09119	0.09153	0.09192	0.09234	0.09272	0.09300	0.09343	0.09416
1		0.09908	0.09866	0.09825	0.09786	0.09756	0.09740	0.09740	0.09756	0.09785	0.09822	0.09861	0.09900	0.09939	0.09988	0.10060	0.10160
2		0.10660	0.10620	0.10590	0.10570	0.10560	0.10570	0.10590	0.10620	0.10650	0.10690	0.10730	0.10780	0.10840	0.10930	0.11040	0.11170
4		0.11750	0.11730	0.11720	0.11720	0.11740	0.11760	0.11790	0.11820	0.11850	0.11900	0.11960	0.12040	0.12140	0.12250	0.12370	0.12500
6		0.13010	0.13020	0.13040	0.13070	0.13100	0.13120	0.13140	0.13160	0.13200	0.13260	0.13360	0.13470	0.13590	0.13700	0.13790	0.13900
Mach = 0.4																	
0.5		0.09266	0.09218	0.09166	0.09114	0.09058	0.09016	0.08995	0.08996	0.09021	0.09067	0.09116	0.09167	0.09214	0.09247	0.09299	0.09388
1		0.09849	0.09798	0.09747	0.09698	0.09659	0.09639	0.09640	0.09661	0.09699	0.09746	0.09795	0.09842	0.09890	0.09947	0.10030	0.10150
2		0.10590	0.10540	0.10500	0.10470	0.10460	0.10470	0.10500	0.10540	0.10580	0.10630	0.10680	0.10740	0.10810	0.10910	0.11040	0.11180
4		0.11660	0.11640	0.11630	0.11640	0.11660	0.11690	0.11730	0.11760	0.11810	0.11870	0.11940	0.12030	0.12140	0.12260	0.12390	0.12530
6		0.12930	0.12950	0.12980	0.13020	0.13060	0.13090	0.13110	0.13140	0.13180	0.13260	0.13370	0.13490	0.13620	0.13730	0.13840	0.13950
Mach = 0.6																	
0.5		0.09164	0.09102	0.09033	0.08961	0.08881	0.08822	0.08792	0.08793	0.08830	0.08896	0.08966	0.09036	0.09099	0.09139	0.09205	0.09331
1		0.09731	0.09663	0.09593	0.09525	0.09470	0.09441	0.09443	0.09474	0.09529	0.09596	0.09663	0.09727	0.09788	0.09864	0.09979	0.10130
2		0.10440	0.10370	0.10320	0.10280	0.10270	0.10280	0.10320	0.10380	0.10440	0.10500	0.10570	0.10650	0.10750	0.10880	0.11030	0.11200
4		0.11500	0.11470	0.11460	0.11480	0.11510	0.11550	0.11600	0.11660	0.11720	0.11790	0.11890	0.12000	0.12140	0.12280	0.12440	0.12600
6		0.12780	0.12800	0.12860	0.12920	0.12980	0.13020	0.13060	0.13090	0.13150	0.13260	0.13400	0.13540	0.13670	0.13800	0.13920	0.14070
Mach = 0.9																	
0.5		0.08694	0.08630	0.08563	0.08494	0.08418	0.08362	0.08334	0.08334	0.08369	0.08432	0.08497	0.08563	0.08626	0.08676	0.08744	0.08858
1		0.09265	0.09198	0.09130	0.09065	0.09012	0.08985	0.08986	0.09015	0.09067	0.09130	0.09194	0.09258	0.09321	0.09397	0.09503	0.09636
2		0.09982	0.09918	0.09866	0.09828	0.09816	0.09829	0.09865	0.09917	0.09977	0.10040	0.10110	0.10180	0.10280	0.10390	0.10530	0.10670
4		0.11110	0.11080	0.11070	0.11080	0.11110	0.11150	0.11200	0.11250	0.11310	0.11380	0.11470	0.11570	0.11690	0.11820	0.11950	0.12090
6		0.12510	0.12530	0.12580	0.12640	0.12690	0.12730	0.12770	0.12800	0.12860	0.12950	0.13070	0.13190	0.13300	0.13400	0.13520	0.13840
Mach = 1.1																	
0.5		0.09231	0.09169	0.09108	0.09047	0.08981	0.08932	0.08908	0.08908	0.08938	0.08991	0.09048	0.09106	0.09165	0.09216	0.09284	0.09382
1		0.10050	0.09991	0.09930	0.09873	0.09828	0.09803	0.09804	0.09829	0.09873	0.09928	0.09985	0.10040	0.10100	0.10180	0.10270	0.10380
2		0.11100	0.11050	0.11000	0.10970	0.10950	0.10970	0.11000	0.11040	0.11090	0.11150	0.11210	0.11280	0.11360	0.11460	0.11580	0.11700
4		0.12680	0.12650	0.12640	0.12650	0.12670	0.12700	0.12750	0.12790	0.12850	0.12910	0.12980	0.13070	0.13170	0.13280	0.13390	0.13510
6		0.14550	0.14570	0.14610	0.14650	0.14700	0.14730	0.14770	0.14800	0.14850	0.14920	0.15010	0.15110	0.15200	0.15290	0.15380	0.15480

Cmα, ARC fin3, A = 50 ft^2

Mach = 1.2

		0.09960	0.09911	0.09863	0.09816	0.09767	0.09731	0.09712	0.09713	0.09734	0.09774	0.09816	0.09861	0.09906	0.09950	0.10000	0.10080
0.5	0.10010	0.09960	0.09911	0.09863	0.09816	0.09767	0.09731	0.09712	0.09713	0.09734	0.09774	0.09816	0.09861	0.09906	0.09950	0.10000	0.10080
1	0.10860	0.10810	0.10760	0.10720	0.10670	0.10640	0.10620	0.10620	0.10640	0.10670	0.10710	0.10760	0.10800	0.10850	0.10910	0.10980	0.11080
2	0.11950	0.11900	0.11860	0.11820	0.11800	0.11790	0.11800	0.11820	0.11850	0.11890	0.11940	0.11980	0.12040	0.12100	0.12180	0.12260	0.12350
4	0.13530	0.13490	0.13470	0.13460	0.13470	0.13480	0.13510	0.13540	0.13580	0.13620	0.13660	0.13720	0.13780	0.13850	0.13930	0.14020	0.14100
6	0.15350	0.15340	0.15380	0.15380	0.15420	0.15450	0.15480	0.15500	0.15530	0.15560	0.15610	0.15680	0.15740	0.15810	0.15870	0.15940	0.16010

Mach = 1.4

		0.09960	0.09911	0.09863	0.09816	0.09767	0.09731	0.09712	0.09713	0.09734	0.09774	0.09816	0.09861	0.09906	0.09950	0.10000	0.10080
0.5	0.21040	0.21000	0.20970	0.20950	0.20920	0.20900	0.20880	0.20870	0.20870	0.20880	0.20900	0.20920	0.20940	0.20970	0.21000	0.21030	0.21070
1	0.21890	0.21860	0.21830	0.21800	0.21780	0.21760	0.21750	0.21760	0.21760	0.21780	0.21800	0.21820	0.21850	0.21880	0.21910	0.21950	0.21980
2	0.22910	0.22880	0.22860	0.22840	0.22820	0.22820	0.22820	0.22830	0.22850	0.22870	0.22890	0.22920	0.22950	0.22980	0.23020	0.23060	0.23100
4	0.24170	0.24150	0.24140	0.24130	0.24130	0.24140	0.24150	0.24170	0.24180	0.24210	0.24230	0.24260	0.24290	0.24320	0.24360	0.24390	0.24430
6	0.25510	0.25500	0.25510	0.25520	0.25530	0.25540	0.25550	0.25570	0.25580	0.25600	0.25620	0.25640	0.25670	0.25690	0.25720	0.25750	0.25780

Mach = 1.65

		0.09960	0.09911	0.09863	0.09816	0.09767	0.09731	0.09712	0.09713	0.09734	0.09774	0.09816	0.09861	0.09906	0.09950	0.10000	0.10080
0.5	0.22390	0.22380	0.22370	0.22360	0.22360	0.22360	0.22360	0.22370	0.22360	0.22360	0.22360	0.22350	0.22360	0.22370	0.22380	0.22390	0.22410
1	0.23280	0.23250	0.23240	0.23240	0.23240	0.23240	0.23240	0.23240	0.23230	0.23240	0.23230	0.23240	0.23240	0.23250	0.23270	0.23280	0.23300
2	0.24310	0.24310	0.24300	0.24300	0.24300	0.24300	0.24290	0.24290	0.24290	0.24290	0.24290	0.24300	0.24310	0.24330	0.24340	0.24360	0.24390
4	0.25580	0.25580	0.25570	0.25570	0.25560	0.25560	0.25560	0.25560	0.25570	0.25570	0.25570	0.25580	0.25590	0.25610	0.25630	0.25650	0.25670
6	0.26890	0.26890	0.26880	0.26870	0.26860	0.26860	0.26860	0.26870	0.26880	0.26880	0.26880	0.26900	0.26910	0.26920	0.26930	0.26950	0.26970

Mach = 1.8

		0.09960	0.09911	0.09863	0.09816	0.09767	0.09731	0.09712	0.09713	0.09734	0.09774	0.09816	0.09861	0.09906	0.09950	0.10000	0.10080
0.5	0.22570	0.22560	0.22570	0.22580	0.22610	0.22630	0.22640	0.22620	0.22590	0.22580	0.22600	0.22570	0.22560	0.22560	0.22560	0.22560	0.22570
1	0.23450	0.23450	0.23460	0.23480	0.23500	0.23510	0.23510	0.23470	0.23450	0.23440	0.23440	0.23440	0.23430	0.23440	0.23440	0.23440	0.23450
2	0.24520	0.24530	0.24550	0.24560	0.24560	0.24550	0.24540	0.24500	0.24490	0.24490	0.24490	0.24490	0.24490	0.24490	0.24490	0.24500	0.24510
4	0.25810	0.25830	0.25830	0.25820	0.25800	0.25790	0.25770	0.25760	0.25760	0.25760	0.25760	0.25760	0.25770	0.25780	0.25790	0.25800	0.25800
6	0.27160	0.27140	0.27110	0.27090	0.27070	0.27070	0.27070	0.27070	0.27070	0.27070	0.27080	0.27080	0.27090	0.27090	0.27100	0.27110	0.27130

Mach = 2.0

		0.09960	0.09911	0.09863	0.09816	0.09767	0.09731	0.09712	0.09713	0.09734	0.09774	0.09816	0.09861	0.09906	0.09950	0.10000	0.10080
0.5	0.22310	0.22310	0.22350	0.22440	0.22500	0.22530	0.22540	0.22540	0.22530	0.22490	0.22530	0.22540	0.22540	0.22530	0.22480	0.22310	0.22340
1	0.23220	0.23260	0.23310	0.23370	0.23400	0.23410	0.23420	0.23390	0.23350	0.23400	0.23410	0.23410	0.23390	0.23350	0.23230	0.23200	0.23240
2	0.24350	0.24390	0.24440	0.24460	0.24470	0.24460	0.24440	0.24370	0.24320	0.24410	0.24440	0.24440	0.24370	0.24280	0.24260	0.24280	0.24310
4	0.25710	0.25730	0.25730	0.25730	0.25710	0.25680	0.25680	0.25570	0.25560	0.25610	0.25680	0.25680	0.25590	0.25580	0.25570	0.25590	0.25610
6	0.27070	0.27050	0.27030	0.27020	0.27000	0.26970	0.26910	0.26870	0.26890	0.26920	0.26950	0.26960	0.26950	0.26960	0.26960	0.26960	0.26970

CM for body alone										
	MACH									
alpha	0.2	0.4	0.6	0.9	1.1	1.2	1.4	1.65	1.8	2
0.5	0.0942	0.0942	0.0942	0.0951	0.1022	0.1028	0.1665	0.1725	0.1733	0.1706
1	0.1897	0.1897	0.1897	0.1915	0.2062	0.2074	0.3355	0.3475	0.349	0.3436
2	0.3916	0.3916	0.3916	0.3952	0.4294	0.4322	0.6887	0.7127	0.7158	0.7049
4	0.8296	0.8296	0.8296	0.837	0.9239	0.9308	1.4385	1.4863	1.4925	1.4709
6	1.2914	1.2914	1.2914	1.3026	1.4527	1.4643	2.2114	2.2828	2.2921	2.2597

CN for body alone										
	MACH									
alpha	0.2	0.4	0.6	0.9	1.1	1.2	1.4	1.65	1.8	2
0.5	0.0193	0.0193	0.0193	0.0194	0.0205	0.0203	0.0287	0.0298	0.0301	0.0295
1	0.0389	0.0389	0.0389	0.0392	0.0415	0.041	0.058	0.0602	0.0609	0.0597
2	0.081	0.081	0.081	0.0816	0.0874	0.0865	0.1207	0.1251	0.1265	0.124
4	0.1741	0.1741	0.1741	0.1753	0.1918	0.1904	0.2576	0.2663	0.2691	0.2642
6	0.2737	0.2737	0.2737	0.2755	0.3054	0.3036	0.4012	0.4141	0.4182	0.411

76

MACH	alpha degs	-8	-7	-6	-5	-4	-3	-2	-1	0	1	2	3	4	5	6	7	8
0.2										fin deflection (degrees)								
	0.5	-0.0674	-0.056	-0.0445	-0.0328	-0.0209	-0.0088	0.0034	0.0158	0.0281	0.0404	0.0526	0.0647	0.0766	0.0883	0.0998	0.1111	0.1221
	1	-0.0395	-0.0281	-0.0165	-0.0046	0.0074	0.0196	0.0319	0.0442	0.0566	0.0688	0.0809	0.0929	0.1046	0.1162	0.1276	0.1388	0.1495
	2	0.0191	0.0308	0.0427	0.0547	0.0669	0.0793	0.0916	0.1039	0.1161	0.1282	0.1401	0.1518	0.1634	0.1747	0.1858	0.1965	0.2067
	4	0.1463	0.1584	0.1706	0.1829	0.1952	0.2075	0.2196	0.2315	0.2434	0.255	0.2665	0.2778	0.2887	0.2991	0.309	0.3182	0.3269
	6	0.2737	0.286	0.2983	0.3105	0.3226	0.3346	0.3464	0.3582	0.3697	0.381	0.3919	0.4023	0.4122	0.4214	0.4301	0.4382	0.4456
0.4	0.5	-0.0694	-0.0579	-0.0461	-0.0342	-0.022	-0.0096	0.003	0.0157	0.0284	0.0411	0.0536	0.0659	0.0781	0.09	0.1017	0.1131	0.1243
	1	-0.0414	-0.0298	-0.0179	-0.0058	0.0065	0.019	0.0317	0.0444	0.0571	0.0697	0.0821	0.0943	0.1063	0.1181	0.1296	0.1409	0.1518
	2	0.0176	0.0294	0.0416	0.054	0.0665	0.0792	0.0919	0.1046	0.1171	0.1295	0.1416	0.1536	0.1653	0.1768	0.188	0.1988	0.2089
	4	0.1455	0.1579	0.1705	0.1832	0.1959	0.2084	0.2208	0.2331	0.2451	0.257	0.2686	0.28	0.2909	0.3014	0.3112	0.3203	0.3289
	6	0.2737	0.2863	0.299	0.3115	0.3239	0.3362	0.3482	0.3601	0.3718	0.3832	0.3942	0.4046	0.4144	0.4235	0.432	0.4399	0.4471
0.6	0.5	-0.0733	-0.0615	-0.0494	-0.037	-0.0242	-0.0112	0.002	0.0155	0.0289	0.0423	0.0555	0.0684	0.081	0.0934	0.1055	0.1173	0.1286
	1	-0.0451	-0.0331	-0.0208	-0.0082	0.0047	0.0179	0.0312	0.0447	0.0581	0.0714	0.0844	0.0971	0.1096	0.1218	0.1337	0.1452	0.1562
	2	0.0144	0.0268	0.0394	0.0524	0.0657	0.0791	0.0926	0.1059	0.1191	0.132	0.1447	0.1571	0.1692	0.181	0.1924	0.2032	0.2134
	4	0.1439	0.157	0.1703	0.1837	0.1971	0.2103	0.2233	0.236	0.2485	0.2608	0.2728	0.2844	0.2954	0.3058	0.3155	0.3245	0.3328
	6	0.2737	0.2871	0.3004	0.3136	0.3266	0.3393	0.3518	0.3641	0.3761	0.3877	0.3987	0.409	0.4187	0.4276	0.4359	0.4433	0.45
0.9	0.5	-0.0892	-0.0751	-0.0608	-0.0462	-0.0313	-0.0161	-0.0006	0.015	0.0306	0.0462	0.0616	0.0767	0.0915	0.1061	0.1204	0.1343	0.1479
	1	-0.0592	-0.0451	-0.0306	-0.0158	-0.0007	0.0147	0.0303	0.0459	0.0615	0.077	0.0922	0.1071	0.1218	0.1362	0.1503	0.164	0.1773
	2	0.0038	0.0183	0.0332	0.0483	0.0638	0.0794	0.095	0.1106	0.1259	0.1411	0.1559	0.1705	0.1849	0.1989	0.2126	0.2256	0.2381
	4	0.1401	0.1554	0.1709	0.1865	0.202	0.2175	0.2326	0.2476	0.2623	0.2768	0.291	0.3049	0.3182	0.331	0.3431	0.3546	0.3654
	6	0.2755	0.2911	0.3066	0.322	0.3372	0.3522	0.3669	0.3814	0.3957	0.4096	0.4229	0.4357	0.4478	0.4593	0.4702	0.4803	0.4897
1.1	0.5	-0.0978	-0.0824	-0.0667	-0.0507	-0.0344	-0.0179	-0.0012	0.0157	0.0326	0.0494	0.0661	0.0826	0.0988	0.1147	0.1304	0.1457	0.1607
	1	-0.0656	-0.0501	-0.0342	-0.018	-0.0016	0.015	0.0319	0.0488	0.0656	0.0824	0.0989	0.1152	0.1313	0.147	0.1625	0.1777	0.1924
	2	0.0029	0.0188	0.035	0.0515	0.0682	0.085	0.1019	0.1187	0.1354	0.1519	0.1681	0.1841	0.1999	0.2153	0.2304	0.245	0.2591
	4	0.1537	0.1703	0.187	0.2039	0.2207	0.2374	0.2539	0.2703	0.2864	0.3023	0.3179	0.3332	0.3481	0.3625	0.3763	0.3896	0.4023
	6	0.3046	0.3214	0.3382	0.3549	0.3714	0.3878	0.4039	0.4199	0.4356	0.4509	0.4659	0.4803	0.4942	0.5076	0.5204	0.5326	0.5441

77

78

degs	-8	-7	-6	-5	-4	-3	-2	-1	0	1	2	3	4	5	6	7	8
1.2																	
0.5	-0.0827	-0.0692	-0.0555	-0.0416	-0.0274	-0.0131	0.0015	0.0161	0.0307	0.0453	0.0598	0.0741	0.0882	0.1022	0.1158	0.1293	0.1424
1	-0.0522	-0.0386	-0.0247	-0.0107	0.0036	0.0181	0.0326	0.0473	0.0619	0.0765	0.0908	0.105	0.119	0.1328	0.1464	0.1596	0.1726
2	0.0131	0.0269	0.041	0.0553	0.0698	0.0844	0.0991	0.1137	0.1282	0.1425	0.1566	0.1706	0.1844	0.1979	0.2111	0.224	0.2364
4	0.1573	0.1717	0.1862	0.2008	0.2154	0.2299	0.2443	0.2585	0.2726	0.2865	0.3001	0.3136	0.3266	0.3394	0.3517	0.3636	0.3751
6	0.3022	0.3168	0.3313	0.3458	0.3602	0.3745	0.3886	0.4025	0.4162	0.4297	0.4429	0.4557	0.4681	0.4801	0.4917	0.5028	0.5134
1.4																	
0.5	-0.0458	-0.036	-0.026	-0.0159	-0.0056	0.0048	0.0152	0.0257	0.0362	0.0467	0.0571	0.0675	0.0777	0.0878	0.0978	0.1077	0.1173
1	-0.0093	0.0006	0.0106	0.0208	0.0312	0.0416	0.052	0.0626	0.0731	0.0835	0.0939	0.1042	0.1144	0.1244	0.1343	0.144	0.1536
2	0.0677	0.0778	0.088	0.0983	0.1088	0.1192	0.1298	0.1402	0.1507	0.161	0.1713	0.1815	0.1915	0.2014	0.2111	0.2207	0.23
4	0.2339	0.2442	0.2546	0.2651	0.2756	0.2861	0.2964	0.3068	0.317	0.3271	0.3371	0.347	0.3567	0.3662	0.3755	0.3846	0.3934
6	0.3991	0.4096	0.42	0.4305	0.4409	0.4512	0.4615	0.4717	0.4817	0.4917	0.5014	0.511	0.5204	0.5296	0.5386	0.5473	0.5558
1.65																	
0.5	-0.029	-0.0211	-0.0131	-0.005	0.0031	0.0112	0.0193	0.0275	0.0356	0.0437	0.0519	0.06	0.0682	0.0762	0.0843	0.0922	0.1
1	0.0071	0.0151	0.0231	0.0312	0.0393	0.0475	0.0556	0.0637	0.0718	0.08	0.0881	0.0963	0.1044	0.1125	0.1204	0.1284	0.1361
2	0.0835	0.0915	0.0996	0.1077	0.1158	0.1239	0.132	0.1402	0.1483	0.1565	0.1647	0.1728	0.1809	0.1889	0.1968	0.2046	0.2123
4	0.2478	0.2559	0.264	0.2721	0.2802	0.2883	0.2965	0.3047	0.3129	0.321	0.3291	0.3371	0.345	0.3529	0.3606	0.3681	0.3755
6	0.4113	0.4194	0.4275	0.4357	0.4439	0.4521	0.4603	0.4685	0.4766	0.4847	0.4927	0.5006	0.5084	0.516	0.5236	0.5309	0.5381
1.8																	
0.5	-0.0239	-0.0165	-0.009	-0.0015	0.006	0.0134	0.0207	0.0281	0.0354	0.0427	0.0501	0.0576	0.0651	0.0726	0.0801	0.0876	0.095
1	0.0123	0.0197	0.0272	0.0346	0.0421	0.0494	0.0567	0.0641	0.0714	0.0788	0.0862	0.0937	0.1013	0.1088	0.1163	0.1237	0.1311
2	0.0886	0.096	0.1034	0.1108	0.1181	0.1254	0.1327	0.1401	0.1475	0.155	0.1626	0.1701	0.1777	0.1852	0.1927	0.2001	0.2075
4	0.2524	0.2597	0.267	0.2743	0.2816	0.289	0.2965	0.3041	0.3117	0.3193	0.3269	0.3344	0.342	0.3495	0.3569	0.3642	0.3713
6	0.4151	0.4224	0.4297	0.4371	0.4446	0.4522	0.4598	0.4675	0.4751	0.4827	0.4903	0.4979	0.5054	0.5128	0.5201	0.5272	0.5342
2																	
0.5	-0.0191	-0.012	-0.005	0.0019	0.0085	0.0149	0.0213	0.0277	0.0341	0.0405	0.0469	0.0534	0.0602	0.0671	0.0742	0.0813	0.0883
1	0.0162	0.0233	0.0302	0.0368	0.0433	0.0497	0.0561	0.0624	0.0688	0.0752	0.0817	0.0884	0.0953	0.1024	0.1095	0.1166	0.1236
2	0.0907	0.0974	0.104	0.1104	0.1168	0.1231	0.1295	0.1359	0.1424	0.1489	0.1557	0.1627	0.1699	0.177	0.1841	0.1911	0.1979
4	0.2497	0.2561	0.2624	0.2688	0.2752	0.2816	0.2881	0.2949	0.3019	0.3091	0.3164	0.3235	0.3306	0.3375	0.3444	0.3512	0.3579
6	0.4075	0.4139	0.4202	0.4266	0.4332	0.4399	0.4469	0.4541	0.4613	0.4685	0.4757	0.4827	0.4897	0.4966	0.5034	0.5101	0.5167

CM, arcf3, A=50, XCG=256.62

alpha degs	MACH	-7	-6	-5	-4	-3	-2	-1	fin deflection (degrees) 0	1	2	3	4	5	6	7	8
	0.2 −8																
0.5	0.1167	0.1138	0.1108	0.1078	0.1047	0.1015	0.0984	0.0951	0.0919	0.0887	0.0856	0.0824	0.0794	0.0763	0.0733	0.0704	0.0675
1	0.2101	0.2071	0.2041	0.201	0.1979	0.1947	0.1916	0.1883	0.1851	0.182	0.1788	0.1757	0.1726	0.1696	0.1667	0.1638	0.161
2	0.4077	0.4046	0.4016	0.3984	0.3953	0.3921	0.3888	0.3856	0.3825	0.3793	0.3762	0.3732	0.3702	0.3672	0.3644	0.3616	0.3589
4	0.8369	0.8337	0.8306	0.8274	0.8242	0.821	0.8178	0.8147	0.8117	0.8086	0.8056	0.8027	0.7999	0.7972	0.7946	0.7922	0.79
6	1.2914	1.2882	1.285	1.2818	1.2787	1.2756	1.2725	1.2694	1.2664	1.2635	1.2607	1.258	1.2554	1.253	1.2508	1.2487	1.2467
	0.4																
0.5	0.1174	0.1144	0.1113	0.1082	0.105	0.1018	0.0985	0.0952	0.0919	0.0885	0.0853	0.0821	0.0789	0.0758	0.0727	0.0697	0.0668
1	0.2107	0.2077	0.2046	0.2014	0.1982	0.1949	0.1916	0.1883	0.185	0.1817	0.1784	0.1753	0.1721	0.1691	0.166	0.1631	0.1603
2	0.4082	0.4051	0.4019	0.3987	0.3954	0.3921	0.3887	0.3854	0.3822	0.3789	0.3758	0.3727	0.3696	0.3666	0.3637	0.3609	0.3582
4	0.8371	0.8339	0.8306	0.8273	0.824	0.8207	0.8175	0.8143	0.8111	0.808	0.805	0.802	0.7991	0.7964	0.7939	0.7915	0.7892
6	1.2914	1.2881	1.2848	1.2815	1.2783	1.2751	1.2719	1.2688	1.2658	1.2628	1.2599	1.2572	1.2547	1.2523	1.2501	1.248	1.2461
0.6																	
0.5	0.1186	0.1155	0.1123	0.1091	0.1057	0.1023	0.0988	0.0952	0.0917	0.0882	0.0847	0.0813	0.078	0.0747	0.0715	0.0684	0.0654
1	0.2119	0.2087	0.2055	0.2021	0.1987	0.1953	0.1917	0.1882	0.1847	0.1812	0.1777	0.1744	0.1711	0.1679	0.1648	0.1617	0.1588
2	0.4091	0.4059	0.4025	0.3991	0.3956	0.3921	0.3886	0.385	0.3816	0.3782	0.3748	0.3716	0.3684	0.3652	0.3622	0.3594	0.3567
4	0.8376	0.8342	0.8307	0.8271	0.8236	0.8201	0.8167	0.8133	0.8101	0.8068	0.8037	0.8006	0.7977	0.795	0.7924	0.79	0.7879
6	1.2914	1.2879	1.2843	1.2809	1.2775	1.2741	1.2708	1.2676	1.2644	1.2614	1.2585	1.2557	1.2532	1.2508	1.2487	1.2467	1.245
0.9																	
0.5	0.1242	0.1205	0.1166	0.1127	0.1087	0.1046	0.1005	0.0963	0.0921	0.0879	0.0838	0.0798	0.0758	0.0719	0.068	0.0643	0.0607
1	0.2179	0.2141	0.2102	0.2062	0.2022	0.198	0.1939	0.1897	0.1855	0.1813	0.1773	0.1733	0.1693	0.1655	0.1617	0.158	0.1545
2	0.416	0.4121	0.4081	0.4041	0.3999	0.3958	0.3916	0.3874	0.3833	0.3792	0.3752	0.3713	0.3675	0.3637	0.3601	0.3566	0.3532
4	0.8464	0.8423	0.8382	0.834	0.8298	0.8257	0.8216	0.8176	0.8137	0.8098	0.806	0.8023	0.7987	0.7953	0.792	0.7889	0.786
6	1.3026	1.2984	1.2943	1.2901	1.2861	1.2821	1.2781	1.2742	1.2704	1.2667	1.2631	1.2597	1.2564	1.2533	1.2504	1.2477	1.2452
1.1																	
0.5	0.1385	0.1338	0.129	0.1241	0.1191	0.114	0.1089	0.1037	0.0985	0.0933	0.0882	0.0832	0.0782	0.0733	0.0685	0.0638	0.0592
1	0.2391	0.2343	0.2294	0.2245	0.2194	0.2143	0.2092	0.204	0.1988	0.1937	0.1886	0.1836	0.1787	0.1738	0.169	0.1644	0.1599
2	0.4553	0.4504	0.4454	0.4404	0.4353	0.4301	0.4249	0.4197	0.4146	0.4096	0.4046	0.3997	0.3949	0.3901	0.3855	0.381	0.3767
4	0.9356	0.9305	0.9254	0.9202	0.915	0.9099	0.9048	0.8998	0.8949	0.89	0.8852	0.8805	0.8759	0.8715	0.8673	0.8632	0.8593
6	1.4529	1.4477	1.4426	1.4375	1.4324	1.4274	1.4224	1.4175	1.4127	1.408	1.4034	1.399	1.3947	1.3906	1.3867	1.3829	1.3794

79

80

1.2 degs	-8	-7	-6	-5	-4	-3	-2	-1	0	1	2	3	4	5	6	7	8
0.5	0.1346	0.1304	0.1262	0.1219	0.1175	0.1131	0.1086	0.1041	0.0996	0.0951	0.0906	0.0862	0.0818	0.0776	0.0733	0.0692	0.0651
1	0.2362	0.232	0.2277	0.2234	0.219	0.2145	0.21	0.2055	0.201	0.1965	0.1921	0.1877	0.1834	0.1791	0.1749	0.1708	0.1668
2	0.4548	0.4505	0.4462	0.4418	0.4373	0.4328	0.4283	0.4238	0.4193	0.4149	0.4105	0.4062	0.402	0.3978	0.3937	0.3897	0.3859
4	0.941	0.9365	0.9321	0.9276	0.9231	0.9186	0.9141	0.9097	0.9054	0.9011	0.8969	0.8928	0.8887	0.8848	0.881	0.8773	0.8738
6	1.4648	1.4603	1.4558	1.4513	1.4469	1.4425	1.4381	1.4338	1.4296	1.4254	1.4214	1.4174	1.4136	1.4099	1.4063	1.4029	1.3996
1.4																	
0.5	0.1896	0.1865	0.1834	0.1803	0.1771	0.1739	0.1707	0.1674	0.1642	0.1609	0.1577	0.1545	0.1513	0.1482	0.1451	0.1421	0.1391
1	0.3563	0.3533	0.3501	0.347	0.3438	0.3406	0.3373	0.3341	0.3308	0.3276	0.3244	0.3212	0.318	0.3149	0.3119	0.3088	0.3059
2	0.7051	0.702	0.6988	0.6956	0.6924	0.6891	0.6859	0.6826	0.6794	0.6762	0.673	0.6699	0.6668	0.6637	0.6607	0.6577	0.6549
4	1.4459	1.4427	1.4394	1.4362	1.4329	1.4297	1.4265	1.4233	1.4201	1.417	1.4139	1.4108	1.4078	1.4049	1.402	1.3992	1.3965
6	2.212	2.2088	2.2056	2.2023	2.1991	2.1959	2.1927	2.1896	2.1865	2.1834	2.1804	2.1774	2.1745	2.1716	2.1688	2.1661	2.1635
1.65																	
0.5	0.1907	0.1883	0.1858	0.1833	0.1808	0.1783	0.1757	0.1732	0.1707	0.1682	0.1657	0.1631	0.1606	0.1581	0.1556	0.1532	0.1508
1	0.3639	0.3614	0.359	0.3564	0.3539	0.3514	0.3489	0.3464	0.3439	0.3413	0.3388	0.3363	0.3338	0.3313	0.3288	0.3264	0.324
2	0.7255	0.723	0.7205	0.718	0.7155	0.713	0.7105	0.708	0.7054	0.7029	0.7004	0.6979	0.6954	0.6929	0.6905	0.688	0.6857
4	1.492	1.4895	1.487	1.4845	1.482	1.4795	1.477	1.4744	1.4719	1.4694	1.4669	1.4644	1.4619	1.4595	1.4571	1.4548	1.4525
6	2.2836	2.2811	2.2786	2.2761	2.2735	2.271	2.2685	2.2659	2.2634	2.2609	2.2584	2.256	2.2536	2.2512	2.2489	2.2466	2.2444
1.8																	
0.5	0.19	0.1877	0.1854	0.1831	0.1808	0.1785	0.1762	0.1739	0.1717	0.1694	0.1671	0.1648	0.1625	0.1601	0.1578	0.1555	0.1532
1	0.3641	0.3618	0.3595	0.3572	0.3549	0.3526	0.3503	0.3481	0.3458	0.3435	0.3412	0.3389	0.3365	0.3342	0.3319	0.3296	0.3273
2	0.7275	0.7252	0.7229	0.7206	0.7184	0.7161	0.7138	0.7116	0.7093	0.7069	0.7046	0.7023	0.6999	0.6976	0.6953	0.693	0.6907
4	1.4977	1.4954	1.4932	1.4909	1.4887	1.4864	1.484	1.4817	1.4793	1.477	1.4746	1.4723	1.47	1.4676	1.4654	1.4631	1.4609
6	2.293	2.2908	2.2885	2.2862	2.2839	2.2815	2.2792	2.2768	2.2744	2.2721	2.2697	2.2674	2.2651	2.2628	2.2605	2.2583	2.2561
2																	
0.5	0.1856	0.1834	0.1813	0.1791	0.1771	0.1751	0.1731	0.1711	0.1692	0.1672	0.1652	0.1632	0.1611	0.1589	0.1567	0.1545	0.1524
1	0.3571	0.3549	0.3527	0.3507	0.3487	0.3467	0.3447	0.3427	0.3408	0.3388	0.3368	0.3347	0.3326	0.3304	0.3282	0.326	0.3238
2	0.7152	0.7132	0.7111	0.7091	0.7072	0.7052	0.7032	0.7012	0.6992	0.6972	0.6951	0.6929	0.6907	0.6885	0.6863	0.6842	0.682
4	1.4754	1.4734	1.4715	1.4695	1.4675	1.4655	1.4635	1.4614	1.4592	1.457	1.4547	1.4525	1.4503	1.4482	1.4461	1.444	1.4419
6	2.2608	2.2589	2.2569	2.2549	2.2529	2.2508	2.2486	2.2464	2.2442	2.2419	2.2397	2.2375	2.2354	2.2333	2.2311	2.2291	2.227

Arc Fin3, XCG=256.62, A=50, Mach=1.4